ROLE OF *ANANAS COMOSUS* DERIVED EXOSOMES IN SCARLESS CUTANEOUS WOUND REPAIR

by
İrem Özkan

Submitted to Graduate School of Natural and Applied Sciences
in Partial Fulfillment of the Requirements
for the Degree of Master of Science in
Biotechnology

Yeditepe University
2020

ROLE OF *ANANAS COMOSUS* DERIVED EXOSOMES IN SCARLESS CUTANEOUS WOUND REPAIR

APPROVED BY:

Prof. Dr. Fikrettin Şahin ……
(Thesis Supervisor)
(Yeditepe University)

Assist. Prof. Dr. Ayşegül Doğan ……
(Yeditepe University)

Assist. Prof. Dr. Hüseyin Abdik ……
(İstanbul Sabahattin Zaim University)

DATE OF APPROVAL: ..../...../2020

ACKNOWLEDGEMENTS

First and foremost, I would like to express my deepest sincere appreciation to my thesis supervisor Prof. Dr. Fikrettin Şahin who motivated and supported me to perform experiments in Molecular Diagnostics Laboratory. I am extremely grateful for his guidance and recommendations throughout my studies.

Special thanks to Mrs. P. Neslihan Taşlı for helping me perform the experiments in this study, answering my numerous questions, and for her intellectual support.

I want to expand my special thanks to Ms. Zeynep Büşra Bolat for believing in me and supporting me for my future endeavors. I couldn't have done it without her.
Many thanks to my lab mates, Mr. Oğuz Kaan Kırbaş, Mr. Sezer Akgöl, Mr. Eslam Essam, Ms. Burcu Şişli, Ms. Zeynep İşlek, Ms. Derya Sağraç, Ms. Ezgi Taşkan, for their continuous support and for always being there when I need it. It was a privilege to have worked with you.

Last but not least, I want to thank my family for growing me into the person that I am today. Even though we have had our ups and downs, you have thought me so much about life, about personal relationships, and how to stay strong during difficult times. Thank you for teaching me that everything happens for a reason.

I would also like to acknowledge Yeditepe University for financial support during my MSc. Studies.

ABSTRACT

ROLE OF *ANANAS COMOSUS* DERIVED EXOSOMES IN SCARLESS CUTANEOUS WOUND REPAIR

Wound healing is a complex and dynamic process involving a great number of cellular interactions based on growth factors, cytokine, and chemokine release. Although many new therapeutic agents are being introduced to the market for their remarkable wound healing capabilities, the problem of why some organisms heal perfectly while others heal with a pathological connective tissue known as a scar remains a mystery. Scar formation is a natural process that occurs after the healing process due to dysfunctionalities in the remodeling phase that may occur either in the epithelial epidermis or the dermis. Reducing scar formation is lately gaining interest as a new area of scientific research. Following the discovery of scarless healing of the fetal skin, an explosive number of studies have highlighted striking differences between fetal and adult human skin in terms of the differences in their extracellular matrix, growth factor, and cytokine characteristics. Despite of the accumulating evidence to mitigate the scar formation, gain or loss of function of no single pathway or cell type has been shown to be responsible for scar formation therefore mimicking the scarless healing remains as a challenging issue. Nonetheless, findings from recent studies have shed light to certain aspects of scarless healing. In this respect, the use of plant-based products in the treatment medical conditions is becoming a matter of preference due to their lower side effects. Taking a parallel approach, this study aimed to evaluate the potential of scar reducing effects of *Ananas comosus* derived exosomes by determining their proliferative, migratory, and angiogenetic activities on the gene and protein expression levels of key factors of wound healing. Our results indicate that these exosomes activate ERK/MAPK and PI3K/AKT pathways and induce cellular proliferation and migration while increasing the ratio of transforming growth factor-β3 (TGF-β3) to TGF-β1, and certain MMPs, which is an indication for suppression of scar formation. Additionally, it has been shown that these exosomes also promote extracellular matrix reconstruction. Based on these results *A. comosus* exosomes emerge as a promising agent that facilitate cutaneous wound healing suppressing formation of scars.

ÖZET

YARA İZSİZ AKUT YARA ONARIMINDA *ANANAS COMOSUS* TÜREVLİ EXOSOMLARIN ROLÜ

Yara iyileşmesi, büyüme faktörleri, sitokin ve kemokin salınımına dayanan çok sayıda hücresel etkileşimi içeren karmaşık ve dinamik bir süreçtir. Dikkat çekici yara iyileştirme yetenekleri için birçok yeni terapötik ajan piyasaya sürülmesine rağmen, bazı organizmaların neden mükemmel iyileşme sorunu yaşarken, diğerleri skar olarak bilinen patolojik bir bağ dokusu ile iyileşme sorunu gizemini korumaktadır. Skar oluşumu, epitelyal epidermiste veya dermiste meydana gelebilecek yeniden şekillenme evresindeki işlev bozuklukları nedeniyle iyileşme sürecinden sonra ortaya çıkan doğal bir süreçtir. Skar oluşumunun azaltılması, son zamanlarda fetüsün skarsız iyileşmesinin keşfi ile bilimsel alanda dikkat çekmektedir. Bu alandaki araştırmaların artmasıyla, fetal ve yetişkin insan derisi arasındaki farklılıklar, hücre dışı matris, büyüme faktörü ve sitokinlerdeki farklılıklarına göre tanımlanmıştır. Skar oluşumunu hafifletmek için mevcut bulgulardan bağımsız olarak, skar oluşumundan tek bir yol veya hücre tipi sorumlu değildir, bu nedenle skarsız iyileşmeyi taklit etmek zor bir konudur. Bununla birlikte, bu alandaki son çalışmalar, skarsız iyileşmenin belirli yönlerini aydınlatır. Öte yandan, bitki kaynaklı ürünlerin tıbbi problemlerde kullanımı, daha az yan etkileri olduğu için giderek daha fazla dikkat çekmektedir. Bu bağlamda, bitki bazlı *A. comosus* türevli eksozomlar, hem gen hem de protein ekspresyon seviyeleri ile skar azaltma oranları ile birlikte proliferatif, migratif ve anjiyogenetik aktiviteleri için test edilmiştir. Sonuçlar, bu eksozomların ERK/MAPK ve PI3K/AKT yollarını aktive ettiğini ve hücresel proliferasyon ve migrasyonu tetiklerken, matriks metallopreteinazlarla beraber büyüme faktörü-β3'ün (TGF-β3), TGF-β1'ya oranı gibi skar oluşumu ile ilişkili proteinlerin oranını arttırdığını göstermiştir. Ek olarak, bu eksozomların ayrıca hücre dışı matris rekonstrüksiyonunu teşvik ettiği gösterilmiştir. Sonuç olarak, sonuçlar *A. comosus* eksozomlarının skar hafifletme yeteneğine sahip kutanöz yara iyileşmesinde umut verici bir ajan olduğunu göstermektedir.

TABLE OF CONTENTS

LIST OF FIGURES

LIST OF TABLES

LIST OF SYMBOLS/ABBREVIATIONS

ADSC	Adipose derived stem cells
AGE	Advanced glycation end-products
AKT	Protein kinase B
COX-2	Cyclooxygenase-2
DFU	Diabetic foot ulcer
DHEA	Dehydroepiandrosterone
DMEM	Dulbecco's modified Eagle's medium
DMSO	Dimethyl sulfoxide
ECM	Extracellular matrix
EGF	Epidermal growth factor
ESC	Embryonic stem cell
EV	Extracellular vesicles
FBS	Fetal bovine serum
FGF	Fibroblast growth factor
GTPase	Guanosine triphosphatase
H_2O_2	Hydrogen peroxide
HA	Hyaluronic acid
HB-EGF	Heparin binding epidermal growth factor
HBOT	Hyperbaric oxygen therapy
HOCl	Hypochlorous acid

HUVEC	Human umbilical vein endothelial cells
IL	Interleukin
iNOS	Inducible nitride oxide synthesis
iPSC	Induced pluripotent stem cell
KGF	Keratinocyte growth factor
MMP	Matrix metalloproteinase
mRNA	Messenger ribonucleic acid
MSC	Mesenchymal stem cell
MTS	3-(4,5-dimethyl-thiazol-2-yl)-5-(3-carboxymethoxy-phenyl)-2-(4-sulfo-phenyl)-2H-tetrazolium
NADPH	Nicotinamide dinucleotide phosphate oxidase
NGF	Nerve growth factor
NO	Nitric oxide
HO	Hydroxyl radical
NPWT	Negative pressure wound therapy
PI3K	Phosphoinositide 3-kinase
PSA	Penicillin, streptomycin, and amphotericin B
ROS	Reactive oxygen species
SLRP	Small leucine rich proteoglycan
STAT-3	Signal transducer and activator of transcription
SPARC	Secreted protein acidic and rich in cysteine
TGF-β1	Transforming growth factor beta1
PDGF	Platelet-derived growth factor

PGE2	Prostaglandin-2
TIMP	Tissue inhibitors of matrix metalloproteinase
TNF-α	Tumor necrosis factor alpha
tPA	Tissue-type plasminogen activator
UCB	Umbilical cord blood
VEGF	Vascular endothelial growth factor

1. INTRODUCTION

Wounds occur when the functional and cellular integrity of the skin is disrupted. In order to restore skin continuity, wound healing, -a 3-consecutive-phase process, takes place in the disrupted area right after the wounding occurs [1]. Despite of the differences in these phases which are known as inflammation, proliferation, and remodeling, concerted action of various interactions and reactions between different cell types, secretion of soluble mediators and changes in the extracellular matrices, all of which become initiated by host mechanisms, are required for wound healing [2, 3]. Novel therapeutics attempt to overcome the complications and the impairments that may occur during wound repair with the help of better understanding of the molecular pathways underlying these circumstances [4]. Molecular mechanisms underlying the wound healing are strictly regulated. This strict regulation lasts throughout the whole tissue repair and it is accomplished by the proper coordination of cell regeneration, proliferation, and increase of the collagen production [1, 5]. Due to the complexity and involvement of interactive processes managed by humoral messengers, the hierarchical and timely organization of these events bears critical importance for proper healing [6]. However, these processes are interrelated and not mutually exclusive, therefore, the characteristics of the wound is the determining factor in deciding to which extent a process is involved during the healing [5, 6].

Time is a crucial variable in determining the type of the wound either as acute or chronic. Healing time curve, also known as dynamic healing trajectory is used to evaluate the healing time of the wounds (Figure 1.1). Ideally, wound healing phases are described as lag phase, logarithmic phase, and waning phase. Nonetheless, the involvement of many cell types and processes during the healing has led to various misconceptions [1]. For example, dynamic healing trajectories have guided scientists in the development of novel therapeutics, however, because they are based on the findings of different studies designed to evaluate different parameters there has been lack of consensus over the ideal targeting phase for optimal clinical outcome [7–12]. After careful considerations it has been stated by FDA that “With respect to outcome measurements, complete rather than partial closure of wounds provides the best objective evidence of clinical benefit and therefore is the preferred primary

endpoint." [13]. However, they also included that as long as the therapeutic under evaluation results in patient's benefit, certain indications of end points may as well be taken under consideration during clinical trials [14]. These trajectories provide scientists the whole continuum of the healing process rather than looking at a single point of the healing process of both chronic and acute wounds [4, 15].

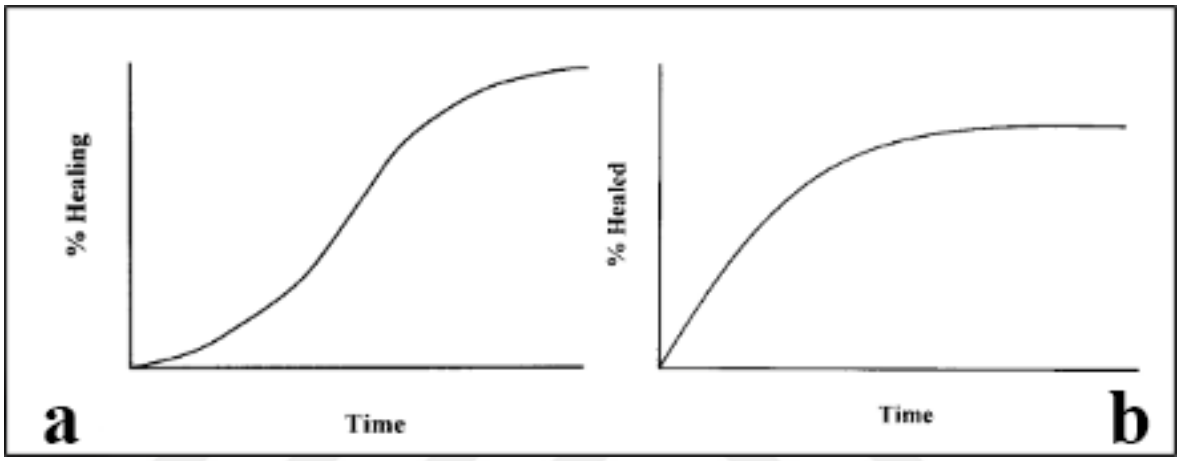

Figure 1.1. Healing curves of (a) acute and (b) chronic wounds [4].

Wound healing involves at least 15 different cell types. Along with inflammatory and immune responses, most of the cellular and physiological mechanisms are originated from the same physiological trajectories [1].

1.1. PHASES OF WOUND HEALING

As it is stated above, wound healing starts right after the wounding occurs involving many cell types, extracellular mediators, and matrices. Even though many of these factors take place in both acute and chronic wound healing, most differ in regards to timing and point of intervention during the repair process [3]. Acute wound occurs in an uninjured tissue after vicious damage and causes loss of function in the tissue. Contrary to the case with chronic wounds in which healing is incomplete and prolonged, acute wound healing is tightly regulated at cellular, molecular, and humoral level [4][16]. Their time of activation begins with the wounding and follows a certain pattern and time sequence throughout the whole

healing process. The sequence of dermal healing process is arbitrarily grouped into inflammation, granulation tissue formation, and remodeling phases.

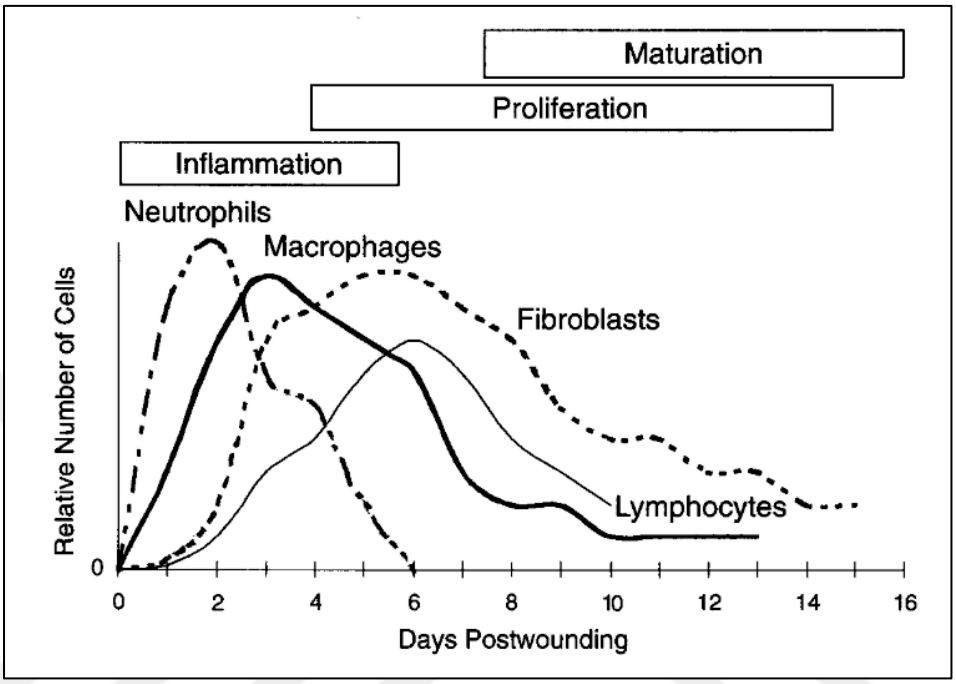

Figure 1.2. Respective time for various cell types to appear during wound repair [17].

1.1.1. Inflammation

Inflammation phase represents the time required for recruiting many cellular elements as well as inflammatory infiltration. The phase starts immediately after the wounding occurs. Upon injury to the vascular network, blood vessels are disrupted which causes bleeding and the outbreak of blood constituents [3]. In order to prevent blood loss, homeostasis is triggered by fibrin clot formation and coagulation [18]. Coagulation and homeostasis are very crucial to prevent exsanguination in order to maintain the tissue integrity of other body parts. Meanwhile, neuroendocrine response mediates the eradication of the injured tissue from the insult site [4].

Platelets that appear at the injury site, are stimulated by thrombin and exposed fibrillar collagens [19]. Collagens serve as a source of proline and hydroxyproline for platelet activation by rapidly adhering to the subendothelial components when the vascular integrity

is disrupted [20]. Once activated, many mediators including von Willebrand factor VIII, thrombospondin, fibronectin, and fibrinogen are released from platelet granules. While others act as ligands, platelet adhesion to fibrillar collagen is arbitrated by von Willebrand factor VIII [21, 22]. Furthermore, release of both thrombin and adenosine diphosphate (ADP) from the existing platelets promotes further platelet recruitment [22]. In order to provide a stable environment for platelet binding, insoluble fibrin matrix is formed by soluble fibrinogen and -therefore- facilitates activated platelet anchorage to fibrin clot via the $\alpha_{IIb}\beta_3$ receptor [23]. All of these events promote platelet aggregation which eventually leads to platelet plug formation [24]. Meanwhile, matrix formed by the conversion of platelet-derived-fibrinogen to fibrin at the platelet aggregation site enhances an inflow of monocytes and fibroblasts acting as a scaffold for the recruitment of other cell types. These cell types may be endothelial cells, neutrophils, monocytes, or fibroblasts [25, 26]. The release of many growth factors and cytokines during wound healing are also controlled by platelets [27].

Growth factors constitute an imperative part of wound repair because they have promoting role in cell migration, proliferation, and intercellular communication [28]. Transforming growth factor beta (TGF- β) epidermal growth factor (EGF), and Platelet-derived growth factor (PDGF) are secreted from platelet granules during clotting and they have a chemotactic and mitogenic impact on both fibroblasts and macrophages that are aggregating at the wound site [29–31]. PDGF is the first growth factor acting as a chemotactic promoting cell migration to the healing wound where its sustained presence for several days after wounding is extremely crucial for the consecutive migration of neutrophils and monocytes [32]. In addition, cellular receptors also execute important roles in responding to certain stimuli. PDGF is also known as an extremely strong chemoattractant for smooth muscle cells and fibroblasts. Nonetheless, chemotaxis of endothelial cells and leukocytes are not affected by PDGF [17]. TGF- β is another growth factor that appears early in the wounding area and it is responsible for triggering fast maturation of collagen and increasing its synthesis even in the initial stages of the wound [33, 34]. Overall, these studies demonstrated that growth factors have predominant roles in the process of the wound repair.

Interleukin-1 (IL)-1, platelet factor-4 (PF4), tumor necrosis factor (TNF)-α, and TGF- β draw in neutrophils to the wounded site [35, 36]. As a result, blood vessels dilate upon the secretion of vasoconstrictors such as prostaglandin 2-α and thromboxane A2 allowing increased cellular trafficking around the wound site. After the coagulation has emerged, capillary permeability increases and leads to matrix protein leakage [37]. Arriving neutrophils in the injury location start clearing the debris and the invading bacteria. Neutrophils succeed this by releasing proteolytic enzymes and reactive oxygen species (ROS) [38, 39]. Towards the end of the coagulation leukocytes produce a wide array of ROS species including nitric oxide (NO), , hydrogen peroxide (H_2O_2), superoxide (O_2^-)hypochlorous acid (HOCl), hydroxyl radical (OH^-), thiyl radicals, and chloramine [40]. Neutrophils remain as the dominant cell type in the injured area until the wound site is cleared from any remaining invading microorganisms and/or debris [41]. Neutrophils produce a sticky, but dynamic surface matrix to be able to hold onto the wound area until their clearance task is complete [42]. After completing their tasks, abundance of neutrophils drastically decrease at the injury site as they are transferred to the wound surface to undergo apoptosis. Further tissue damage is prevented in due to sustained production of ROS [43, 44].

Factor	Concentration	Effect	Mechanism
Platelet-derived growth factor	ng range max at 5–10 ng/mL	↑	
Interferon-γ	1–100 U/mL 1–1000 U/mL	↑ ↓	Lengthening of G_0/G_1 and G_2
Transforming growth factor-β	0.1–1 ng/mL 1–10 ng/mL 0.1–1 ng/mL	↑ ↓ →	Via release of PDGF[121]
Fibroblast growth factor		↑	
Epidermal growth factor	max at 20 ng/mL	↑	
Interleukin-1		↑ ↓	Via release of PDGF
Tumor necrosis factor-α	0–1.2 nM Low High	→ ↑ ↓	Via increase of PDGF

Figure 1.3. Effect of growth factors on fibroblast proliferation [17].

Growth factors, including PDGF, TGF- β, and PF4 are important for attracting neutrophils in the earlier phases. Later on, they contribute to the attraction of circulating monocytes to the damaged site together with leukotriene B_4, nerve growth factor (NGF), vascular endothelial growth factor (VEGF), monocyte chemoattractant protein (MCP)-1, inflammatory protein (MIP)-1α, and collagen [37, 45]. Around 48 or 96 hours post-injury, integrin receptors on monocytes help them attach to the fibrin clot. Thus monocytes will differentiate into macrophages. Activation of macrophages is extremely critical both for moving forward towards the proliferative phase and inducing angiogenesis, collagen synthesis, fibrosis, reepithelization, and synthesize inducible nitride oxide (iNOS) [46–48].

Activated macrophages in wound healing produce nitric oxide, which is renowned for its antimicrobial activity. In addition to its antimicrobial activity, synthesized nitric oxide exerts several important effects for the healing process [49, 50]. Therefore, if needed other cells involved in tissue regeneration such as endothelial cells, fibroblasts, lymphocytes and monocytes may be turned on to generate nitric oxide [51–54]. Strikingly, significantly low levels or absence of nitric oxide have been reported in the impaired wounds suggesting that nitric oxide may contribute to wound healing via its properties other than antimicrobial ones [17, 55]. Activated macrophages also release many enzymes such as collagenases for clearing the wound and they also secrete cytokines such as TNF-α and ILs (IL-1, IL-6, IL-12) to engage fibroblasts in collagen production as well as to promote further macrophage infiltration [56, 57]. At lower doses, TNF-α activate neutrophils and monocytes to induce antimicrobial activity. TNF-α also stimulates proinflammatory cytokines IL-1, and specialized cytokines such as IL-6 and IL-8. If found in excess concentrations, TNF-α activity increases the core temperature and hepatic acute phase protein production [58]. VEGF which is accountable for nearly half of the angiogenesis is also excessively secreted by macrophages [59]. Macrophage activation also triggers lymphocyte activation and in return they release interleukins and interferons (IFN) as a part of paracrine mechanism [58]. As the inflammatory phase starts to fade out, macrophages shift from pro-inflammatory to anti-inflammatory phenotype as they begin to express IL-10, IL-1 receptors to initiate the cell proliferation and granulation tissue formation phases, respectively [60].

1.1.2. Proliferative Phase

Main purpose of this stage is to restore damaged or lost layers of the skin by contraction and fibroplasia. Although there are no strict criteria describing boundaries between the phases of the tissue regeneration process, it is made up of re-epithelization, angiogenesis (re-vascularization), granulation, and contraction. This stage of the regeneration process is the major step for the closure of the lesion and establishing an epithelial barrier of the activated keratinocytes. The start of the proliferative phase is determined by both the decline of the inflammatory response and secretion of growth factors and cytokines by platelets which can typically take place at around 48 hours after the damage and may last up to 14 days [61].

1.1.2.1. Re-epithelization

In order to close the wound, new epithelium needs to be constructed. Re-epithelization phase includes both proliferation and migration of the keratinocytes to the lesion site. The re-epithelization process varies between partial (only epidermal) and full-thickness (both dermal and epidermal) wounds.

In partial thickness wounds, re-epithelization may be initiated in the hair follicles and other skin appendages. Epidermal cells generated by the hair follicles are descendants of the cells resident to the hair bulge which is the germinative portion of the hair. Although, their exact contribution throughout the entire process has not been demonstrated except for their contribution to the acute phase of re-epithelization, this pool of cells of the hair bulge are recognized for their stem cell properties of high proliferation and multipotent differentiation potential [62, 63]. During migration, the proliferative potential of the epidermal cells is inactivated. So far, it is believed that these cells migrate towards the injury site under the influence of “free edge” effect [18, 64]. According to a study conducted with organotypic wound healing model, basal cells were also present in the injury site in addition to retrovirally labeled keratinocytes. This situation is called “leapfrog” [65]. This effect is believed to be activated with the loss of cell-cell interaction which keeps them silent when the skin integrity is intact and keratinocytes are neatly attached to the basal lamina via their anchoring hemidesmosomes [64]. Although major migration and proliferation is initiated

from neighboring epidermal cells during wound healing, the contributory role of hair follicular cells need to be further investigated.

Another explanation to why keratinocytes move toward the wounded area may be due to the fact that keratinocytes at the edge can -not only- differentiate, but also proliferate in response to atypical integrin expression in an intact skin [64, 66]. When the integrity is ruptured, hemidesmosome attachments via the anchoring α6β4 integrins of the keratinocytes to the basal lamina is dissolved, hence they start to express pro-migratory α5β1, αvβ6 fibronectin/tenascin, αvβ5 vitronectin receptors, while relocating α2β1 collagen receptor to pursue migration towards the wounded area [67–70]. Furthermore, the migrating cells alter their expression profile and start expressing the cell surface marker CD 44 and others that are expressed by squamous cells [18]. Additional movements are accomplished through establishing actinomyosin filaments and adhesion complexes [71]. Both fibrin clot established during the initial stages of inflammation as an interface between the wound normal dermis are cleared by the matrix proteins secreted from migrating keratinocytes which at this time start to change their adhesive characteristics [72, 73]. Plasmin, a leading fibrinolytic enzyme, is derived from plasminogen inside the clot and is activated by either tissue-type plasminogen activator (tPA) or urokinase-type plasminogen activator (uPA). Migrating keratinocytes up-regulates these activators [64, 74]. Wound healing also involves various members of the matrix metalloproteinase (MMP) family of enzymes (MMP-1, -2, -3, -10, -14, -19, and -28). MMP-9, which cleaves anchoring fibril collagen type VII and collagen type IV are also upregulated. MMP-9, which becomes highly upregulated in the migrating keratinocytes, plays a major role in freeing keratinocytes from basal lamina as the detachment the keratinocytes from the surface is crucial for proper healing to [75]. On the other hand, MMP-1 levels increase only in those keratinocytes migrating freely at the basal lamina and MMP-10 expression levels are found to be upregulated among impaired wounds [76]. Altogether, these findings suggest that cell-matrix interactions regulate the MMP expression levels, which need to be kept under a tight control to prevent the occurence of chronic wounds. Once the normal homeostasis of MMPs and tissue inhibitors of metalloproteinases (TIMPs) disrupted, wound fails to heal properly and may trigger development of chronic wounds [77]. Once the wound area is covered with keratinocyte monolayer, new stratified epidermis is built up starting from the wound margins, super basal

cells stop producing integrins and keratins and rather enter a differentiation program in the unwounded area [78].

Once the migration ceases, growth factors such as TGF-α, EGF family members, heparin binding epidermal growth factor (HB-EGF), induce keratinocyte proliferation which eventually form an adequate cell supply to close the wound properly. Macrophages and epidermal keratinocytes at the injury site are responsible for the production of these growth factors [79]. Moreover, various studies demonstrated that exogenous application of these growth factors to burn wounds has shown enhanced healing and re-epithelization [80, 81]. The mechanism of action of the growth factors involved in cell motility among fibroblasts and epithelial cells take place via activating guanosine triphosphatase (GTPase) rac *in vitro*[82–84]. In addition to the EGF family, which has been considered as the key regulator for many years, both keratinocyte growth factor (KGF) and fibroblast growth factors (FGF) (especially -2, -7, -10, and -22) are claimed to play a critical roles during epithelization [85]. KGF (also known as FGF2) exerts its effects on keratinocytes through FGF2IIIb receptor and increases mitogenic and proliferative activity [86, 87]. Besides, upregulation of FGF-7 and -10 is thought to assist the clearing the reactive oxygen species from the wound area to prevent ROS related apoptosis in the healing tissues [88]. Moreover, cytokines such as TNF-α, , IL-1α, and IL-6 , induce the proliferation of keratinocytes through different mechanisms [89]. For example, while IL-1α promotes upregulation of FGF-7, IL-6 indirectly affects signal transducer and activator of transcription (STAT)-3 pathway promoting keratinocytes migration [90, 91].

Among all of these growth factors, the role of TGF-β remains debatable. TGF-β, which consists of 3 different isoforms (TGF-β1, -2, -3), are differentially expressed by different cell groups resident to the skin at steady state levels [92]. Although it is known that the expression of TGF-β varies throughout the acute wound healing, there is no clear information on the expression levels of individual isoforms [93]. TGF-β released by keratinocytes is an important growth factor for fibronectin deposition in ECM. Additionally, increase in fibronectin levels may also promote epidermal migration. To the contrary, the

enhanced expression of TGF-β levels results in inhibition of keratinocyte proliferation. This situation also downregulate the TGF-β release in fibroblasts [94–96].

TGF-β also plays different roles in both partial and full thickness wounds. While it is shown to be effective in re-epithelization in partial wounds, surprisingly it displays exactly opposite effects in full thickness wounds where it is inhibiting re-epithelization [97]. In full thickness wounds basement membrane is destroyed, therefore both epidermis and dermis need to be restored. In order to achieve this goal, migration of the keratinocytes alone, which is sufficient to support wound healing in partial-thickness wounds, need to be supported by the epithelial cells located under the skin that -not only- proliferate, but also send out specific signals such as EGF and TGF-α to reconstruct basal membrane as a defensive barrier [98]. For the complete healing of the full thickness wounds, fibroblasts, endothelial cells, and keratinocytes move and divide, granulate and accompanied by proper vasculogenesis. In accordance with these data, role growth factors and that of TGF-β require an in-depth research to understand their role in healing precisely [99].

The degree of keratinocyte proliferation differ for each wound, and depends on the cell differentiation, growth factor availability, and attachment of the cells to the basal lamina [100]. Regardless, the synergy between ECM, growth factors, cytokines, and integrins regulate the keratinocyte proliferation and migration throughout the course of re-epithelization. How and why keratinocyte proliferation stops is still unclear, however, contact inhibition is one of the suggested possibilities. Another candidate that accounts for the cessation of keratinocyte proliferation can be adhesion and re-assembly of formed hemidesmosome to the basal lamina and abrogation of MMP expression. Once the activation of keratinocytes stops and they return to their inactivated forms and start to differentiate marking the beginning of the stratification phase.

1.1.2.2. Granulation Tissue Formation

Approximately 4 days after the wound insult, granulation tissue formation starts with new stroma invading the wound space, meanwhile the keratinocytes go back to their inactivated

phase and form a safe barrier [3]. Epidermis migrates towards the wound from wound margins after type VII collagen fibrils and anchoring hemidesmosomes are formed [101]. Fibroblasts invading the wound site begin proliferating and synthesizing collagen along with another pool of fibroblasts so-called wound fibroblasts which are already present at the wound site. Wound fibroblasts have less proliferating capacity compared to that fibroblasts coming from peripheral tissues [39, 102, 103]. This situation is thought to be because of the lag time needed for fibroblasts to exit the quiescence state [104]. Collagen synthesis by the fibroblasts is induced by TGF-β1 secreted by macrophages and once the fibroblasts starts synthesizing collagen they -themselves- turn into myofibroblasts to facilitate the wound contraction [105, 106]. Furthermore, TGF-β activates K5 and K14 markers specific to the basal cells to reduce proliferation of keratinocytes to revert them into basal cell phenotype [107]. Deficiency in TGF-β levels is shown to suppress granulation tissue formation *in vivo* [108]. In fact, many growth factors at the injury site behave as chemotactants and as mitogens for wound fibroblasts [109]. Autocrine and paracrine signaling among fibroblasts is induced by PDGF and EGF which then trigger the synthesis of structural molecules for the provisional matrix acting as a scaffold for cell migration and attachment [32]. Building blocks of this matrix are collagen type III, fibrin, elastin, laminin, glycosaminoglycans, fibronectin, and hyaluronic acid (HA) [110, 111]. Amount of granulation tissue formation is limited by the available fibrin and fibronectin molecules because fibroblasts rely on fibronectin to migrate towards wound site [110]. Fibroblasts are responsible for synthesizing structural molecules of ECM, therefore they hold an important place in the deposition and remodeling the matrix. Consequently, fibroblasts, which generally reside in a collagen I rich matrix need to re-adjust their collagen receptors to upregulate integrin synthesis that bind vitronectin, fibrin, and fibronectin that are required for fibroblast migration [64]. While macrophages, and platelets continuously supply growth factors, countless new capillaries surrounding the new stroma provide oxygen and nutrients necessary for the cellular metabolism [3]. About a week after the wounding, myofibroblasts start expressing α-smooth muscle actin. Then they become capable of creating strong contractile forces for wound contraction [112].

1.1.2.3. Wound Angiogenesis

Following the fibroblast activation, angiogenesis, formation of the new blood vessels from existing ones, takes place in order to deliver oxygen and nutrients to the wound area and remove waste. Angiogenesis is induced by growth factors released from macrophages such as FGF2 and by vascular endothelial growth factor (VEGF) released from endothelial cells. Both of these angiogenic factors are of critical importance as the lack of FGF2 has been shown to obstruct angiogenesis and the lack of VEGF leads impaired healing in diabetic mice [113–115]. Although VEGF expression levels are quite low among intact skin cells, its expression peaks after the injury due to hypoxia caused from the injury [116]. VEGF is also expressed by macrophages and keratinocytes at the wound site upon stimuli coming from KGF and TGF-α [117, 118]. In order to form new capillaries endothelial cells must be activated for migration towards the wound site, $\alpha_v\beta_3$ integrins at the tips of newly forming capillaries are up-regulated. Therefore, any kind of disturbance to integrin upregulation leads to impaired healing [119, 120]. Furthermore, VEGF receptor 1 (VEGFR2/F1t1) and VEGF receptor 2 (VEGFR2/F1k1) found on endothelial cells are responsible for VEGF activation upon stimuli [121]. Other growth factors such as TGF-β, IL-1, TNF-α, FGF-10, PF-4, and PDGF contribute to the endothelial cell activation [122]. Proliferating endothelial cells at the wound site forms tubular structures and supply blood flow to the area which causes the pink granular appearance [64]. Just like any other migratory movement, proteases are tightly regulated to degrade basal lamina in order to make a way for the newly formed capillaries, a process also known as sprouting [123]. As an ECM protein, laminin is essential for endothelial proliferation and tube formation [124].

1.1.2.4. Wound Contraction

Approximately a 50 percent decrease in the wound size is the result of wound contraction. The contraction takes place when the wound edges start to be drawn to closer to each other [125]. In accordance with this fact, cells organize to minimize the ECM that needs to be re-established [126]. Myofibroblasts which are responsible for the majority of the contractile forces start synthesizing α-smooth muscle actin along with desmin and myosin [127]. Due to their similarities, myofibroblasts are proposed to be morphologically similar to smooth muscle cells and fibroblasts [128]. These actin-rich myofibroblasts constitute the prominent

part of the granulation tissue, thus they are the determining factor on accomplishing a successful wound healing. [18]. When compared to the other cells like endothelium or leukocytes, myofibroblasts strictly regulate their integrin receptor expression for a firmer grasp onto the ECM. Moreover, compared to other cell types they have the ability to align themselves according to wound contraction which allows them to contract just like a muscle [129]. Contractions stimulate collagen type I and III to be pulled towards the newly formed ECM [130]. While collagen type I is the dominant type found on the normal dermis, collagen type III, which is the major type found in the fetal dermis, is synthesized at high levels during healing [131]. Normally, fibronectin fibrils of fibroblasts keep them attached to the ECM via $\alpha_2\beta_1$ collagen transmembrane proteins. These fibronectin fibrils carry the tension most of the time and elongate cordially with actin stress fibers [132]. After the wounding occurs and the fibroblasts start migrating, secreted TGF-β1 and PDGF induce a change in their phenotype transforming them into profibrotic type so that the new collagen-rich matrix can be formed [133]. Collagen is the driving force for pulling up and fixing the tissue during wound closure. Although growth factor stimulation is mandatory for contraction, IL-8 is found to be inhibitory for wound contraction. This situation may explain why prolonged inflammatory phase leads to impaired wound healing [134]. Over all, during wound contraction tissue matrix is organized in a manner to reduce the time required healing and minimizing the wound.

1.1.3. Remodeling

As the third phase of the healing process, remodeling starts approximately 2 weeks post injury and it lasts up to 2 years [135]. The purpose of this stage is to rearrange ECM components, that are synthesized indiscriminately, and to provide maximum strength to the healing tissue which only re-gains 20 percent of their pre-injury strength during the first 3 weeks [3]. While granulation tissue is remodeled, less cellular and vascular scar tissue forms and ECM and cellular components of the wound continuously change throughout this step. Therefore, ECM components at the wound margin substantially differ from those at the wound center both quantitively and qualitatively at any given time. Distance from the wound margin and time passed since the injury are also determining factors for the composition of granulation tissue [6]. However, this stage heavily depends on the tight regulation of synthesis and degradation of collagen. Thus, synthesis of new collagen and the breakdown

of the existing collagens by collagenases are tightly controlled during the conversion of newly formed collagen type III to collagen type I. In normal tissues, collagen type I constitute up to 90 percent of the dermis while collagen type III is limited to 10 percent, 20 percent at most [102, 136]. On the other hand, granulation tissue in healing injuries is composed of up to 30 percent of collagen type III, while collagen type IV has been reported in some studies [137, 138]. Replacement of collagen types is also facilitated with the appearance of fibronectin which assists the phagocytosis of collagen type III [25].

Collagenases are released from different sources including keratinocytes, fibroblasts, endothelial cells, and inflammatory cells [139–141]. Among collagenases, MMPs released from fibroblasts, and endothelial cells in scar tissue help degrade hyaluronic acid and fibronectin in order to reduce granulation tissue to organize the skin tissue for the better. Although these collagenases catalyze cleaving of collagens, they all have different preferences. MMP-1, for example, acts on collagen type III, MMP-8 acts on collagen type I, and MMP-13 is able to cleave all collagen type-I, II, and -III [142]. Furthermore, there is a difference between in the time of releases for these MMPs. While some of them like MMP-8 is preserved in the neutrophil granules and can be released right after injury, others for example MMP-1 needs to be expressed by switching on relevant gene expression [143, 144]. Collagenases are specific enzymes that can cut collagens at specific sites so that they can be more susceptible to further cleavage by other proteases. Hence, a tight regulation of MMPs and TIMPs is mandatory which is controlled by cytokines, ECM, and certain cytoskeleton components [145, 146]. Among cytokines TGF-β1 is responsible for tight regulation of the these collagenases by both inducing fibroblastic collagen production and restricting MMP activity [147].

Later in this phase, just like myofibroblasts, other cells such as macrophages and neutrophils are not needed anymore. Although the exact mechanism of action is not deciphered yet, they leave the wound site and/or some undergo apoptosis [148]. Revascularization in the scar tissue results in less capillary network among mature scars, therefore the wounds look less red over time [148]. Thrombospondin 1 as well as other antiangiogenic factors like Secreted Protein Acidic and Rich in Cysteine (SPARC) peptides is found to play a crucial role in the

revascularization [149, 150]. In the case of a major injury, epithelial stem cells, which are responsible for producing hair follicles and sweat glands, do not re-appear in the scar tissue unlike keratinocyte stem cells, which is able repopulate epithelial barrier indefinitely. In the literature, this phenomenon is described as needing a specific niche or microenvironment for stem cells to live on [151, 152].

All in all, remodeling phase constitute a greater part of the wound healing and many major events such as collagen storing as well as its production and bonding of formed collagens with intermolecular cross-links explains why this phase lasts so long [153]. Regardless, wounds are only able to re-gain at most 70 percent of original mechanical strength that they used to have before the injury [154]. As it was made clear so far, normal response to the injuries are controlled in a timely manner and they are organized neatly throughout the whole process. Despite the unmatched healing capacity of the skin, some injuries especially full thickness wounds end up with scars.

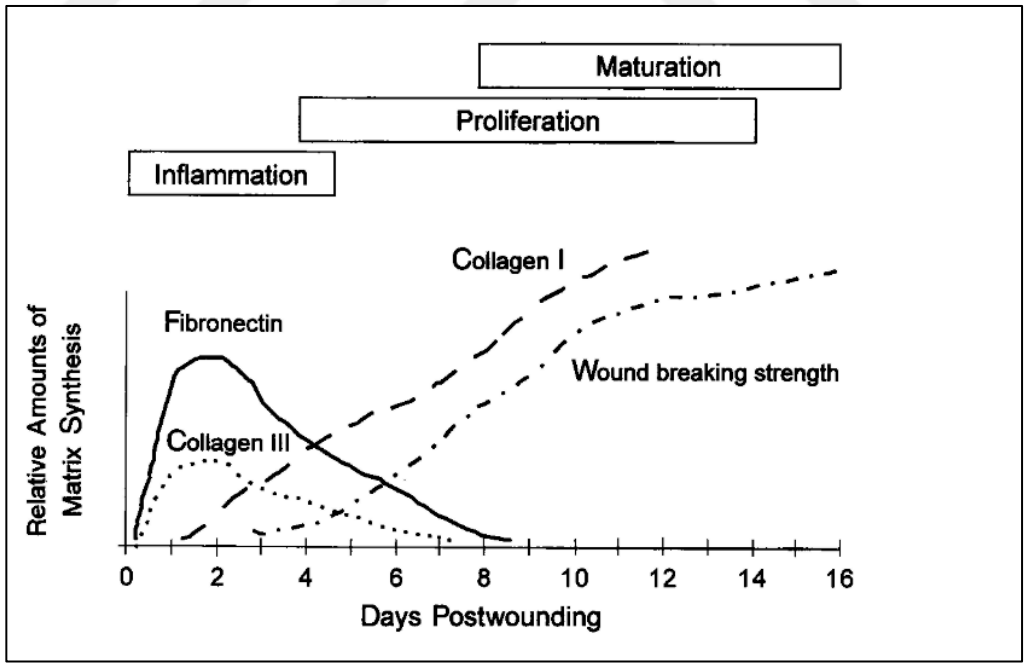

Figure 1.4. Wound matrix components and their deposition throughout the healing time period [17].

1.2. SCARRING

Some adult human wounds may heal with scarring due to dysfunctions in the remodeling phase in order to protect body from infections and dehydrations [148]. These dysfunctionalities generally appear in the two different compartments of the skin, which are epithelial epidermis and the dermis. Excessive synthesis of collagen leads them to be crosslinked anomalously [155]. Two different types of scars known as keloids and hypertrophic scars may be caused from extravagant presence of ECM proteins, myofibroblasts, growth of the scar tissue by activated connective tissue cells or dermis inflammations [112]. Both scar types is pathologically different and possess structurally and molecularly distinct properties. Hypertrophic scars, which are seen after wounding, do not past beyond the wound sites since the excess collagen is reduced over time. However, keloids move beyond the original wound site and they are generally larger [156]. Regardless, the degree of scar formation is unpredictable and depends on the various factors such as race, genetics, sex, age, site of the injury as well as the greatness of the insult [157]. Hypertrophic scars are seen more often than keloids on 4 mm above the skin surface and they develop approximately 6 weeks following the insult and may last up tos 6 months [158]. At first, they appear red but may become pale with age. Loosely arrayed collagen fibers in hypertrophic scars present a wavy but parallel pattern to the epidermis [159]. Contrarily to hypertrophic scars, keloids take up to 3 months to develop and they do not regress spontaneously over time but rather grow like a benign tumor [160]. Although the exact pathological mechanism of keloids are not very well understood, inflammation is prevalent and collagen fibers are randomly scattered and much thicker than hypertrophic scars [161]. Regardless, what these both scar types have in common is the uncoordinated state of cytokine secretion. In order to develop better healing agents, it is important to better comprehend the healing mechanisms of the fetus that provides a unique environment for scarless wound healing [162, 163].

1.2.1. Wound Healing Deficiences Causing Scarring

Functionality of the dermis along with vascular and nervous system in the epidermis are disrupted in scar tissue. Collagen accumulation and their abnormal linkage causes weaker skin. Stimulated by growth factors such as PDGF,TGF-β, and Insulin-like growth facor

(IGF), myofibroblasts and fibroblasts synthesize ECM components and collagen which in the end speeds the scar formation [164]. The balance between synthesis and degradation of collagen is altered in scars resulting in keloids to have 20 fold higher collagen synthesis while hypertrophic scars synthesize up to 7 fold more collagen than that of normal skin cells [165]. Normally, the ratio of collagen type III and collagen type I among skin cells is 1:5 however, this ratio shift to 1:6 in hypertrophic scars and to 1:17 in keloids [161]. Small leucine rich proteoglycan (SLRP) decorin controls the collagen fibrillogenesis by regulating both collagen formation and degradation upon stimulation by TGF-β signalling during wound healing [166]. Decorin binds to TGF-β via the core protein which leads to downregulation of TGF-β production hence less fibrosis in hypertrophic scars [167, 168]. During scarring, decorin levels are downregulated and pro-fibrotic actions of TGF-β signaling pathway persists [169]. As it has been mentioned earlier, TGF-β isoforms show different functions in scar formation. In wound fluid, the major isoform found is TGF-β1, but other two isoforms also contribute the wound healing [170, 171]. TGF-β induces many different pathways during wound healing including but not limited to those related to chemotaxis, remodeling of ECM, and angiogenesis [29]. TGF-β1 is shown to be the most substantial isoform in the scar formation. Fetal mice expressing less TGF-β1 shows scarless healing of the wounds similar to the case in rats which were injected with TGF-β1 and TGF-β2 neutralizing antibodies [172, 173]. In scarless fetal wounds, TGF-β3 expression is upregulated, while TGF-β1 levels remain unhanged. In contrasts, during scar formations, TGF-β1 expression increases while TGF-β3 expression is downregulated [174]. Furthermore, exogenous treatment with TGF-β3 leads to less scar formation. These results suggest that the determining factor for scar formation lies in the relative proportion of TGF-β isoforms [157].

Moreover, to what extent the scar formation will occur is also affected by variety of other specific molecular pathways and factors. For example, ECM components like fibrin-fibronectin levels, tenascin and hyaluronic acid found in ECM components are increased in scars, thus fibronectin production is halted and in return fibroblast migration is delayed [175, 176]. As a major ECM glycoprotein tenascin C is able to both stimulate and inhibit the cell proliferation. Its interaction with fibronectin promotes adhesion of fibroblasts, endothelial cells and many more in order to promote cell migration and contraction to promote scarless

healing [177, 178]. Tenascin C expression is not observed in the scar tissue once the wound contraction is completed [179]. However, during inflammation, fibrosis and neovascularization among excessive scars, its expression is highly upregulated and may prolong fibrosis [180]. Wound contraction occurs when collagen type I is being synthesized and one of the key modulators of this phase is the ubiquitously found seven transmembrane G protein coupled CXCR3 receptors. The receptor stops fibroblast and endothelium migration to the injury site and promotes keratinocyte migration, thus faster re-epithelization [155]. Growth factor induced fibroblastic and endothelial cell migration is stopped by suppressing m-calpain. It has been shown in animal studies that in the absence of this receptor, the wound experiences the regenerative phase over and over again and even undergo through inflammation phase repeatedly leading to the hypercellularity and hypertrophic scarring [181]. Although CXCR3 receptor is expressed by variety of cell types such as fibroblasts, keratinocytes, and endothelial cells, its ligands CXCL10/IP-10 and CXCL11/IP-9 are expressed by different cells in a timely manner. CXCL10/IP-10 is expressed by neovascular and endothelial cells that appear deep in the dermis while CXCL11/IP-9 is expressed by re-differentiating keratinocytes [182]. When CXCR3 signalling is absent, fibroplasia creates a relatively immature matrix, allowing more inflammatory cells to invade the wound area, thus wounds mature more slowly with immature and weakened dermis [183].

Overall, timely penetration of relevant cell types into the wounds is a critical step for regenerative healing with minimal scar formation. Although pro-scarring and anti-scarring mechanisms have been studied intensively in an attempt to achieve minimal scarring, the focus has been shifted to understanding of the molecular and cellular mechanisms of fetal healing that has the ability to heal wounds without any scars.

1.2.2. Fetal Wound Healing

Regarded as an example for scarless healing, fetal wound healing can heal bone and skin wounds in a regenerative manner until gestational week 24. Wound healing process widely differs between adults and gestation stage fetuses which have numerous advantages like amniotic fluid or aseptic environment that may contribute the scarless healing. Regardless,

the most impressive characteristics of fetal healing is the speed at which scarless regeneration takes place and its tissue-specificity [162]. Fetal wound healing diverges from adult healing both quantitatively and qualitatively during the inflammatory and regenerative phases. Molecular processes regarding the ECM components account for these differences. However, following the 24 weeks of gestation, fetal skin repair becomes the same as that of adult [184].

The most striking difference between adult and fetal wound healing processes is acute inflammation. Fetal wounds take place in a sterile, warm amniotic environment rich of growth factors, however this alone is not sufficient for scarless healing since among the late stage fetuses scarring still occurs [134]. Fetuses have relatively lesser platelet degranulation and aggregation to the wound site for minimal acute inflammatory response that consists of mainly macrophages and lesser extent lymphocyets and leukocytes. Reduced inflammatory response results in reduced phagocytic activity hence a small amount of neutrophils invades the wound site. Additionally, fetal platelets reduces the amount of TGF-β1 and fibrogenic PDGF production which in the end contribute to scarless healing [185]. Additionally, TGF-β1/TGF-β3 ratio is less in fetal wounds. Regardless the different isoforms, they all bind to the same receptors TGF-βRI and TGF-βRII. Among fetal wounds, TGF-β3 is expressed in greater amount while TGF-β1 and TGF-β2 expressions are downregulated. Up-regulated TGF-β3 expression suppresses the inflow of the macrophages and monocytes to the injury site while increasing the expression of fibronectin and collagen. Regardless, increased levels of TGF-β1 leads to scar formation even in fetuses.[186]. Moreover, pro-inflammatory chemokines such as IL-6 and IL-8 are reduced while anti-inflammatory cytokines such as Il-10 are highly expressed in fetal wounds [187, 188]. Availibility of stem-like cells are another aspect of scarless fetal wound healing.

Fetal ECM events, on the other hand, constitute a big part of scarless wound healing, including cell adhesion, differentiation, and proliferation. One of the noteworthy differences is the proliferation rate of fetal fibroblasts which proliferate faster and migrate upon both intrinsic and extrinsic signals [189]. As fibroblasts migrate to the insulted area and lay down ECM components like collagen type III, fetal fibroblasts possess a more secretory

phenotype, therefore they perform better in coordination compared to the adult fibroblasts [190]. Collagen synthesis as well as its deposition and crosslinking patterns also differ between adults and fetuses. The ratio of collagen type III over collagen type I in the healed fetus wounds is 3:1 however, this ratio is 1:3 in adults [191]. Fetal wounds deposit collagen type III in a fine reticular network that is identical to the pattern found in the uninjured skin. Increased collagen type I in adult wounds provide strength to the wound however this hinders cell migration [192]. Moreover, the high ratio of MMP over TIMP favors remodeling and ECM degradation over ECM deposition in the wound site [193]. Additionally, fetal fibroblasts also express more glycosaminoglycans such as HA which stays in the wound site for longer periods of time and makes the fetal wounds softer. High level of HA is important for scarless healing as it enables a higher rate of growth factor and cytokine binding in the ECM [194, 195]. Softness of the ECM leads to a mesenchymal pheotype which increases the survival rate of the cells and drive a scarless healing . Although proteoglycan levels such as that of SLRP decorin increase upon injury among fetal wounds, their concentration is still less than that found in adults [195, 196]. Along with decorin, fibromodulin which is another modulator of collagen fibrillogenesis, possesses antiscarring properties by suppressing TGF-β activity [197]. Earlier deposition of tenascin C also contributes to the rapid re-epithelization hence reducing inflammatory cell appearance. While cell movement is facilitated by tenascin, fibronectin which appears approximately 4 hours post-injury in fetuses, facilitates anchoring. On the other hand, fibronectin appearance is not seen until 12 hours after the wound occur in adults [198]. Prostoglandins, which control various aspects of inflammation, are mediated by cyclooxygenase-2 (COX-2). Low levels of COX-2 and prostaglandin-2 (PGE2) is observed at relatively low levels [199].

1.3. CHRONIC WOUNDS

In chronic wounds, cytokines, growth factors, proteins, and several types of cells responsible in healing are not organized as in the case of acute wounds. Compared to acute wounds, less amount of growth factors are secreted in chronic wounds in a prolonged inflammatory phase [200]. Chronic wounds have poor functional and anatomic outcomes and they are mostly recurrent in 70 percent of the patients. Chronic wounds approximately last up to 13 months and decrease the quality of life [201]. Majority of chronic wounds are associated with venous stasis ulcers, , diabetic ulcers resulting from diabetes mellitus, pressure necrosis, and

vascular insufficiency [16]. Diabetic ulcers, for example, arise in diabetic patients who are unable to sense and relieve their cutaneous pressure. Diabetic patients usually have significantly high blood glucose and are severely immunocompromised [135]. Moreover, ischemia seen with this disease reduces the oxygen and nutrients provided to tissues, and predisposes to infections due to impaired chemotaxis [202].

Since MMPs are pivotal in cleavage of collagen and elastin, altered MMP expression levels is frequently encountered to contribute chronic wound development and many other vascular diseases [203]. Enhanced MMP activation also degrades PDGF and other vital growth factors. Moreover, chronic wounds have reduced TIMP levels which inhibit MMPs [204]. the prolonged inflammatory phase that causes increased inflow of macrophages and neutrophils to the wound site is one of the implications of the chronic wounds [205]. These pro-inflammatory cells promote hyper-induction of pro-inflammatory cytokines such as TNF-α, IL-1, and IL-6. Degradation of newly formed ECM is also facilitated by ROS which are being produced in high numbers by immune cells [206]. High levels of proteases, degradation of ECM, reduced growth factor levels in the wound area, and prolonged inflammatory response are major causes of the chronic wounds thus, its treatment includes modalities such as applying ECM, growth factors, , skin engraftment, and negative pressure wound therapy (NPWT) [207]. However, all of these novel therapies are highly costly. Therefore, factors contributing to the chronic wound development need to be better understood in order to obtain complete healing.

1.4. FACTORS AFFECTING WOUND HEALING

Since wound healing process consists of many integrated phases, many systemic and local factors may interfere with this process. While local problems are directly related to the wound itself, systematic problems are related to the overall health status of the individual [208]. Regardless, systematic factors that are contributing to the pathology of the chronic wounds act through the local factors.

1.4.1. Local Factors That Influence Wound Healing

Local factors, which may delay the normal wound healing process, can be divided into oxygenation, foreign body, infection, and venous sufficiency.

1.4.1.1. Oxygenation

Cell metabolism during wound healing as well as the energy production by ATP is highly depended on oxygenation. Moreover, tissue oxygenation is needed to prevent the inflammation via increasing superoxide production which is a requirement to kill the pathogens. Therefore, efficient elimination of pathogens is heavily depended on available oxygen [209]. In addition, oxygenation promotes neo-vasculogenesis, activates the cells needed for healing, and ensures required cell migration to the wound [210].

Since vascular system is damaged during injury, hypoxia is inevitable in wounds at a time when neighbouring metabolically active cells require high amounts of oxygen. In addition, several systemic conditions such as advanced age or presence of a diabetic condition may lead to improper oxygen inflow due to damaged vascular integrity. Therefore, it is not a surprising fact that chronic wounds also develop during highly hypoxic conditions [211]. Hypoxic wounds creates an oxygen gradient between the wound and the nearby undamaged tissues. This gradient promotes the oxygen diffusion to the hypoxic tissue [209]. Oxygen gradient starts from the wound centre where hypoxia is found most densely and gradually decreases towards the edge of the wound [212]. Although temporary hypoxia induces wound healing, prolonged hypoxia caused by systemic conditions leads to delays in wound healing. Production of cytokines and growth factors by the macrophages are also induced by hypoxia. In response to hypoxia, PDGF, VEGF, TNF-α, and TGF-β are produced and they stimulate cell proliferation, migration, and chemotaxis. Cytokine production as well as other metabolic fuctions also depend on the availability of ATP produced by glycolysis. However, in the subsequent stages of the healing process, cells switch to oxidative phosphorylation for ATP production. Additionally, ROS production in the form of hydrogen peroxide (H_2O_2) or

superoxide (O^2) increases during both hypoxic and hyperoxic conditions and it stimulates cell motility and angiogenesis [213].

Oxygen availability is crucial for sustaining the healing, however, hypoxia occurs naturally in all wounds. Besides, hypoxia controls cytokine and growth factor release as well as initial ROS production. Hyperbaric oxygen therapy (HBOT) is one of the theraupeutic options to overcome hypoxia, however, its availiability is limited and its effectiveness require further study [208]. Optial levels of oxygen for an effective wound healing need to be determined in future clinical studies.

1.4.1.2. Infection

Underlying skin compartments become susceptible to microorganisms once the skin integrity is disrupted. Although inflammation phase of the wound healing eliminates any remaining invaders from the wound site, sometimes this phase fails and microorganisms may proliferate inside the wound and cause infection. The infection may spread to the other uncontaminated tissues during invasive infections [214]. Contamination refers to the situation when the microorganisms in the wound site do not replicate during sustained colonization resulting in a limited number of microorganisms producing biofilm. Local infection occurs when the microorganisms infect the granulation tissue only [215]. Bacterial invasion and endotoxins lead to a prolonged inflammation phase and -hence- prolonged manifestation of interleukin-1 and TNF-α (pro-inflammatory cytokines). In the continuous presence of these cytokines, the wound becomes chronic and cannot heal. As the inflammation step lasts longer, MMP levels also increase and they start to degrade the ECM while levels of TIMPs decrease. In this mayhem, growth factors degrade [216].

Host response is usually the determining factor for the outcome of microbial infections as all of the inflammatory cell activity, pathogenicity, virulence, and number of microorganisms at the wound site depends on it. Higher than 10^5 CFU/gr tissue in an intact skin generally signals microbial infection. Some bacterial species such as β-hemolytic may cause infections even under 10^5 CFU/gr tissue since they have a high virulence factor [217].

Some biofilms form more protected microenvironments, therefore raise the antibiotic resistance. Due to increased resistance and protection provided by firmer biofilms, the bacteria from the phagocytic activity exacerbate the development of chronic wound [218]. *Pseudomonas* spp. and *Staphylcoccus* spp. are both found in acute and chronic wounds. Specifically *Pseudomonas* spp. form biofilm layer containing polysaccharides, nucleic acids, and proteins [219].

It is crucial to prevent chronic wound formation that result from infections and prolonged inflammatory response. Therefore, microbial contamination needs to be removed from the wound site either by using antibiotics or other therapeutic interventions such as use of silver containing byproducts. Major side effects of these treatments such as antibiotic resistance or silver toxicity are burdens that need to be dealt with in order to revert microbial infection [220]. Aside from bacterial infection other foreign body formations caused from fungal infections are also present in burn wounds. Mortality rate of the fungus infection is rather high. On the other hand, the number of available antifungal agents is limited [221]. Therefore, there is an immediate need for novel antimicrobial and antifungal agents.

1.4.2. Systemic Factors Influencing Wound Healing

personal factors such as age, nutritional habits, sex, and the presence of comorbidities of the individual are directly related to systemic factors which are related neither to the wound itself nor its location.

1.4.2.1. Age

According to the World Health Organization (WHO) elderly population, a term that is used to describe people of age of 60 or over, is growing fast than any other age group due to improved medical conditions. Increased age is a major risk for impaired wound healing as age related changes at the cellular level cause delays in wound healing. However, these delays are time-dependent only, therefore, they do not affect the quality of the healing [222]. Inflammatory response is considered as the major retarding factor because it results in

subdued T-cell infiltration into the wound area, reduced macrophage activity, and altered chemokine production with the increased age [223]. According to a study, where old and young mice with no other systemic differences were compared in their wound capabilities, old mice suffered from poor skin tensile strength, poor growth factor release, decreased cell proliferation rate, and delayed cell activation compared to younger animals. Increased age also impedes collagen synthesis, angiogenesis, and re-epithelization [224]. Although each phase of the wound healing characteristically changes with the increased age, conflicting results have been reported for the inflammation phase. Alpha granule release including TGF-β, TNF-α, and PDGF increases with age while nitric oxide release and vasoactive mediator amounts decrease. Both platelet adherence to the endothelium and -hence- their aggregation is enhanced with age. Even though leukocytes secrete more inflammatory mediators with the increased age, leukocyte proliferation decreases with the same parameter [225, 226]. On the other hand, in the proliferative phase, endothelial cells, keratinocytes, and fibroblasts have rather decreased proliferation rate in aged animals [227]. Collagen synthesis and turnover, angiogenesis, wound strength, and re-epithelization rates are either reduced or delayed with the increasing age [224].

1.4.2.2. Chronic Diseases

Chronic diseases such as cancer, coronary artery disease, diabetes mellitus, peripheral vascular disease compromises wound healing. Diabetic patients suffer from impairments in acute wound healing and nearly 15 percent of these patients are prone to developing chronic diabetic foot ulcers (DFUs) [208]. Several extrinsic factors such as infection, callus formation, neuropathy, pressure, vasculopathy, and trauma contribute to formation of DFUs. Moreover hyperglycemia and resulting ROS production from hypoxic conditions also contribute to extensive cellular and tissue damage. Impaired wound healing during diabetic conditions are also linked to the formation of advanced glycation end-products (AGEs) and their receptors (RAGE), especially under hyperglycemic conditions [228]. AGEs produced under hyperglycemic conditions lead to improper ECM formation which as a result prevent the docking of the immune cells, cell migration, and collagen formation. Tissue destruction in DFUs is usually aggravated by the skyrocketed MMP levels which are usually 60 times higher than that of normal acute wounds [229]. Further tissue damage occurs via production of excessive Protein Kinase C that promotes DFU formation by fuelling further ROS

production via nicotinamide dinucleotide phosphate oxidase (NADPH) [230]. Abnormalities in the immune system also contribute the formation of DFUs such as degenerated chemotaxis of leukocytes, dysfunctionalities in fibroblasts and epidermal cells. Abnormalities in these mechanisms make the wound susceptible to bacterial invasion and delayed healing among diabetic patients [231, 232]. Among diabetic patients and *in vivo* animal models, chronic inflammation, decreased levels of growth factors, dysfunctionalities in angiogenesis, inadequate granulation tissue, and collagen formation are common. In contrast to acute wounds, diabetic ulcer fibroblasts have little proliferative and migratory properties [233]. VEGF secretion, levels of PDGF, IL-8, IL-10, IGF-1, iNOS in keratinocytes and endothelial cells are downregulated in DFUs [234, 235]. All of these factors discussed above contribute to impairment of wound healing among diabetic patients.

Apart from diabetes mellitus, venous insufficiency is an important systemic factor leading to impaired wound healing. Chronic venous insufficiency is the leading factor contributing to the lower ulcers [236]. Defects in blood flow direction and pressure diminish the effectiveness of the valves which in the end results the accumulation of blood in the lower leg since the blood can no longer circulate away from the site. Overloaded blood in deep veins harasses the muscles in the area and the resulting chronic hypertension, which is a gateway to the venous ulcer formation, occurs [237]. Hypertension widens the capillary pores allowing the fibrinogens leak through and form an outer layer that prevents nutrient and gas exchange. In the end necrosis, ischemia, and ultimately ulcer develop. Accumulated leukocytes, on the other hand, produce high amounts of proteases and inflammatory cytokines such as TNF-α that increases inflammatory response.

Obesity has been an exponentially growing health issue over the past three decades. Risk of having co-morbidities such as heart failures, diabetes, cancer, stroke, sleep apnea and hypertension increases with obesity [208]. Obese patients face many complications such as infections, hematoma seroma, and ulcers. With increased weight, skin starts to fold over on itself and the moisture between these folds provide an ideal habitat for microbial growth and damages the tissue. Prevalence of infections in obese patients is rather high due to cytokines released from adipose tissue [238]. There are high numbers of pressure related ulcer and

injuries in obese individuals due to hypo-vascularity and ischemia. Oxygen supply is usually not efficient therefore anoxygenic conditions may be observed under subcutaneous adipose tissue due to poor vascularity which also prevents the delivery of sufficient nutrient supply [239, 240].

1.5. PRESENT WOUND HEALING TECHNIQUES AND POTENTIAL CARE

Skin forms a protective barrier for the tissues and organs underneath from the exterior damage. When the skin integrity is disrupted, wound healing mechanisms take place in order to restore the integrity. Acute wounds that heal normally does not require intensive medical care. However, cases of non-healing wounds caused by chronic diseases that impose an enormous burden to the healthcare systems and the economy, is now an epidemic since the number of these patients are increasing more than ever [241]. In the light of findings from recent studies, better perceival of the molecular and cellular details of the healing cascades offers new promises for the development of novel therapeutics. Current treatment methods include administration of cytokines, growth factors, stem cells, and other small molecules with the assistance of the light sensor technology that provides a high-resolution detection of the wound environment.

1.5.1. Standard Wound Healing Procedures

Current wound healing methods are generally used for the treatment of chronic wounds and they are generally used in combination with conventional healing modalities. Current methods involve skin autografts, wound dressings, and tissue engineering.

1.5.1.1. Skin Autografts

As a gold standard, split-thickness autograft entails harvesting full thickness tissue from a donor. According to the studies conducted on this very subject, healing time lasted over a 6-week-period, excluding the 4 weeks required for preparation of the split-thickness autograft [242]. Although the benefits of this method for the healing of chronic wounds are far better than those offered by others, this method comes with several downsides such as the obvious

scarring and frequent contraction of the wound area which are inversely related to the amount of dermis delivered to the area [243]. Besides, complications such as pain and infection as well as limited amount of available donor skins especially in cases where greater than 20 percent total body surface area is required for the treatment make this treatment option deficient [244, 245]. Another complication with the skin substitutes arise when the donor skin is mismatched with the patient's age and proliferation rate of the cells [246]. In order to eliminate problems caused from split skin autografts, cultured autologous grafts have been developed. For this purpose, keratinocytes are of great advantage as they both respond and secrete their own growth factors and other modulators for signalling and growing [247]. Studies showed that cell proliferation is high in patients aged between 22-27 years old compared to that of adults who are 60-82 years old. Moreover, fetal foreskin keratinocytes are able to grow and proliferate in response to growth factors secreted by other new-born cells [246, 248]. Contrarily, proliferation of adult keratinocytes were proven to be limited when they were incubated in a new-born conditioned medium and similarly new-born keratinocytes were not stimulated to proliferate in an adult cell conditioned medium [246]. These studies prove that responsiveness of the cells and aging are strictly related to one another and this relation between the two affect the healing time [249]. As a treatment method for the chronic wounds, autografts consisting of cultured autologous keratinocytes were first used clinically in 1981. In this method, cells were harvested via biopsy, and grown *in vitro* in a 3T3-fibroblast-cell-conditioned medium supplemented with other growth factors [250][251]. Healing time of the wounds estimated to last for about 3 to 4 weeks and these cultured autologous grafts can be used for both acute and chronic wound treatment with no further complications such as rejection [252, 253]. Regardless, the success of the grafts rely on the attachment of the exogenous keratinocytes to the basement membrane since non-attached grafts cannot proliferate and differentiate [254]. Although infection was commonly seen among 40 percent of the patients, nearly 30 percent of the leg ulcer patients benefited from this treatment [255]. However the side effects of this treatments such as infection rate should not be underrated [256].

1.5.1.2. Wound Dressings

As a common practice, several methods such as cotton, synthetic bandages, gauzes have been used in the treatment of wounds. Major objective of these applications are to prevent

infection and keep the wound area moisten. With the help of advancement in the technology, new dressing methods provide optimal conditions for oxygen circulation, antimicrobial surface, and moisture for the wound environment [257]. Scaffolds have gained more of an interest recently, because they have great compatibility with the skin cells. There are several biocompatible types of scaffold systems. Currently, chitosan, hyaluronic acid, collagen, and silicon-based dressings are available in the market and other potential biomaterials such as gelatine, cellulose, and hydrocolloid dressings are being studied for potential usage [258, 259]. Problems encountered during skin engraftment have given rise to developments in wound dressings as they are used as carrier mediums and they also ease the wound contraction, ulceration, and blistering at the wound site. As mentioned before, hyaluronic acid (HA) is found in the ECM and made up of disaccharide units. Although HA is used for drug delivery method for various therapeutic approaches, biodegradation and biocompatibility of the hyaluronic acid support cell growth and proliferation [260, 261]. Studies showed that in order to promote cell growth and proliferation, HA must be broken down, because the biodegradation by-products of HA promote to epithelial cell proliferation [262, 263]. When in intact, HA facilitates cell movement and cell migration during wound healing. Another thing to consider when using HA as a wound dressing is its molecular weight. While low molecular HA was shown to be pro-inflammatory, high molecular weight HA also prevent the nourishment of the regenerating wound area. Medium molecular weight HA is considered beneficial for wound treatment because it upregulates adhesion molecules during the treatment [264, 265]. Although HA treatment is highly beneficial for nearly 79 percent of the DFU patients, its usage is limited among high risk patients [266].

Collagen is also used for wound dressing as biobrane dressings for burn patients. The nature of this dressing allows blood clot formation and sera around the injury in order to increase re-epithelization [267]. Despite numerous advantages including the decrease in the healing time for up to 5 days, utilization biobrane dressing clinically is limited since it fails to decrease inflammation. Additional studies showed that in addition the its high prices, biobrane is also associated with increased infection rates [268, 269].

Hydrogels, as an important dressing type, are made up of water and swellable polymers. They can also stimulate various part of wound healing process and are sustainable on wounds. A dressing should also be able to provide water permeability and moisture to retain the wound fluid so that microbial infection can be prevented. Different kinds of wound dressings have been introduced lately and they are shown to have healing capacities for acute and chronic wounds [270]. Novel formulations for chemicals and substances are constantly being improved as the dressing materials currently used in the clinic is only providing a suitable environment and removing the waste from the wound area.

1.5.2. Potential Wound Treatment

All of the healing precautions mentioned beforehand require repeated processes not to mention exposing cells to the high concentrations of the active molecules. Although enhanced therapeutics allow a controlled release while sustaining these active molecules, the problem is not fully solved. Therefore, use of growth factors, cytokines, and other active ingredients have been incorporated into scaffolds and dressings.

1.5.2.1. Growth Factors and Delivery of Other Molecules

Macrophage and neutrophil recruitment to the wound location are managed by platelets and their growth factor secretion. When they bind to ECM, they are transformed into macrophages and start to secrete interleukins, TNF-α, FGF-2, IGF-1, TGF-β, PDGF, and VEGF [256]. For the treatment of DFU, gels containing up to 3 dosages of the PDGF has been approved by the FDA [271]. Despite its controversial results, utilization of PDGF gel have spurred an interest in growth factor enriched dressing/scaffolds. There are numerous different growth factors involved in wound healing. FGF family, for example, has 23 different members and among this family, only FGF-1, -2, -7, -10, and -22 are associated in the healing process through activation of Ras/MAPK, PI3K/Akt pathways [3]. FGF loaded collagen sponge enhanced healing time 24 percent for chronic traumatic ulcers and the sponge also enhanced the wound closure rate by 68 percent within 21 days [272]. In a similar study, FGF-2 has been integrated into chitosan film and found to be effective in wound contraction, granulation tissue formation, and re-epithelization [273]. TGF-β family, on the

other hand, have more than 30 members but only TGF-β1, TGF-β2, and TGF-β3 are proved to be involved in the healing and display opposing results in regards to scarring. Regardless, wound contraction and re-epithelization in acute wounds in rabbits was improved by TGF-β integrated collagen scaffold application [274].

In addition to growth factors, inflammatory mediators are also targeted in chronic wounds. In contrast to growth factor delivery, gene delivery is more stable and lasts longer. Gene delivery is a more effective option since growth factor delivery may fail due to their degradation and metabolic inhibition. Gene delivery is performed either *in vivo* or *ex vivo* conditions via transient expression with episomal vectors (non-viral vectors) or integrating the target gene to the host chromosome which is more stable [275]. Gene delivery when performed with viral vectors has some risks, including promoting carcinogenesis, mutagenesis, and boosting immune responses [276]. However, viral vectors have more efficiency and infectivity rates in contrast to non-viral vectors which are generally used during clinical trials. Inhibition of inflammatory mediators can be accomplished via small interfering ribonucleic acid (siRNA) sequence specific gene delivery systems [277]. For example, tumor suppression gene (p53) and pro-inflammatory genes (SMAD3) can be silenced around the wound site to assist healing [278, 279]. Moreover, microRNA-based targeting is being studied as a potential therapeutic. microRNAs are small non-coding RNA molecules that regulate gene expression post-transcriptionally. They can bind to messenger RNAs (mRNAs) and control their translation, alternatively they can also target mRNAs for degradation [280, 281]. Even though gene therapy offers many advantages, including controlling the location of gene delivery, this system still requires many optimizations and safety to be used in clinically.

1.5.2.2. Stem Cells in Wound Repair

Stem cells described as self-renewed, proliferating cells and are capable of differentiating into different cell types. Stem cells derived from bone marrow, umbilical cord blood (UCB), foreskin cells, and peripheral blood are good candidates for treating acute and chronic wounds as they are able to replace lost or damaged tissue. Stem cells also contribute to the cellular functions through paracrine signalling in chronic wounds. In addition, mesenchymal

stem cells (MSCs) were demonstrated to improve healing, promote angiogenesis, and granular tissue formation [282, 283]. Due to difficulties in harvesting bone marrow stem cells, researchers shifted their focus on other types of stem cells such as induced pluripotent stem cells (iPSCs) and embryonic stem cells (ESCs). These type of cells are shown to be effective for skin regeneration. Embryonic stem cells, however, exhibit high incidence of pluripotent activity that last through several passages *in vitro*. Due to their high pluripotency, ESCs were hypothesized to promote healing by the proven means of paracrine signalling and differentiation into the lineage found in both epidermis and dermis to reconstitute a complete skin [284, 285]. However, there are several ethical and legal controversies about the clinical use of ESCs, therefore they cannot be used for clinical studies. Instead of ESCs, iPSC has been introduced in order to eliminate issues that arise from clinical use of ESCs. Nonetheless, the reprogramming capacity of iPSCs is not as efficient and they may cause carcinogenesis in patients [286]. Therefore, regarding the ethical guidelines MSCs from adult tissues are the safest option for skin regeneration. Among mesenchymal stem cells, adipose derived stem cells (ADSCs) are very popular due to the convenience in their isolation and high abundance [287]. Seeded on a cell-derived matrix, ADSCs induced wound healing, vasculogenesis, and angiogenesis among full thickness cutaneous wound models in murines and they also show reduced scarring [288, 289]. Umbilical cord blood (UCB) derived stem cells appear as an alternative source. These stem cells were tested on dermal cells and they were shown to differentiate into keratinocytes effectively [290]. Several studies performed with different types of stem cells proved that while some stem cells like ESCs are superior for wound treatment, other types like UCB stem cells are much more effective in chronic wound treatment [291].

Encouraging findings with stem cells have led scientists to incorporate them in the formulations of dressings and scaffolds to promote adhesion, migration, and proliferation. Further investigations are being carried out to isolate, characterize, and deliver stem cells to the wound area. Whether pluripotent or multipotent, stem cells may solve the major problem of impaired healing and scarring of wounds. Even though MSCs have much to offer in this regard, their safety and ethical utilization must be kept in mind like it is the case of iPSCs and ESCs in terms of the judicial concerns regarding their use in the clinic. Thus, there is an

increasing demand for cost effective, novel, safe, user friendly, and accessible wound healing agents.

1.6. EXTRACELLULAR VESICLES

Nearly all cell types secrete lipid-bilayered extracellular vesicles (EVs). Main purpose of EVs is to deliver specific cellular cargo by acting as cellular messengers. The cargo that EVs carry vary based on the conditions of the cells. Therefore EVs have the potential to alter characteristics of other cells as well [292]. Extracellular vesicles that perform cellular communication are divided into exosomes, small vesicles, apoptotic bodies, large oncosomes, and exomeras. These EVs are found in large quantities among body fluids, such as saliva, blood, breast milk, and they are defined by various overlapping definitions based on their biogenesis [293]. Among all the extracellular vesicles exosomes is the class that has been most intensively studied.

1.6.1. Exosomes

Exosomes carry lipids, mRNAs, proteins, and have a membrane made of lipids. Although when first discovered 3 decades ego, exosomes were thought to be garbage bins which are removing redundant proteins of the cells are now thought to be new promising therapeutic agents [294]. The importance of the exosomes were first recognized with the discovery that their content may be taken up by other cells. Later on it was discovered that the cell-to-cell communication executed by exosomes were to play a major part in pathology of several diseases such as neurodegenerative disorders, diabetes, liver disease, and many more [295, 296]. Recently the relationship between cancer metastasis and exosome relation has been discovered.

1.6.2. Exosome Biogenesis & Exosomal Content

Underlying mechanisms of exosome biogenesis is not completely defined, however, several pathways related to its biogenesis has been discovered.

Due to their morphological resemblance, exosomes are generally and interchangeably referred as multivesicles bodies (MVBs) in various research papers. However, vesicles with the size of 30-150 nm are defined as exosomes while vesicles between 100-1000 nm are considered as MVBs. Regardless, exosome biogenesis start with inward budding of membranous endosomes and then they are released into plasma membrane which is now they turn into early endosomes. Early endosomes later on turn into multivesicular bodies by the accumulation of intraluminal vesicles (ILV) which contain , nucleic acids, proteins and membrane associated molecules. These ILVs are rich in tetraspanins like CD9 and CD63 and these ILVs are controlled by endosomal sorting complex required for transport (ESCRT). Cargo sorting of the exosomes requires the presence of ESCRT. After maturation, MVB are either transferred to membrane for fusion and exosome release or they are sent to lysosome for lysosomal degradation [297].

Exosomal content differ for each cell type. ExoCarta database contain the most recent version for exosomes coming from different background and origins. According to this database, exosomes contain 9769 different proteins, 3408 mRNA, and 1116 different lipid content [298]. Although specific protein content vary for each individual cell, some proteins like fusion proteins (tetraspanin, integrins), membrane trafficking proteins (Rab proteins, GTPases), MVB formation related proteins (ALIX, TSG101), chaperones (Heat shock proteins HSP-60, -70, -90) are augmented in exosomes [299]. Even though exosomes are indirectly generated from the plasma membrane, their protein content is determined according to their cell of origin where they are secreted from. For instance, antigen presenting proteins are found in greater extent in antigen presenting cell derived exosomes and molecules while tumor derived exosomes are rich in tumor promoting proteins.

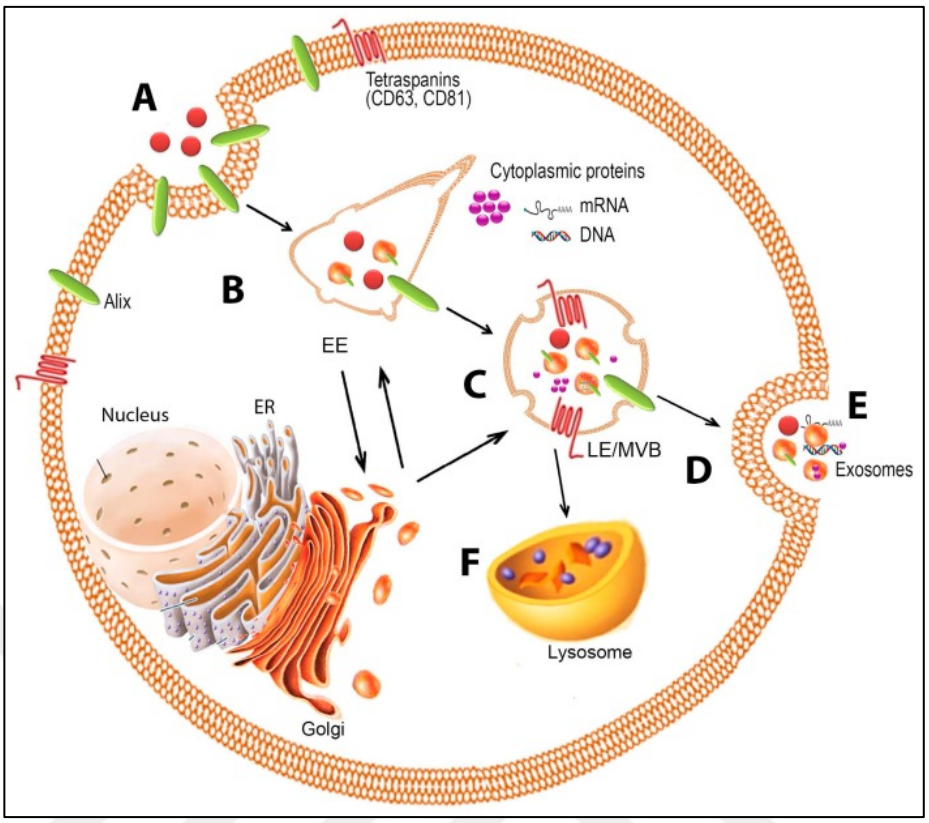

Figure 1.5. Cellular perspective of exosome biogenesis and release [294].

In addition to proteins, exosomes are also rich in lipids in the form of cholesterol, diglycerides, glycerophospholipids or glycosylceramides and therefore they are excellent lipid carriers [300]. There are reports suggesting that lipid content of exosomes like docosahexaenoic acid and lysophosphatidylcholine promote antigenic capacity of dendritic cells. In contrast, if exosomes are high in prostaglandin PGE2 levels, they are found to contribute tumor evasion and promotion [301].

Just like lipids and proteins, functional RNA content of exosomes are also important for their functionality. These RNA molecules can be mRNAs, miRNAs, and lncRNAs [302]. It has been shown that functionality of miRNA are especially preserved in recipient cells. Functionality of miRNA are especially important since some exosomal pathways may therefore eliminate tumor-suppressor miRNAs that block the development of tumor metastasis [303].

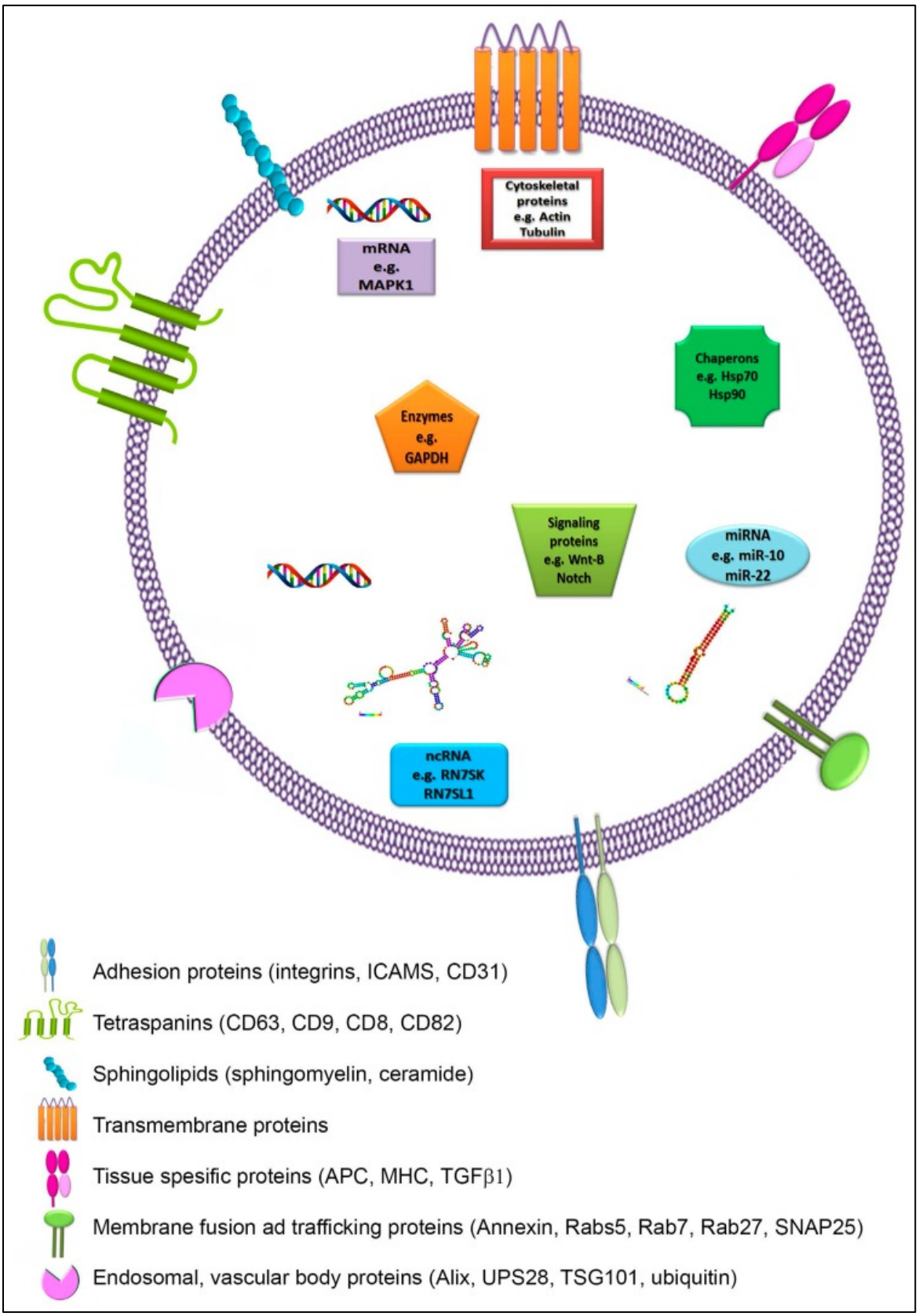

Figure 1.6. Molecular composition of exosome [294].

1.6.3. Mechanisms of Uptake of Exosomes

Exosome biogenesis is poorly understood; therefore exosomal uptake is still open for debate. Whether it is cell type-specific or involves membrane fusion in the form of endocytosis needs further investigation. So far many theories have been suggested including but not limited to antigen recognition, juxtacrine signalling, fusion, phagocytosis, and micropinocytosis. Among all, antigen specificity has been shown for antigens and MHC class I & II proteins and presence of MHC proteins on exosomes solely depend on the protein expression in the parent cell. Juxtaposition of ligands and receptors found both on exosomes and recipient cells are required for juxtacrine signalling and exosomal uptake. In the fusion process, exosomal membrane fuses with that of recipient cells and exosomal content is directly released into the cytoplasm of the recipient cell. On the other hand, since phagocytosis is directly related to actin-mediators, it requires either specific opsonin receptors or scavenger receptors. Macropinocytosis is also driven by actin filaments to shape invagination to take in the vesicle [304].

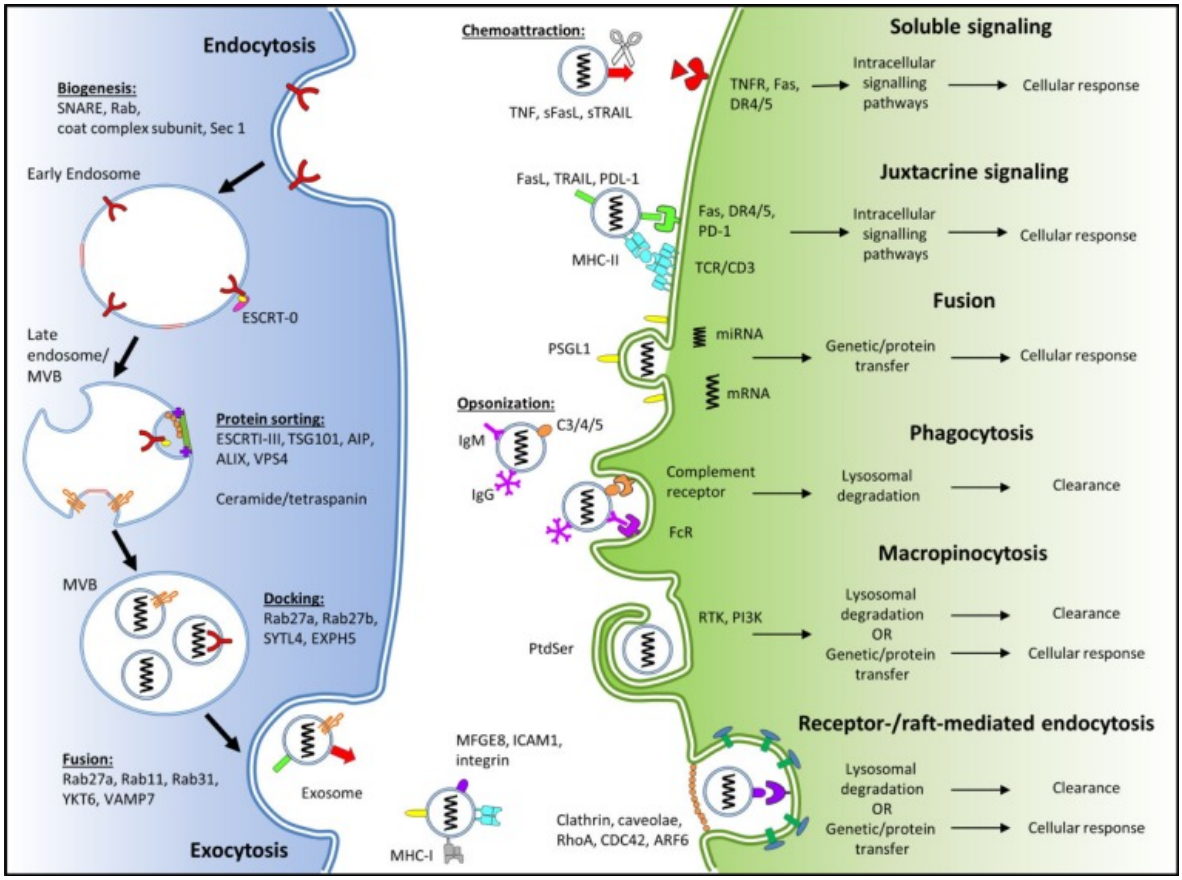

Figure 1.7. Biogenesis and internalization of exosomes [304].

1.6.4. Extracullular Vesicles from Plants

When first discovered in mammalian cells, the exosomal research area has exploded. Unfortunately, exosome research on plant area had lacked an interest for many years. The active research on plant exosomes has started after researchers in Indiana University worked on deciphering the mechanisms how plant cells die in 2012. From their studies on *Arabidopsis thaliana* they discovered persistent presence of round structures between their cell wall and plasma membrane. Surprisingly, older studies dating back to 1960s has also pointed the presence of such structures inside the plants [305]. What is more striking than the presence of these membrane bound vesicles that Innes and colleagues have captured these membrane bound vesicles fusing with plasma membrane and release their cargo between cell wall and its membrane [306]. Since mammalian exosomes are discharged when MVBs fuse with plasma membrane, the similarity between mammalian exosomes and these

membrane bound plant vesicles has started an interest on the presence of plant exosomes. When compared to plant exosomes, mammalian exosomes have comparatively studied in much detail, therefore there are many reports for their isolation and usage. Despite the great acknowledgement of the importance of exosomes in mammalian cellular communication, nothing was known about the significance of plant EVs except their existence by old microscopic images. However, plant exosomes are now known to have a role in immune response which have eventually caused the investigation of EV isolation methods from plant cells [307]. Studies on plant exosomes mainly depend on the utilization of transmission electron microscopy. These researches suggest that, EVs in plant tissue start proliferating upon fungal/pathogen attack and accumulate around the attack site [308, 309]. Potential role of plant EVs are especially intriguing due to the prevalence of EVs during infection [310].

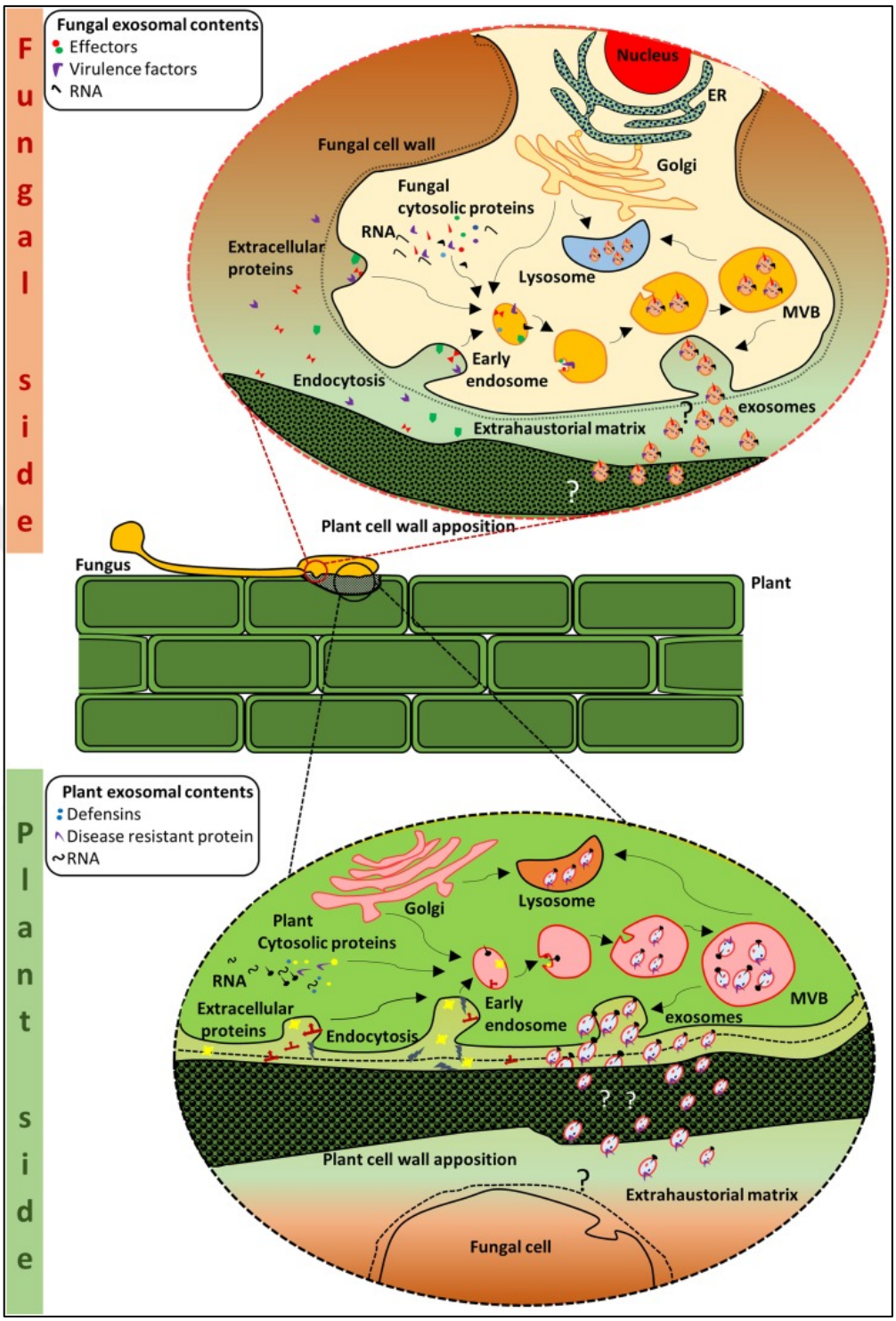

Figure 1.8. Crosstalk between plant cell and fungal invasion [311].

The need for developing green, biocompatible and sustainable products are ever increasing in the past few years. Extracellular vesicles from plants and mammalian cells are relatively

attracting attention recently. In the light of these circumstances, medicinal plants play a leading role for their regenerative roles. Among medicinal plants, *A. comosus* has long been used for its digestive aid and remedy for skin disorders by native cultures [312]. The active compound of *A. comosus* is bromelain which is derived from its stems and fruits. In the literature, bromelain has been suggested for its various therapeutic benefits such as anti-edematous analgesic and anti-inflammatory [313, 314]. Mainly, the proteolytic component of bromelain is suggested to be responsible for its therapeutic effects such as reduced levels of PGE, inflammation and pain [315–317]. Due to the ever increasing interest in both medicinal plants and the existence of plant exosomes, the role of exosomes of these medicinal plants are now being studied in much greater interest for their possible role for complementary medicine.

1.7. THE AIM OF THE STUDY

Exosomes are the main components of the cellular communication. So far, it has been established that various cell types secrete exosomes that vary in their cellular content. Even though medicinal uses of plants is nothing new, plant exosomes are freshly discovered area that needs further investigations and research. As always, there is an unprecedented interest in the use of medicinal plant.

For that purpose, this study will be aimed to; (a) isolating and characterizing *A. comosus* exosomes; (b) evaluate the effect of exosomes *in vitro* on dermal cell line for proliferative, migrative and angiogenetic capabilities; (c) investigate changes in gene and protein levels and figure out if these exosomes possess any anti-scar properties.

2. MATERIALS AND METHODS

2.1. MATERIALS

2.1.1. Chemicals

DMEM high glucose (Gibco 41966, Thermo Fisher Scientific, USA), DMEM low glucose (Gibco 31885, Thermo Fisher Scientific, USA), Heat inactivated Fetal Bovine Serum (FBS) (Gibco 10500-056, Thermo Fisher Scientific, USA), Penicillin-Streptomycin (PS) (Gibco 15140-122, Thermo Fisher Scientific, USA), Dimethyl Sulphoxide (DMSO) (Santa Cruz Biotechnology sc-202581, USA), Phosphate Buffered Saline (PBS) (Lonza BE17-517Q, Switzerland), Trypsin-EDTA (Gibco 25200056, Thermo Fisher Scientific, USA), 4 6, 6-diamidino-2-fenilindol DAPI (DS1306, ThermoFischer Scientific, USA), PKH26 (PKH26GL, Sigma-Aldrich, USA), PKH67 (PKH67GL, Sigma-Aldrich, USA), The Muse® Cell Cycle Kit (MCH100106, Merck Millipore, USA), Human Pro-Collagen I alpha 1 ELISA Kit (ab210966, abcam, USA), RayBio® Human TGF-beta 1 ELISA Kit (#ELH-TGFb1, RayBiotech, USA), The Human Matrix MetalloProteinase 3 (Hu MMP3) ELISA kit (BMS2014-3, ThermoFisher Scientific, USA), Human MMP-1 ELISA Kit (EHMMP1, ThermoFisher Scientific, USA), Human VEGF ELISA Kit (KHG0111, Invitrogen, USA), Polyethylene glycol (#81310, Sigma-Aldrich, USA), Dextran (#9004-54-0, Sigma-Aldrich, USA), TRIzol™ Reagent (15596-018, ThermoFisher Scientific, USA), Anti-CD9 antibody (ab2215, Abcam, USA), Anti-CD63 antibody (ab8219, Abcam, USA), Anti-Hsp70 antibody (ab61907, Abcam, USA), Aldehyde/Sulfate Latex Beads,4 percent w/v, 4 μm (A37304, ThermoFisher Scientific, USA), RIPA Lysis and Extraction Buffer (#89900, ThermoFisher Scientific, USA), 4-20 percent Mini-PROTEAN TGX Protein Precast Gel (#4561094DC, Biorad, USA), Page Ruler Protein Ladder (26619, ThermoFisher, USA), QuantiTect SYBR Green PCR Kit (204145, Qiagen, USA), iScript™ cDNA synthesis kit (#1708890, BioRad, USA), CellTiter96 AqueousOne Solution (#G3582,; Promega, Southampton, UK), CytoSelect™ 24-Well Cell Migration and Invasion Assay (8 μm, Colorimetric Format) (CBA-100-C, Cell BioLabs), Bovine Serum Albumin (BSA) ($0332-100G, VWR LifeScience), Mounting media (F4680-25, Sigma, USA), Anti-Collagen I antibody (ab34710, Abcam, USA), Anti-Fibronectin antibody (ab2413, Abcam, USA), ERK1/2

antibody (16443-1-AP, Proteintech, USA), SMAD3 antibody (25494-1-AP, Proteintech, USA), Goat anti-rabbit IgGH&L (Alexa Fluor® 647) (ab150079, Abcam, USA), Phospho-p38 MAPK (Thr180/Tyr182) (D3F9) XP® Rabbit mAb(#4511S, Cell Signaling, USA), Phospho-p44/42 MAPK (Erk1/2) (Thr202/Tyr204) Antibody (#9101S, Cell Signaling, USA), AKT Antibody (#9272, Cell Signaling, USA), Anti-beta-actin antibody (STJ97714, St John's Laboratory, USA), Goat Anti-Rabbit IgG H&L (HRP) (ab6721, abcam, USA).

2.1.2. Consumables

Cell culture flasks T25, T75, T150, (#90025, #90075, #90150, TPP, Switzerland), Serological Pipettes 5,10,25,50 mL (SP-5-C,SP-10-C SP-25-C,SP-50-C, CAPP, Germany), Microcentrifuge tubes 1.5, 2 mL (078.03.002, 078.03.003, Isolab, Germany), Micropipette tips 10,200,1000 µL (301-03-051, Axygen, USA) Falcon tubes 15,50 mL (LB.IS.078.02.003, Isolab, Germany), 2 mL Cryotubes (091.11.102, Isolab, Germany), Micropipette 2.5,10,20,200,1000 µL (2231300002, Eppendorf, Germany), Countess Cell Counting Chamber Slides (#C102288, Thermo Fisher, USA), Multipipette 100 µL (Eppendorf Research, Germany), Graduated Cylinder 100, and 1000 mL (Isolab, Germany), Whatman Paper (Isolab, Germany), Nitrocellulose Membrane (GE Healthcare, USA), 8-well Chamber Slide (PEZGS0816, Millicell EZ Slide, USA), Pipette pump (#156403, Integra, Japan).

2.1.3. Instruments

Laminar Flow Cabin (Heal Force Class II Biosafety Cabinet A2, China), CO_2 incubator (In-Vitro Cell ES NU-5800, NuAire, USA), Inverted Microscope (Nikon Eclipse, TS100, Netherlands), Low-Speed Centrifuge (Gyrozen 416, Korea), -80°C freezer (New Brunswick, U410, Germany), Microplate reader (Bio-tek ELx800, USA), Mini Trans-Blot Cell Blotting System (Bio-Rad, USA), High-Speed Centrifuge (Sigma Aldrich 3-18KS, Germany), Shaking Water Bath (Stuart SBS40, UK), Nano-Drop 2000 (Thermo Fisher Scientific, USA), Thermal Cycler (Biorad Mycycler 1709703, USA), CFX96 Real-Time PCR (Bio-Rad, C1000 Touch, USA), Liquid Nitrogen Tank (Air Liquide Arpege 140, UK), pH Meter (Milwaukee Mi151, USA), Vortex (Dragon Lab, MX-F, China), Heating Block

(WiseTherm, HB-R, Switzerland), Incubator Shaker (New Brunswick Innova 4330, USA), Magnetic Stirrer (Heidolph MR3004, Germany), Mini-PROTEAN Tetra Cell Electrophoresis System (Bio-Rad 165-8001, USA), Fluorescence Microscope Axio Vert. A1 (Zeiss, Germany), Confocal Laser Scanning Microscope (Zeiss LSM 700, Germany), Weighing Machine (Shimadzu, AUW220D, Japan), FACS Calibur (BD Biosciences, USA), ChemiDOC XRS+Gel Imaging System (Bio-Rad Universal Hood 2, USA), Guava easyCyte Flow Cytometers (Merck Milipore, Germany), Muse® Cell Analyzer (Merck Millipore, USA), ELISA plate reader (Biotek, USA), FACS Calibur (BD Biosciences, USA).

2.1.4. Cell Lines

- Primary neonatal human dermal fibroblasts (HDF) were isolated from human foreskin according to the protocol described in the literature [318].
- Human umbilical vein endothelial cells (HUVEC), ATCC-CRL 1730.
- Human keratinocyte (HaCaT), CLS 300493, DKFZ, Heidelberg.

2.2. METHODS

2.2.1. Exosome Isolation from Pineapples

Pineapples were purchased from a local store in Turkey and the crusts were skinned. Pineapple was sliced into small slices and then grounded in a laboratory blender. In order to obtain the juice, plant debris is pelleted with centrifuge at 1000 g for 30 minutes. Exosome isolation was carried out according to the aqueous two-phase system (ATPS) procedure described in the literature [319]. In brief, ATPS isolation solution was prepared with Dextrean (DEX) (Sigma 31392) and Poly(ethylene glycol) (PEG) (Sigma, 81310) and mixed in distilled water. Then, 20 ml of plant lysate is mixed with 20 ml of ATPS isolation solution and centrifuged at 1000 g for 10 minutes to separate phases. After the centrifugation 80 percent of the volume is discarded and the same amount of the ATPS isolation solution was added and then centrifuged at the same speed. Once the centrifugation steps are over, upper phase of the system was discarded and the exosome containing bottom phase is filtered through 0.22 μm filters.

2.2.2. Exosome Characterization and Quantification

Exosome characterization was carried out in via nanoparticle tracking analysis (NTA), flow cytometry and exosome quantification was carried out via Lowry protein analysis. By using NTA system, exosome quantification and size distribution were determined with 488 nm laser. Samples were diluted accordingly to the suggested concentration range 1:40 with distilled water as instructed in the instrument manual. Nanoparticles were captured to the video with 60 second intervals for at least 5 takes and the analysis was performed via NTA software version 3.3.301. Capture and analysis settings can be observed in the figure 2.1 below;

Capture Settings

Camera Type:	sCMOS
Laser Type:	Blue488
Camera Level:	14
Slider Shutter:	1259
Slider Gain:	366
FPS	25.0
Number of Frames:	1498
Temperature:	15.0 - 15.0 °C
Viscosity:	(Water) 1.134 - 1.136 cP
Dilution factor:	4 x 10e1

Analysis Settings

Detect Threshold:	4
Blur Size:	Auto
Max Jump Distance:	Auto: 8.9 - 19.7 pix

Figure 2.1. Settings for capture and analysis of nanoparticle tracking analysis

Surface antigens of the exosomes were also analysed with flow cytometry. After the particle number of the exosomes in one ml was calculated with NTA, 5 µg of exosomes were attached to the 5 µl of latex beads (4 percent w/V, 4 µm) made of aldehyde/sulfate (ThermoFisher, A37304) and incubated at room temperature for 15 minutes on a shaker. Then, exosomes were incubated for 2 hours with 2 percent BSA prepared in PBS to prevent non-specific antibody binding. Following incubation, glycine was added to the mixture for

a final concentration of 100mM. Then this mixture was incubated on a shaker for 30 minutes. After the incubation, cold PBS was added to the mixture which was then centrifuged at 2700 g for 3 minutes. Exosomes then resuspended in PBS and aliquoted into different tubes with respective antibodies CD9 (Biolegend 124808), CD 63 (Biolegend 143904) and HSP70 (Biolegend 648004) and were kept with conjugated antibodies overnight. Following day, exosomes were centrifugation at 2700 g for 3 minutes to pellet then. They were resuspended with 1:100 diluted Alexa Fluor 488 (Abcam, ab150077) antibody and read via Flow Cytometry. Exosome quantification was evaluated via Lowry protein assay kit as it is a generally accepted method for EV quantification and results were based on BSA assays. 4 µl of exosomes were combined with 16 µl distilled water and 5 µl of the mixture was dispersed in 3 different wells of 96-well plates in 5 µl. Each well was filled with 25 µl of Reagent A solution and 220 µl of Lowry B solution and incubated for 30 minutes. The plate was read at 750 nanometer Multiscan Spectrophotometer (Biotek, USA) and based on known absorbance values of BSA standards concentrations of unknown samples were calculated.

2.2.3. Cell Culture

Primary neonatal human dermal fibroblasts, human umbilical vein endothelial cells (HUVEC, ATCC-CRL 1730), and human keratinocyte (HaCaT) (CLS 300493, DKFZ, Heidelberg) were cultured in complete Dulbecco's Modified Eagle Medium (DMEM) with 10 percent (v/v) Fatal Bovine Serum (FBS) and 100 units/ml Penicillin / Streptomycin / Amphotericin (1 percent) antibiotics. T25, T75, T125 flask were gradually used to grow and incubate cells in Nuaire NU5510/E/G incubator at 37ºC in a highly humidified atmosphere (RH 80 percent) with 5 percent CO_2 and 95 percent (v/v) air. Cells were observed daily and passaged once they reached 70 to 80 percent confluency.

2.2.4. Cell Passaging

ESCO Labculture Class II Biohazard Safety Laminar Flow cabinet was used for cell passage. Cells were detached from flask by 0.05 percent (w/v) trypsin by incubating for 4 minutes at 37ºC. Once the cells were collected from the flask, activity of trypsin was halted with by adding complete medium. Sterile flask was used to collect the cells into and they were

precipitated by centrifuging at 300xg for 5 minutes. Fresh growth media was used to resuspend the cell pellet. Following the passage, 10 µl of the re-suspended cells was placed in a hemocytometer and the number of the cells were counted under inverted light microscope.

2.2.5. Cell Viability

The viability of primary neonatal human dermal fibroblasts (HDF) isolated from human foreskin cells in Molecular Diagnostics Laboratory (Yeditepe University, Turkey), human umbilical vein endothelial cells (HUVEC), and human keratinocyte (HaCaT) skin cells were investigated via MTS assay (3-(-4,5-dimethyl-thiazol-2-yl) – 5 - (3-carboxymethoxy-phenyl)-2-(4-sulfo-phenyl)-2H-tetrazolium(. 5 different concentrations of pineapple exosomes starting from 25 µg/ml to 150 µg/ml (25-, 50-, 75-, 100- and 150 µg/ml) were prepared in DMEM with 10 percent fetal bovine serum (FBS) (#10500-064, Invitrogen, UK) and 1 percent of penicillin, streptomycin and amphotericin B (PSA) (#15240-062, Invitrogen, UK). Cells were counted and $5x10^3$ cells/well seeded on 96-well plates (#CLS6509, Corning Plasticware, Corning, NY) and incubated 24 hours at beforementioned conditions in section 2.2.3. After 24 hours, the cells were attached to the well plate and their medium was changed with prepared concentrations of DMEM medium starting from 25 µg/ml up to 150 µg/ml. Viability of the cells after exosome treatment were detected at the same time for the following 3 days (respective 24-, 48- and 72 hours) via MTS assay. PBS-glucose solution was mixed with MTS solution to make a final concentration of 10 per cent. Prepared with MTS, PBS-glucose solution was given to the cells. Cells were incubated with PBS-glucose solution for 1 hour at 37^{o}C in a highly humidified atmosphere (RH 80 percent) with 5 percent CO_2 and 95 percent (v/v) air. Absorbance of the wells were measured in ELISA plate reader (Biotek, USA) at 490nm.

2.2.6. Cell Cycle Analysis

In order to detect the implications of exosomes on cell cycle, cell cycle analysis was executed by Muse Cell Analyzer according to manufacturer's instructions. In brief, 2 x 10^5 cells/well were seeded on 6 well plates. After 24 hour and they were attached to the flask surface, they

were treated with 100 µg/ml exosomes for respected 12th, 24th and 48th hours. Cells removed by trypsinization were collected into falcon tube including their treatment medium and then for 5 minutes they were centrifuged at 300 x g. Following the centrifugation cells were washed with PBS and pelleted again to be fixed with 70 percent ethanol. After 1 week, cells pelleted and then incubated for 30 minutes in 200 µl Muse cell cycle kit (MCH100106, Merck Millipore) solution. Following the incubation, 10000 cells were read and analysed via Muse Cell Analyzer and all of the time interval experiment was replicated at least 5 times.

2.2.7. Exosome Uptake Analysis

Exosome taken inside by the cells was visualized with exosome uptake analyses. At first, cell nucleus was dyed with Hoechst dye (#62249, Thermo-Fischer Scientific, Massachusetts, USA) with a final concentration of 1µg/ml as suggested in the manufacturer's protocol. Then, attached cells were dyed with CellTracker^{TM} Red CMPTX Dye (#C34552, Thermo-Fischer Scientific, Massachusetts, USA) in accordance with manufacturer's protocol. In brief, lyophilized CMPTX dye was prepared in DMSO with a final concentration of 10 mM as a stock solution. To prepare working solution, stock solution is diluted to 25 µM in a serum free medium. Prepared in medium, the dye was then given to the attached cells and they were incubated at 37^{o}C with 5 percent CO_2 and 95 percent (v/v in a highly humidified atmosphere (RH 80 percent)) air for 30 minutes. In the meantime, exosomes are dyed with Paul Karl Horan (PKH) 67 Green Fluorescent Cell Linker Kit for overall labelling of the cell membrane (#PKH67GL, Merck, Darmstadt, Germany) as per manufacturer's guidance. In short, 1 ml of Diluent C from the PKH67 kit mixed with 4 µl of the PKH67 dye then it is mixed with 1 ml of exosome (1:1 ratio is kept in all circumstances) solution, mixed thoroughly for 30 seconds. After that exosomes and the dye were kept at room temperature for 5 minutes. Once the exosomes are thoroughly dyed, the remaining dye is removed via exosome spin columns (MW 3000) (#4484449, Thermo-Fischer Scientific, Massachusetts, USA) by centrifuging exosomes at 750 g for 2 minutes. After remaining dye is removed, exosomes were given to the cells dyed red with CMPTX dye in a complete medium. Pictures of HUVEC and HaCaT cells were taken with Fluorescence Microscope at respective 30 minutes, 1-, 2-, 3-, 4-, 6-, 12-, 24- and 48th hours and those of fibroblast were taken at 12th and 24th hours.

2.2.8. Scratch Assay

Scratch assay was conducted with the object of detecting the effects of pineapple exosomes on cell migration and wound closure. $2x10^5$ cells were seeded on 6 well plates and incubated at 37°C in conditions mentioned in section 2.2.3. After cells were attached to the wells, they were scratched by 1000 µl sterile micropipette tip and observed under microscope. Then the cells were washed with PBS twice immediately after. The medium of the cells was changed with either exosome including treatment medium or control medium without exosomes. Cells, then, incubated at 37°C in conditioned mentioned in section 2.2.3. Scratch photographs were taken at the beginning and at the 16th hour via inverted microscope (Carl Zeiss Microscopy, LLS, Thornwood, NY, USA). Wound closure rate analysis were measured by using Image analysis Software (ImageJ, NIH, Bethesda, MD) program based on the initial edges (Ai) subtracted by final distance (Af) between the wound edges divided by the initial distance and the total result was multiplied with 100. The overall equation used is;

$$\text{per cent wound closure} = [(\text{Ai-Af})/\text{Ai}] \text{ x } 100 \qquad (2.1)$$

2.2.9. Transmembrane Cell Migration Assay

Migration plates were kept in 2-8°C until use and they were warmed up at room temperature under sterile conditions. HaCaT and HUVEC cells were prepared in 5 x 10^5 cells/ml in suspension. 500 µl of complete medium and 500 µl of complete medium with 100 µg/ml pineapple exosomes were supplied to the lower well of the migration plate to be used as control and treatment respectively. 300 µl of the cell suspension solution was transferred to the top side of the migration inserts. Migration inserts were then incubated in incubator for 24 hours. After 24 hours, cell media was aspirated and the interior part of the insert was swabbed with cotton-tipped swabs. Then the inserts were taken to the clear wells and dyed with 400 µl of Cell Stain Solution and kept at room temperature for 10 minutes. In order to remove any remaining dye from the inserts, they were washed with distilled water thoroughly. After the dye remnants were cleared, the inserts were then air-dried. After that,

inserts were placed under inverted light microscope and picture of the migrated cells were taken from 5 different areas.

2.2.10. Transmembrane Cell Invasion Assay

Invasion plates were kept in 2-8ºC until use and they were warmed up at RT. Membrane layer of the invasion inserts were rehydrated with the annexing of 300 µl of warm serum-free medium inside the inner compartment. For 1 hour, the insert was incubated with the medium. HaCaT and HUVEC cells were prepared in 5 x 10^5 cells/ml in suspension. After incubation, rehydration buffer was discarded. 500 µl of complete medium and 500 µl of complete medium with 100 µg/ml pineapple exosomes were transferred to the bottom side of the invasion plate to be used as control and treatment respectively. 300 µl of the cell suspension solution was transferred to the top side of the migration inserts. Migration inserts were then incubated at 37ºC in an incubator with relative humidity at 80 per cent, 5 percent CO_2 and 95 percent (v/v) air for 24 hours. After 24 hours, cell media was aspirated and the interior part of the insert was swabbed with cotton-tipped swabs. Then the inserts were taken to the clear wells and dyed with 400 µl of Cell Stain Solution and kept at RT for 10 minutes. In order to take off any remaining dye from the inserts, they were washed with distilled water thoroughly. Inserts then were placed under inverted light microscope and picture of the migrated cells were taken from 5 different areas.

2.2.11. Cellular Reactive Oxygen Species Detection

1 x 10^5 cells were seeded on 6 well plates and incubated at 37ºC overnight according to the conditions mentioned in section 2.2.3. 24 hours later cells were either given 50- or 100-µg/ml exosome, control cells were treated with growth medium. Following day, they were harvested including their corresponding media and treated with 1 µM and 10 µM of 2',7'–dichlorofluorescin diacetate (DCFDA) dye in PBS for 30 minutes. Following incubation, cells were treated 50 µM of tert-Butyl Hydroperoxide (tBHP) to stimulate oxidative stress on cells. Cells were treated with tBHP for 4 hours. The amount of ROS produced within cells were detected by FACS Calibur Flow Cytometry (BD Biosciences, USA).

2.2.12. Angiogenesis Assay

HUVEC cells were cultured on Matrigel (#354234, Corning, USA) in order to evaluate pineapple exosomes effect on tube formation. Tube formation assay was conducted in accordance with the manufacturer's instructions. 24-well plates and micropipette tips were pre-chilled and Matrigel matrix is thawed at 4°C overnight. While keeping 24-well plate on ice, 10 mg/ml chilled Corning Matrigel matrix was added to each well. In order to remove any air bubbles that may be present in wells, the plate was centrifuged at 300 g at pre-cooled centrifuge at 4°C for 10 minutes. After centrifugation, the plate is incubated at 37°C incubator for 30 minutes to allow polymerization of the corning Matrigel matrix. After the matrix polymerized, $4x10^4$ HUVEC cells per well were seeded onto the matrix with control medium and also with medium including 100 µg/ml pineapple exosomes. Cells then incubated at 37°C in conditions mentioned in section 2.2.3. Tube-like formation of the cells become visible around 7 hours. Tube formation photos from randomly selected five different areas were taken at 7^{th} and 20^{th} hour with an inverted microscope (Nikon Eclipse TS100, Nikon, Tokyo, Japan). The analysis of the tube formation was conducted with WimTube Angiogenesis Analysis (Wimasis, Germany).

2.2.13. RNA Isolation for Gene Analysis

2×10^5 cells/well were seeded on 6 wells and then incubated at 37°C in a highly humidified atmosphere (RH 80 percent) with 5 percent CO_2 and 95 percent (v/v) air overnight and then treated with either growth medium or 100 µg/ml of *A. comosus* exosomes. 24 hours later, cells were harvested and total RNA from each cell line isolated by using Trizol™ reagent (#15596026, Thermo-Fischer Scientific, Massachusetts, USA) consistent with the manufacturer's instructions. First, 400 µl of Trizol was mixed with the cell pellets and incubated for 5 minutes. 100 µl of chloroform was mixed thoroughly with the each sample and incubated for 3 minutes. In order to separate the sample into 3 distinct phases, they were centrifuged at 12,000 x g for 15 minutes. Following, upper colourless phase was carefully taken into a new tube and then 200 µl isopropanol was added, mixed and then incubated for 10 minutes. Samples were centrifuged again at 12,000 x g for 10 minutes. Then, RNA samples were collected as white gel-like form at the bottom of the tube. Contrarily,

supernatant that does not contain RNA was discarded. 400 µl of 75 percent of ethanol was mixed/vortexed thoroughly. The sample was then centrifuged for 5 minutes at 7500 x g. Following the centrifugation, the pellet was airdried for approximately 5 minutes. 30 µl of RNase/DNase free water was used to dissolve RNA samples. Concentrations of the samples were measured with Nanodrop.

2.2.14. Quantitative Real-Time Polymerase Chain Reaction (RT-PCR) Assay

Primer-BLAST online software of the National Center for Biotechnology (NCBI, Bethesda, MD) was used to design target primers that are synthesized by Sentegen Biotech (Ankara, Turkey). As a housekeeping gene, glyceraldehyde-3-phosphate dehydrogenase (GAPDH) gene was employed to normalize the gene expressions. Complementary DNA (cDNA) from total RNAs was synthesized by BioRad iScript™ cDNA Synthesis kit (#1708891, BioRad, USA) in accordance with the manufacturer's suggestions (Table 2.1).

In order to prepare master mix for RT-PCR, QuantiTect SYBR Green PCR Kit (#204145, Qiagen, Hilden, Germany), dH_2O, and 10 pmol of each primer (sequences of the primers were given in Table 2.4) was mixed and distributed to respective wells for RT-PCR. 800 ng of cDNAs was also added to accomplish a final volume of 10 µl. The RT-PCR experiments were run via iCycler RT_PCR system (Bio-Rad, Hercules, CA). Data normalization of the gene expressions was normalized against their respective GAPDH values to represent as fold changes.

Table 2.1. BioRad iScript™ cDNA synthesis kit reaction establishment

iScript Kit Components	**Volume per Reaction (µl)**
5X iScript Reaction Mix	4
iScript Reverse Transcriptase	1

Nuclease-free water	Variable
RNA template	Variable
Total Volume	20

Table 2.2. BioRad iScript™ cDNA synthesis kit reaction protocol

Priming	5 minutes at 25 °C
Reverse Transcription	20 minutes at 46 °C
RT inactivation	1 minute at 95 °C
Hold	4 °C

Table 2.3. RT-PCR settings

Cycle	**Repeat**	**Step**	**Duration**	**Temperature**
Initial Denaturation	1	1	5 minutes	93 °C
Denaturation	40	1	60 seconds	93 °C
Annealing		2	60 seconds	55 °C
Extension		3	60 seconds	72 °C
Final Extension	1	1	10 minutes	72 °C
Melt Curve	110	1	12 seconds	-0.5 °C/cycle
Hold	1	1	-	4°C

Table 2.4. Primers used in RT-PCR assays

Gene	Species	Orientation	Sequence
AKT	Human	Forward	5’-GGGACCTGAAGCTGGAGAA-3’
		Reverse	5’-CCTGGTTGTAGAAGGGCAGG-3’
Laminin	Human	Forward	5’-CACATGTCCGTCACAGTGGA-3’
		Reverse	5’-TAGAGGCTGACCACCTCCTC-3’
MMP2	Human	Forward	5’-AGCGAGTGGATGCCGCCTTTAA-3’
		Reverse	5’-CATTCCAGGCATCTGCGATGAG-3’
MMP9	Human	Forward	5’-GCCACTACTGTGCCTTTGAGTC-3’
		Reverse	5’-CCCTCAGAGAATCGCCAGTACT-3’
Vimentin	Human	Forward	5'-TGCAGGAGGCAGAAGAATGGTACA-3'
		Reverse	5'-TTCCATTTCACGCATCTGGCGTTC-3'
α-smooth	Human	Forward	5'-AGACATCAGGGGGTGATGGT-3'
		Reverse	5'-ATCTTTTCCATGTCGTCCCAGTTG-3'
TGF-β1	Human	Forward	5’-TACCTGAACCCGTGTTGCTCTC-3’
		Reverse	5’-GTTGCTGAGGTATCGCCAGGAA-3’
TGF-β3	Human	Forward	5’-TGGCTGTTGAGAAGAGAGTCC-3’
		Reverse	5’-TCATCCTCATTGTCCACGCC-3’
Col1A1	Human	Forward	5’-CCACGCATGAGCGGACCCTAA-3’
		Reverse	5’-ATTGGTGGGATGTCTTCGTCTTGG-3’
Col3A1	Human	Forward	5’-TGGTCTGCAAGGAATGCCTGGA-3’
		Reverse	5-‘TCTTTCCCTGGGACACCATCAG-3’
Fibromodulin	Human	Forward	5’-AGGATCAATGAGTTCTCCATCAGC-3’
		Reverse	5’-TTGATCTCGTTCCCGTCCAG-3’

GAPDH	Human	Forward	5'-TTCGACAGTCAGCCGCATCTTCTT-3'
		Reverse	5'-ACCAAATCCGTTGACTCCGACCTT-3'

2.2.15. Enzyme-Linked Immunosorbent Assays

2.2.15.1. Human MMP1 ELISA

2 x 10^5 cells/well were grown in 6-well plates and incubated at 37^{o}C in a highly humidified atmosphere with conditions mentioned in section 2.2.3. Following the incubation, cells were treated with 100 µg/ml pineapple exosomes and control cells were given fresh medium. Then, the medium of the cells was collected and centrifuged respectively for 5 minutes at 300 x g to get rid of any cell remnants. The supernatants that will be used within 24 hours were stored at 2-8^{o}C and for long term storage, they were aliquoted and stored at -80^{o}C. Human MMP1 ELISA kit is composed of lyophilized recombinant Human MMP-1 Standard, anti-Human MMP-1 Precoated 96 well Strip Plate, Biotinylated Antibody Reagent,, 20X Wash Buffer, TMB Substrate, Streptevidin-HRP Reagent, Stop Solution, 5X Assay Diluent, and plate sealer. In order to start the ELISA procedure all the reagents were warmed to RT (18 – 25^{o}C) before use. To prepare 0.1 µg/ml standard solution lyophilized standard sample that comes with the kit was centrifuged and dissolved with 1X Assay Diluent. Then the standard solution was diluted according to manufacturer's instructions. 100 µl of standards duplicates along with triplicates of the samples were added appropriate wells of the anti-Human MMP-1 precoated 96-well Strip Plate and incubated with gentle shaking for 2 and a half hour at RT. Following the incubation, wells were cleaned with 300 µl of 1X Wash Buffer at least 4 times for 5 minutes. Once the wells were washed, each well was treated with 100µl of 1X biotinylated antibody and for 1 hour, they were incubated at RT with gentle shaking. Then, wells were washed with 300 µl of 1X Wash Buffer at least 4 times for 5 minutes once again. 100 µl of Streptavidin-HRP solution was transferred into appropriate wells. For 45 minutes samples were incubated in this solution at RT. Following, wells were cleaned with 300 µl of 1X Wash Buffer at least 4 times for 5 minutes once again. Each well was then treated with 100 µl of TMB Substrate and then incubated in dark for 30

minutes at RT. In order to stop the reaction, stop solution of 50 µl was combined and the absorbance values of the wells were evaluated with an ELISA plate reader both at 450 nm and 550 nm. The values obtained from 550 nm reading was subtracted for correcting the imperfections in the microplate. The results of the respective wells were computed from the standard curve generated by standard values.

2.2.15.2. Human MMP-3 ELISA

2 x 10^5 cells/well were grown in 6-well plates and incubated at 37ºC in a highly humidified atmosphere with conditions mentioned in section 2.2.3. Following the incubation, cells were treated with 100 µg/ml pineapple exosomes and control cells were given fresh medium. Then, the medium of the cells was collected and centrifuged respectively for 5 minutes at 300 x g to get rid of any cell remnants. The supernatants that will be used within 24 hours were stored at 2-8ºC and for long term storage, they were aliquoted and stored at -80ºC. Human MMP3 ELISA kit is composed of lyophilized recombinant TMB Substrate, Human MMP-3 Standard, 20X Wash Buffer, anti-Human MMP-3 Precoated 96 well Strip Plate, Stop Solution, Biotinylated Antibody Reagent, Streptevidin-HRP Reagent, 5X Assay Diluent, and plate sealer. In order to start the ELISA procedure all the reagents were warmed to RT (18 – 25ºC) before use. To prepare 8 ng/ml standard solution, lyophilized standard sample that comes with the kit was centrifuged and dissolved in distilled water. Then, the standard solution was diluted according to assay kit. To start the assay, wells were treated with 400 µl Wash Buffer twice. After that, while 100 µl of 1X Assay Buffer was transferred to blank wells, 90 µl of 1X Assay Buffer was transferred to the sample wells. 10 µl of the samples were then transferred to their appropriate wells and then 50 µ of Biotin-Conjugate was transferred into each well. For 2 hours, samples were incubated with gentle shaking at RT. After the incubation, wells were washed with 1X Wash Buffer 6 times. After the wash, the wells were treated with 100 µl of previously prepared Streptavidin-HRP and then they were incubated for 1 hour at RT with gentle shaking. Then, wells were washed with 1X Wash Buffer 6 times. 100 µl of TMB Substrate Solution was transferred into each well. After the addition of this substrate, samples were incubated in dark for 30 minutes. Once a dark colour has been developed by the highest sample of standard solution, 100 µl of Stop Solution was combined in the mix. The absorbance values of the wells were evaluated with an ELISA plate reader at 450 nm with 620 nm as a reference wave length. The results of the respective wells were computed from the standard curve generated by standard values.

2.2.15.3. Human VEGF ELISA

2 x 10^5 cells/well were grown in 6-well plates and incubated at 37ºC in a highly humidified atmosphere with conditions mentioned in section 2.2.3. Following the incubation, cells were treated with 100 µg/ml pineapple exosomes and control cells were given fresh medium. Then, the medium of the cells was collected and centrifuged respectively for 5 minutes at 300 x g to get rid of any cell remnants. The supernatants that will be used within 24 hours were stored at 2-8ºC and for long term storage, they were aliquoted and stored at -80ºC. Human VEGF ELISA kit is composed of lyophilized Hu VEGF standard, Standard Diluent Buffer, Incubation Buffer, Anti-VEGF antibody coated plate, Hu VEGF Biotin Conjugate, 100X Streptavidin-HRP, 25X Wash Buffer, Streptavidin-HRP diluent, stop solution, Stabilized chromogen tetramethylbenzidine (TMB) and plate covers. In order to start the ELISA procedure all the reagents were warmed to RT (18 – 25ºC) before use. To prepare 10,000 pg/ml standard solution, lyophilized standard sample that comes with the kit was centrifuged and dissolved in standard diluent buffer. Then the standard solution was diluted in accordance with the manufacturer's suggestions. In order to begin the assay, 50 µl of the Incubation Buffer was transferred to wells and then 100 µl of standard sample was transferred to their corresponding wells. Sample wells were added both 50 µl of sample and 50 µl of Standard diluent buffer. Samples were incubated at RT for 2 hours. Then protein remnants were removed from the wells by washing them 4 times with 1X wash buffer. Following, 100 µl of Hu VEGF Biotin Conjugate solution was transferred to the wells and then for 1 hour they were incubated at RT on gentle shaker. Wells were washed 4 times with 1X wash buffer and 100 µl of Streptavidin-HRP solution was transferred to wells. For 30 minutes, wells were incubated at RT. Again, wells were washed 4 times with 1X wash buffer. Following, well were treated with 100 µl of Stabilized Chromogen for 30 minutes of incubation in dark. In order to stop the substrate reaction, wells were treated with 100 µl of stop solution. ELISA plate reader at 450 nm was used to evaluate the absorbance values of the wells. The results of the respective wells were computed from the standard curve generated by standard values.

2.2.15.4. Human TGF-beta 1 ELISA

2 x 10^5 cells/well were grown in 6-well and incubated at 37°C in a highly humidified atmosphere with conditions mentioned in section 2.2.3. Following the incubation, cells were treated with 100 µg/ml pineapple exosomes and control cells were given fresh medium. Then, the medium of the cells was collected and centrifuged respectively for 5 minutes at 300 x g to get rid of any cell remnants. The supernatants that will be used within 24 hours were stored at 2-8°C and for long term storage, they were aliquoted and stored at -80°C. Human TGF-beta 1 ELISA kit is composed of TGF-beta 1 microplate, HRP-streptavidin concentrate, standard protein, 20X wash buffer concentrate, stop solution, TGF-beta detection antibody, TMB one-step substrate reagent, assay diluent and plate cover. In order to start the ELISA procedure all the reagents were warmed to RT (18 – 25°C) before use. to prepare 4,000 pg/ml standard solution, lyophilized standard sample that comes with the kit was centrifuged and dissolved in 1X assay diluent. Then the standard solution was diluted according to the assay kit. Standard solutions and the samples were added as 100 µl of each to their respective wells in duplicates. Samples were incubated for 2.5 hours at RT on gentle shaker. Wells were cleaned with 300 µl of 1X wash buffer 4 times. Each well was treated with 100 µl of 1X biotinylated antibody for 1 hour at RT. Following, wells were washed with 1X wash solution for 4 times. Then wells were incubated in 100 µl of Streptavidin for 45 minutes. After that, wells were cleaned with 1X wash buffer for 4 times. 100 µl of TMB one-step substrate was transferred to the wells. The wells were incubated in dark with this substrate for 30 minutes at RT with gentle shaking. In order to halt the substrate reaction, 50 µl of stop solution was transferred to the wells. ELISA plate reader at 450 nm was used to evaluate the absorbance values of the wells. The results of the respective wells were computed from the standard curve generated by standard values.

2.2.15.5. Human Pro-Collagen I alpha 1 ELISA

2 x 10^5 cells/well were grown in 6-well plates and incubated at 37°C in a highly humidified atmosphere with conditions mentioned in section 2.2.3. Following the incubation, cells were treated with 100 µg/ml pineapple exosomes and control cells were given fresh medium. Then, the medium of the cells was collected and centrifuged respectively for 5 minutes at 300 x g to get rid of any cell remnants. The supernatants that will be used within 24 hours

were stored at 2-8°C and for long term storage, they were aliquoted and stored at -80°C. Human Pro-Collagen I alpha 1 kit is composed of 10X Wash Buffer PT, 50X Cell Extraction Enhancer Solution, 10X Human Pro-Collagen I alpha 1 Capture Antibody, TMB Development Solution, 10X Human Pro-Collagen I alpha 1 Detector Antibody, 5X Cell Extraction Buffer PTR, Antibody Diluent CPI - HAMA Blocker, sample diluent, Pre-Coated 96-Well Microplate, Human Pro-Collagen I alpha 1 Lyophilized Recombinant Protein, stop solution, and plate seals. In order to start the ELISA procedure all the reagents were warmed to RT (18 – 25°C) before use in order to prepare 31,250 pg/ml standard solution, lyophilized standard sample that comes with the kit was centrifuged and dissolved in sample diluent NS. Then the standard solution was diluted according to the assay kit. In order to start the assay, both standards and samples were added to their appropriate wells for 50 µl each. 50 µl of antibody cocktail was also combined into each well. Samples were and incubated at RT with gentle shaking for 1 hour. Following, cells were cleaned with 1X wash buffer thrice and 100 µl of TMB development solution was transferred to the wells. The solution was incubated in the dark for 10 minutes. To halt the substrate reaction, 100 µl of stop solution was added. ELISA plate reader at 450 nm was used to evaluate the absorbance values of the wells. The results of the respective wells were computed from the standard curve generated by standard values.

2.2.16. Immunocytochemistry Analysis

Hacat and HUVEC cells were seeded in 8-well chambers with a density of 3 x 10^3 cells/well and incubated at 37°C in a highly humidified atmosphere (RH 80 percent) with 5 percent CO_2 and 95 percent (v/v) air overnight for cell attachment. After the cells were attached to the surface, control groups were treated with complete DMEM medium and treatment group was treated with 100 µg/ml pineapple exosomes. Cells were then incubated for another 24 hour. Following the 24 hour incubation with exosomes and normal complete medium, medium of the cells were discarded. For 20 minutes at 4°C, cells were fixated with 4 percent (w/v) paraformaldehyde (PFA). Following that, permeabilization of the cells were supplied with the addition of pre-prepared 0.1 percent (v/v) Triton X-100 in PBS. Cells were incubated with Triton X-100 for 10 minutes at RT. Then cells were washed with 1X PBS in 0.1 percent (w/v) Tween® 20 Detergent (PBS-T) for 5 minutes thrice. Non-specific binding of primary antibodies was inhibited by incubating cells in a blocking solution of 5 percent

(v/v) BSA (VWR Life Science) for 30 minutes at 4°C with gentle shaking. Again fixated cells were washed with PBS-T for 5 minutes thrice. Then they were incubated with primary antibodies of Anti-Collagen I antibody (ab34710, Abcam, USA), Anti-Fibronectin antibody (ab2413, Abcam, USA), ERK1/2 antibody (16443-1-AP, Proteintech, USA), SMAD3 antibody (25494-1-AP, Proteintech, USA) according to their respective dilutions as shown in table 2.5 overnight. The very next day antibodies were collected for further use and they were stored at -20°C. Meanwhile, cells were washed with PBS-T for 5 minutes thrice to remove any primary antibody remnants. Goat anti-rabbit IgGH&L (Alexa Fluor® 647) was used on cells as secondary antibody. For 1 hour, cells were incubated in dark with secondary antibody at 4°C with gentle shaking. To remove any secondary antibody remnants, cells were washed with PBS-T for 5 minutes thrice again. Again in dark, nucleus dye DAPI (ThermoFischer Scientific, USA) was given to the cells for 15 minutes at 4°C. Following the nucleus dye, cells were again washed with PBS-T for 5 minutes, twice. Then, any liquid from the surface was airdried and slides were closed with mounting medium (Sigma, USA) and cells were observed under Confocal Laser Scanning Microscope (Zeiss LSM 700, Germany).

Table 2.5. Antibody dilutions for immunocytochemistry analysis

Antibody	**Used Dilution**
Anti-Collagen I antibody (ab34710)	1:200
Anti-Fibronectin antibody (ab2413)	1:200
ERK1/2 antibody (16443-1-AP)	1:25
SMAD3 antibody (25494-1-AP)	1:25
goat anti-rabbit IgGH&L (ab150079)	1:500

2.2.17. Total Protein Isolation from Whole Cell Pellets

2 x 10^5 cells/well were grown seeded on 6-well plates and incubated at 37ºC in conditions mentioned in section 2.2.3. After overnight incubation, cells were given 100µg/ml pineapple exosomes in complete medium. Following day, cells were trypsinized including the treatment medium as well and centrifuged at 350 x g for 5 minutes. After washing the pellet with PBS, cells were pelleted and taken on ice. The cell pellet taken on ice treated with RIPA lysis buffer containing 1 percent (v/v) protease inhibitor cocktail, 1 mM PMSF and 1mM Na3VO4 for protein isolation. After 30 minutes incubation on ice, samples were centrifuged at 14,000 x g for 15 minutes in a precooled centrifuge. Supernatants were transferred into sterile Eppendorf tubes. Lowry Method was used to determine the concentrations of isolated proteins. Lowry method was performed according to the instructions mentioned in Section 2.1.2. Once the protein concentrations were acquired, 15 µg of proteins were aliquoted into Eppendorf tubes to prevent them from continuous freeze thaw cycles each time and stored at -80ºC.

2.2.18. Sodium Dodecyl-Sulfate Polyacrylamide Gel Electrophoresis (Sds-Page)

SDS-PAGE was used to separate isolated proteins according to their molecular weight. 2x Laemmli buffer was mixed with 20 µg of protein at 95ºC for 7 minutes and then spinned. Ready-to-use 4-20 percent Mini-PROTEAN TGX Protein Precast Gel (BioRad, USA) and they were placed into mini-PROTEAN Tetra cell Electrophoresis apparatus in a tank. The tank was filled with 1 x running buffer containing 192 mM glycine, 25 mM Tris pH 8.5 and 0.1 percent (w/v) SDS. Protein marker and the samples run at 90V at first and then at 120V for separation until the bromophenol blue dye reaches to the end.

2.2.19. Immunoblotting

After the proteins were separated on SDS-PAGE gel, they were transferred to the nitrocellulose membrane (0.22 µm) via wet blot transfer system. In order to use wet blot transfer, mini Trans-Blot Cell Blotting System was used. At first, sponge pads, whatman papers and the membrane were soaked into 1X transfer buffer composed of 192 mM glycine,

25 mM Tris-Base pH 8.3 and 20 percent(v/v) methanol. The sandwich model was established onto the black side following the order of sponge pad, whatman paper, gel, membrane, whatman paper and sponge pad. The sandwich is pressed together in the blotting cassette and placed into the blotting apparatus. The tank including an ice block was filled with 1X transfer buffer. The conditions for transfer are 350 mA for 1 hour. Immediately after the transfer ended, the membrane was blocked with 5 percent BSA in 1X Tris-Buffered Saline, 0.1 percent (w/v) Tween® 20 Detergent (TBS-T) buffer (1 M Tris-HCl pH 7.4, 9 per cent NaCl, and 0.5 percent Tween 20). After the blocking, appropriate antibodies were given in 5 percent BSA according to the dilutions given on table 2.6. Samples on primary antibodies were incubated overnight at 4ºC. For further use, antibodies were collected and stored at -20ºC. Membranes were washed with 1x TBS-T buffer for 5 minutes thrice. Appropriate secondary antibodies (anti-rabbit IgG or anti-mouse IgG) were prepared in 5 percent BSA in TBS-T. Membranes were then treated with secondary antibody for 1 hour. Membranes were taken into 1x PBS after the secondary antibody incubation and treated with ECL Substrate for 3 minutes at RT to be visualized via ChemiDoc XRS+Gel Imaging System (Bio-Rad Universal Hood 2, USA).

Table 2.6. Antibody dilutions for western blot analysis

Antibody	**Used Dilution**
AKT antibody (#9272)	1:1000
p-p38 antibody (#4511S)	1:1000
p-p44/42 antibody (#9101S)	1:1000
Anti-beta-actin antibody (STJ97714)	1:1000
Goat Anti-Rabbit IgG H&L (HRP) (ab6721)	1:2000

2.3. STATISTICAL ANALYSIS

All data presented in the results part (Section 3) were given in either means ± standard deviation (SD) or means ± standard error of the mean (SEM). Standard deviation of the experiments were calculated from three to ten independent experiments. Parametric statistics between 2 data set were compared using two-tailed multiple t-test. One-way analysis of variance (ANOVA) followed by Geisser-Greenhouse correction was used for more than 2 different conditions by using GraphPad Prism 6 (GraphPad Software, USA) and differences were considered statistically different where *$P \leq 0.05$, **$P \leq 0.01$. Tube formation and tube length analysis was conducted by Wimasis Image analysis.

3. RESULTS

3.1. EXOSOME CHARACTERIZATION BY SURFACE ANTIGEN DETECTION VIA FLOW CYTOMETRY

Exosome characterization was performed according to the surface proteins found on their membranes. These surface markers are tetraspanin proteins of CD9, CD63, and HSP70 which are found in high amounts on the exosome membrane. Presence of these markers were detected by using magnetic beads that were coated with their appropriate antibodies against these proteins (Figure 3.1). Negative control was used as beads with no exosomes and other beads of CD9, CD63, nad HSP70 was tested positive for exosomes at 94 percent, 97 percent and 85 percent respectively.

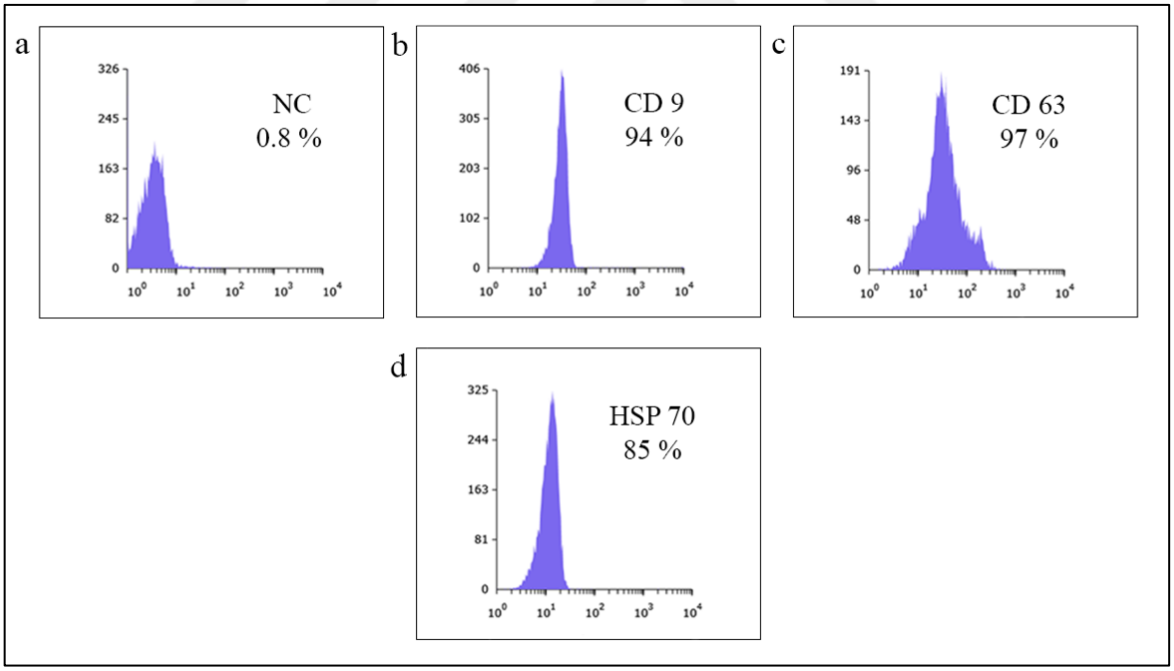

Figure 3.1. Characterization of *A. comosus* exosomes via flow cytometry. (a) Representative flow cytometry of negative control, 0.8± 0.91 percent (b) Representative flow cytometry of CD9 protein found on the exosomes, 94±0.1 percent, (c) Representative flow cytometry of CD63 protein found on the exosomes, 97± 2.61 percent, (d) Representative flow cytometry of HSP70 protein found on the exosomes, 85± 3.14 percent.

3.2. EXOSOME SIZE AND PARTICLE NUMBER DETECTION VIA NTA

NTA was used to detect the variety of the exosome size and particle concentration while observing the Brownian motion of exosome. According to graph 3.2 size of the exosomes are averaged with a mean of 149.6±9.3 nm and mode at 163.6±12.7. On the other hand, exosome concentration were determined as 4.59 x 10^8±9.41 x 10^7 particles/ml and particle number by frame was 2.9 ± 0.7 particles/frame (Figure 3.2).

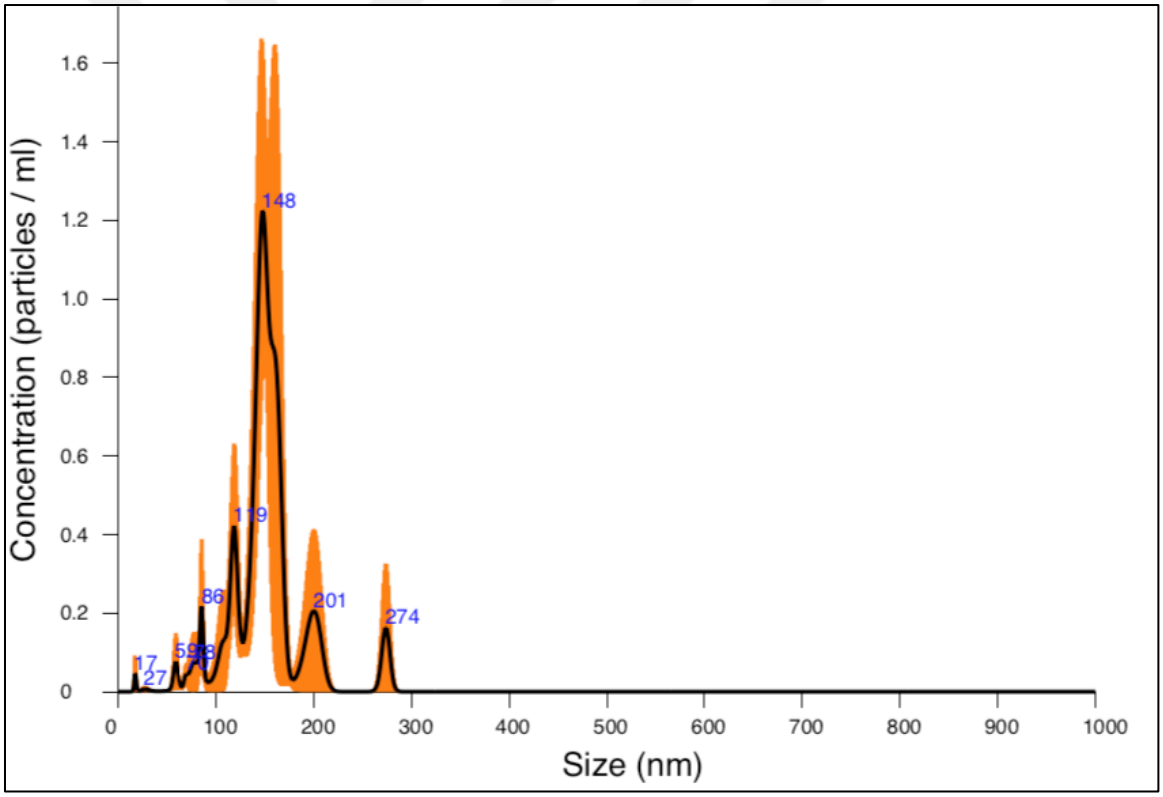

Figure 3.2. Nanoparticle tracking analysis results showing averaged finite track length adjustment concentration / size.

3.3. TIME DEPENDENT CELLULAR UPTAKE OF EXOSOMES

Functionality of the *A. comosus* derived exosomes were determined by time dependent cellular uptake to see if these exosomes may be taken by dermal cells as a sign of cross-kingdom communication. Isolated exosomes were dyed with PKH67 dye and given to keratinocytes, endothelial cells and fibroblasts. Internalization of exosomes was observed at various time points with fluorescence microscopy. The results displayed that exosome internalization has started about an hour past the treatment and the intensity of exosomes gradually increases at $2^{nd,}$, 3^{rd}, 4^{th}, 6^{th}, 12^{th} and 24^{th} hours in keratinocytes and endothelial cells (Figure 3.3, Figure 3.4). Fibroblasts exhibit strong Exosomal uptake at both 12^{th} and 24^{th} hours after treatment (Figure 3.5). However, both exosome intensity and number start to fade during 48^{th} hour among HaCaT and HUVEC cells.

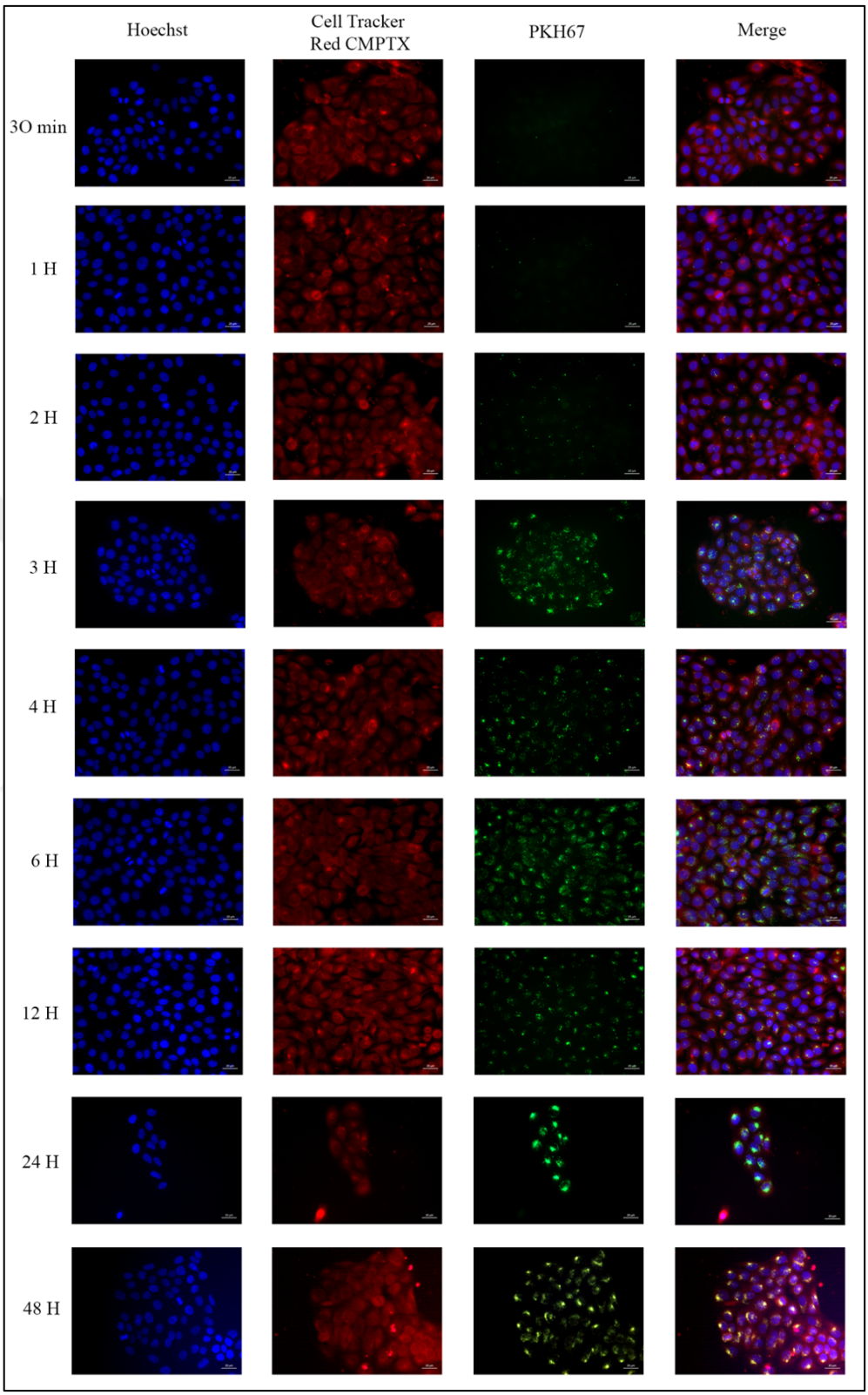

Figure 3.3. Time dependent exosome uptake of HaCaT cells. (40X magnification, scale bar at 20µm.

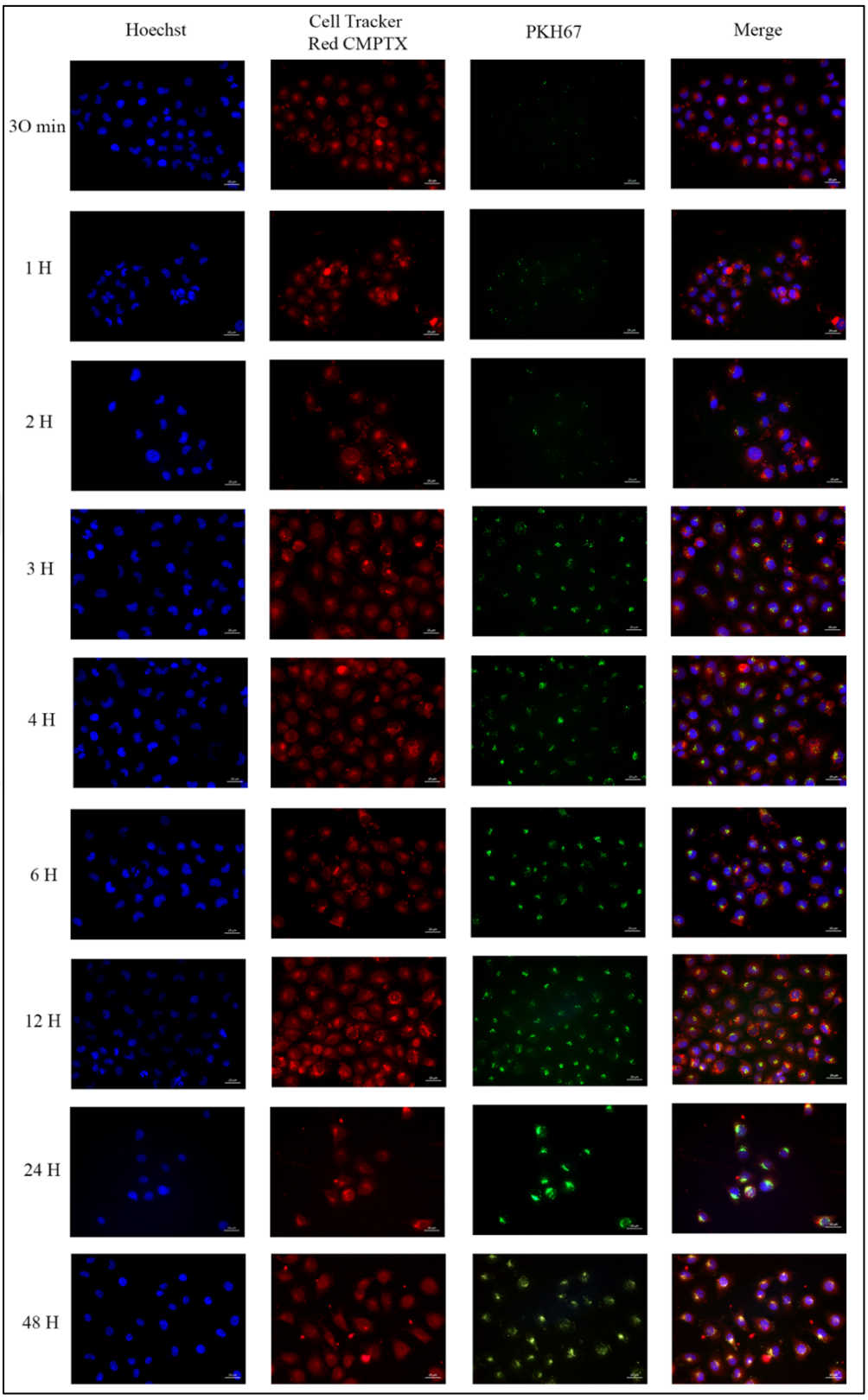

Figure 3.4. Time dependent exosome uptake of HUVEC cells. (40X magnification, scale bar at 20µm

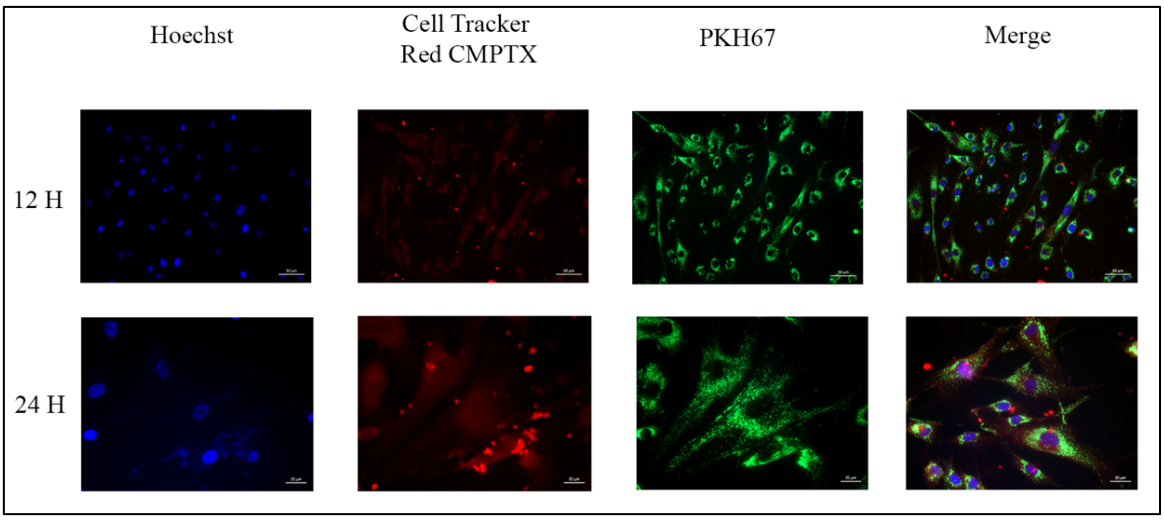

Figure 3.5. Time dependent exosome uptake of fibroblast cells. (40X magnification, scale bar at 20µm

3.4. CELL PROLIFERATION

Upon characterization, the effect of the exosomes on dermal cells (HaCaT, HUVEC, and Fibroblast) were determined with MTS assay, which depends on the mitochondrial activity. Results revealed that increasing doses of the exosomes significantly increase the cell proliferation and viability.

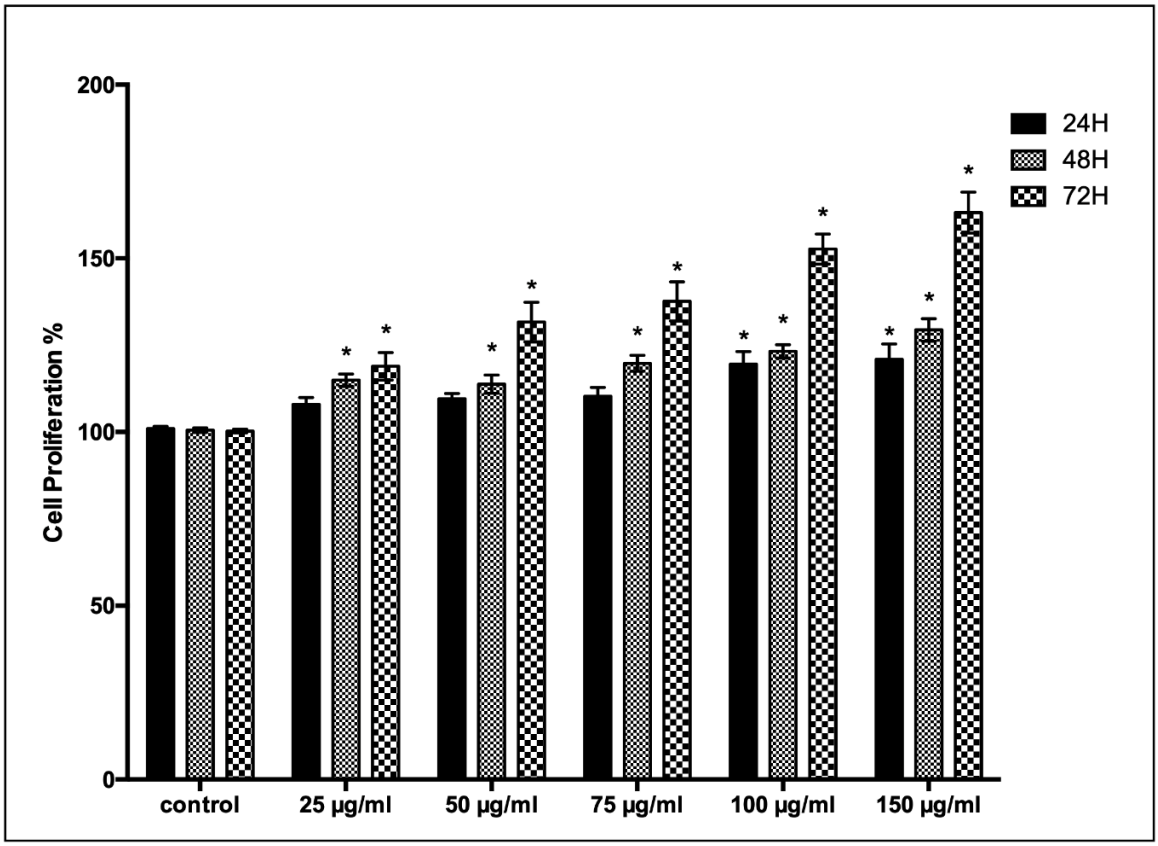

Figure 3.6. The effects of *A. comosus* exosomes on HaCaT cell proliferation. Control is negative control performed with complete growth medium, *P<0.05, control was accepted 100 percent for each day respectively.

Although low doses of exosomes up to 75 µg/ml did not cause a significant increase in the cell number within 24 hour, both 100 µg/ml and 150 µg/ml exosome application cause up to 30 percent significant increase in the cell number within the first day. A significant increase in the cell number is apparent for concentrations between 25 and 150 µg/ml exosomes during the 48 hour time period with respect to their growth medium treated controls (P<0.05). However, up to 70 percent of increase in the cell number among HaCaT cells is particularly evident for specific 100 and 150 µg/ml exosome treatments. While exosome treatment caused a significant differences for the most part of the treatments, the only statistical difference between experimental groups was that of between 24 hour and 72 hour (Figure 3.6) (P<0.05).

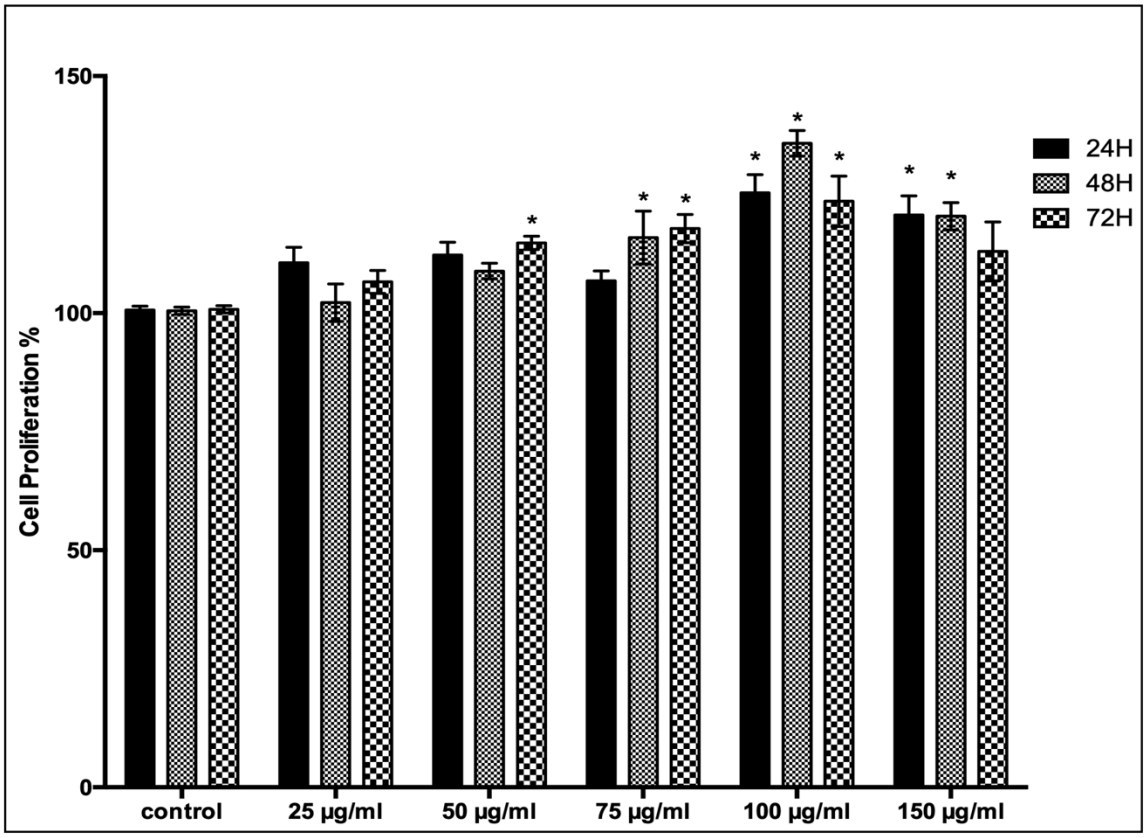

Figure 3.7. The effects of *A. comosus* exosomes on HUVEC proliferation. Control is negative control performed with complete growth medium, *P<0.05, control was accepted 100 percent for each day respectively.

On the first day of the treatment, HUVEC cells did not demonstrate a significant increase in the cell number for lower doses (25 to 75 µg/ml), however higher doses (100 and 150 µg/ml) of the exosome treatment cause a significant proliferation rate among cells starting from 24th hour. Although 50 µg/ml exosome treatment causes up to 10 percent significant increase on the 72nd hours, application of 100 µg/ml exosome led to approximately 35 percent of cell number increase among endothelial cells at 48th hour (P<0.05). Conversly, 150 µg/ml exosome application significantly increased the cell number for the first 2 days however, it did not cause any significant increase on day 3 (Figure 3.7). Contrarily to HaCaT cells, there was no significant difference between any day (P<0.05).

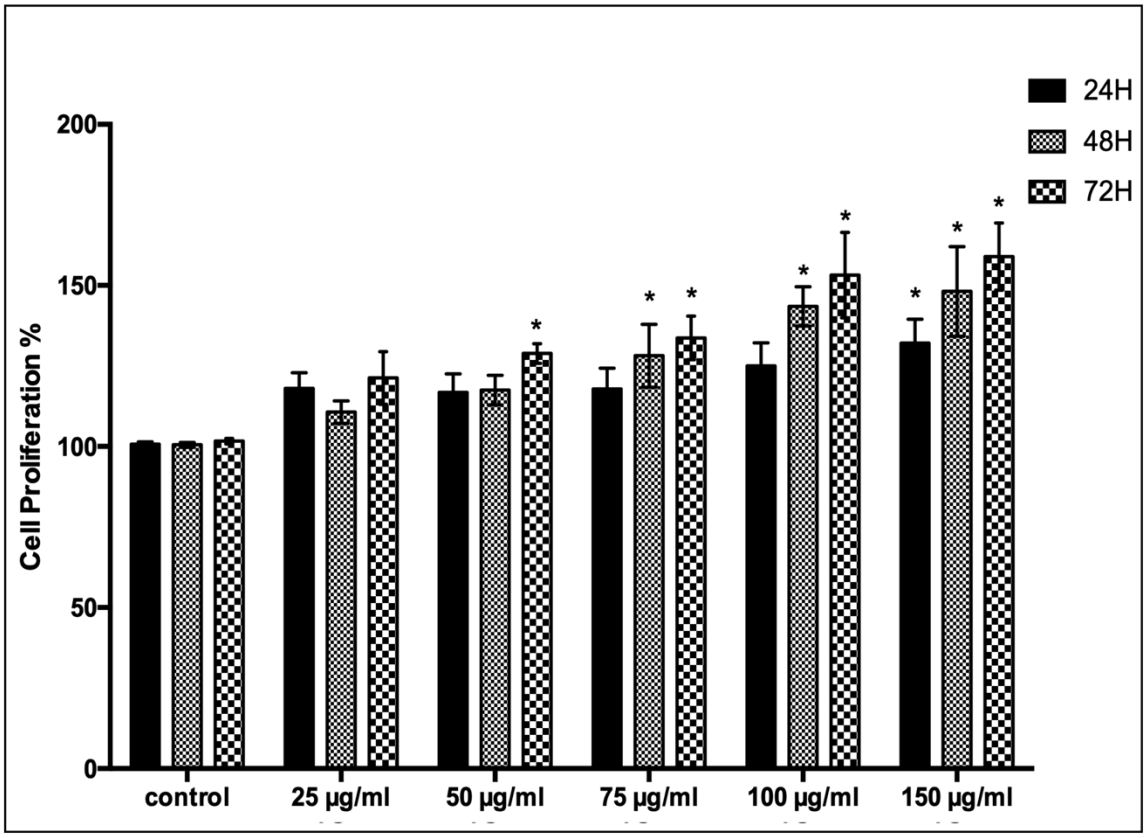

Figure 3.8. The effects of *A. comosus* exosomes on fibroblast cell proliferation. Control is negative control performed with complete growth medium, *P<0.05, control was accepted 100 percent for each day respectively.

Just like HaCaT and HUVEC cells, proliferation of human fibroblasts did not significantly changed with the application of lower doses (25 µg/ml and 50 µg/ml) of exosome treatment during 24 and 48th hours. However, fibroblast cell number significantly increased with 50 µg/ml exosome treatment on day 3. Regardless, 100 µg/ml exosome treatment caused a significant increase for each day and nearly 45 percent more cell proliferation was observed on the 48th hour of the treatment (Figure 3.8) (P<0.05).

3.5. CELL CYCLE ANALYSIS

To evaluate how *A. comosus* exosomes affect dermal cell proliferation, cell cycle analysis was carried out. Cell cycle analysis of HaCaT, HUVEC and fibroblasts were determined at

12^{th}, 24^{th} and 48^{th} hours after exosome treatment with a growth medium treated control. According to the results, application of exosomes did not change significantly any phases of the cell division for the first 12^{th} hour. However, during the 24^{th} hour, number of cells in the M phase increased by 21 percent significantly with respect to control cells which were treated with growth medium. When the cells reach to 48^{th} hour, no significant difference between the phases was observed. However cell number that was in G0-G1 phase was higher among exosome treated cells (Figure 3.9).

HUVEC cells, on the contrary, responded to 100 µg/ml exosome treatment straight away. The number of cells in the G2-M phase were significantly rose by 13 percent while that of in the S phase significantly decreased by 16 percent. Moreover, at 24^{th} hour, number of cells in phases significantly increases by 4 and 6 percent respectively. Interestingly no significant change was observed at 48^{th} hour between treated and control cells (Figure 3.10).

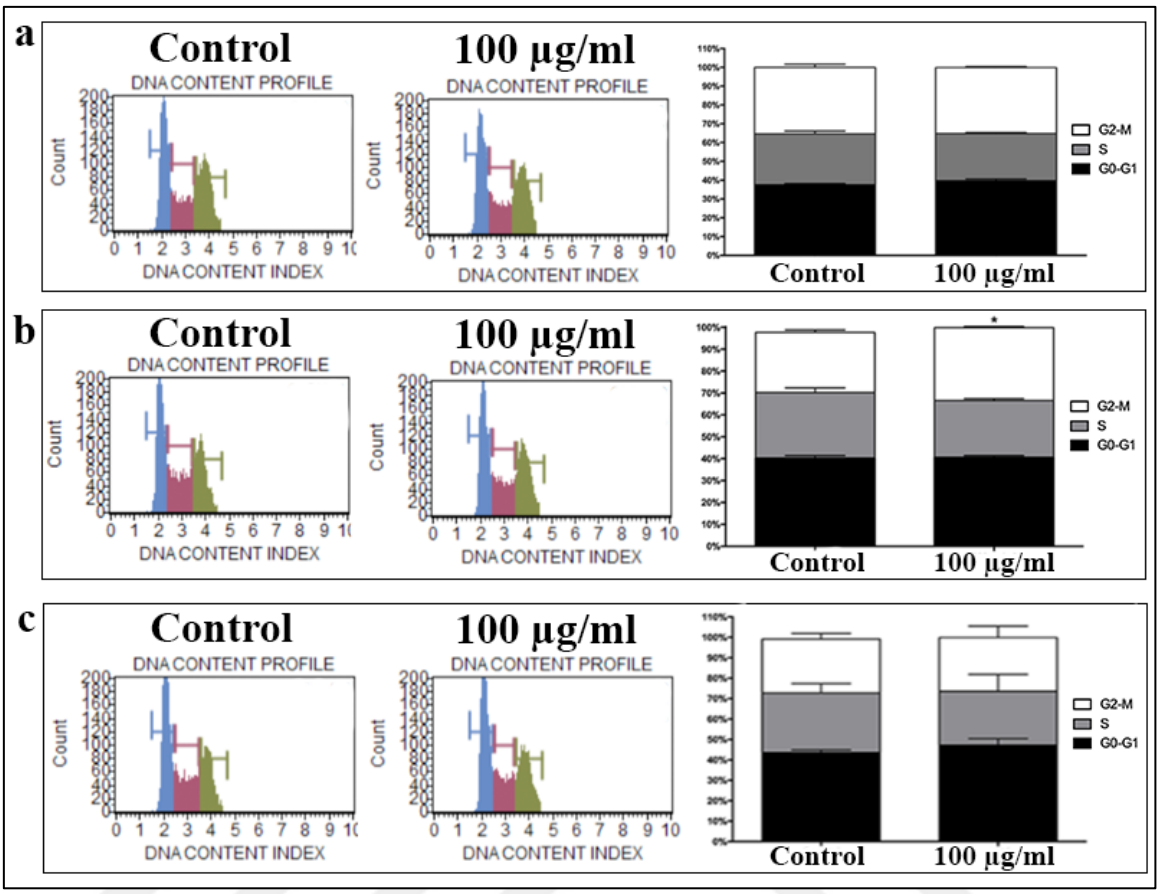

Figure 3.9. Cell cycle analysis of HaCaT cells upon exosome treatment. (a) Cell cycle results of HaCaT cells at 12th hour. (b) Cell cycle distribution of HaCaT cells at 24th hour. (c) Cell cycle distribution of HaCaT cells at 48th hour. Data are shown with ± SEM, n=4, *P<0.05

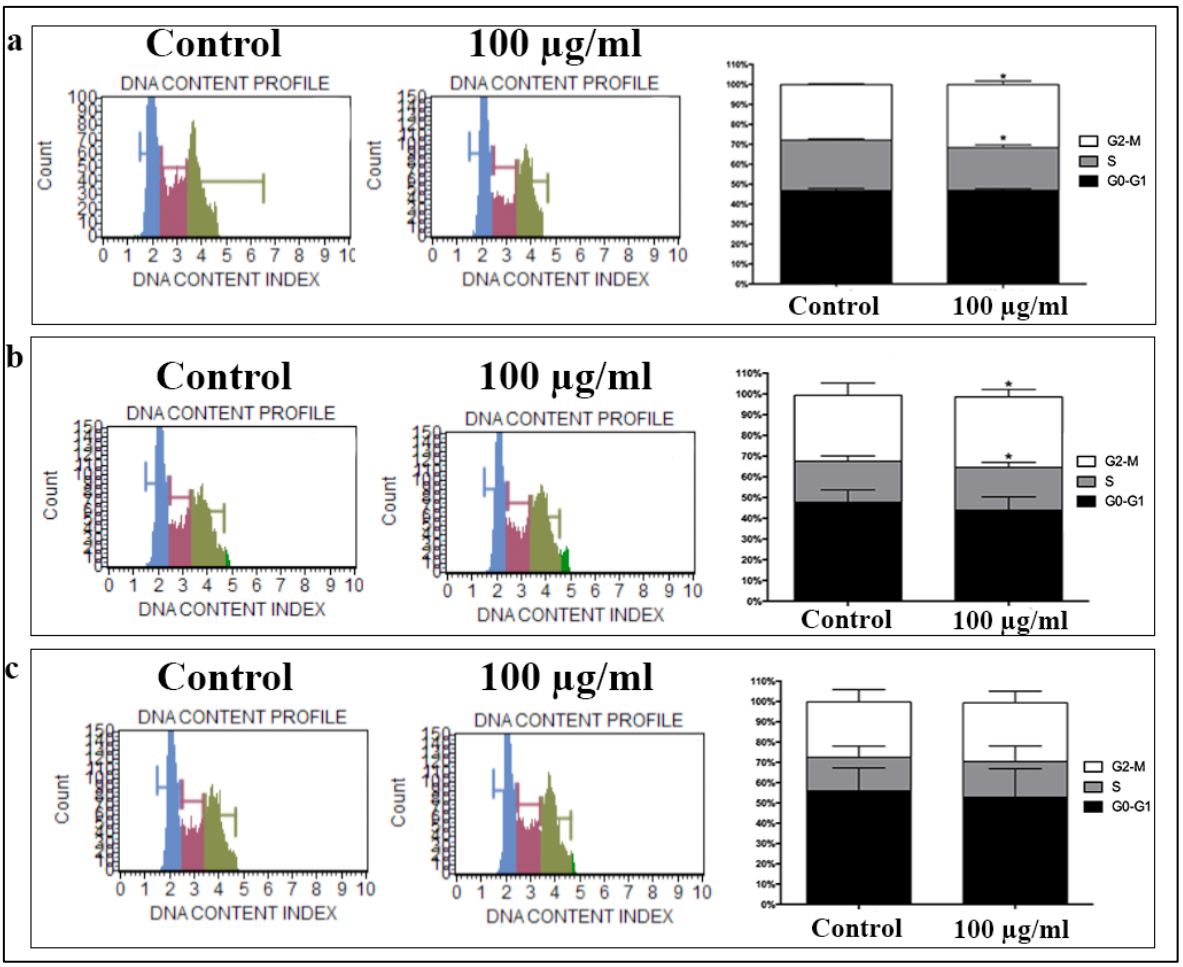

Figure 3.10. Cell cycle analysis of HUVECs upon exosome treatment. (a) Cell cycle distribution of HUVECs at hour 12th. (b) Cell cycle distribution of HUVECs at hour 48th. (c) Cell cycle distribution of Fibroblasts at 48th hour. Data are shown with ± SEM, n=4, *P<0.05

Upon treatment with 100 µg/ml of exosomes, fibroblasts immediately transitioned to S phase from G0-G1 phase. Cell number that are in the S phase rose by 29 percent. Later on, percentage of cells found at both S and G2-M phases significantly increased by 18 percent and 3 percent at 24th hour. Similarly to other 2 cell lines, no significant change between control and treated cell cycles at 48th hour was seen (Figure 3.11).

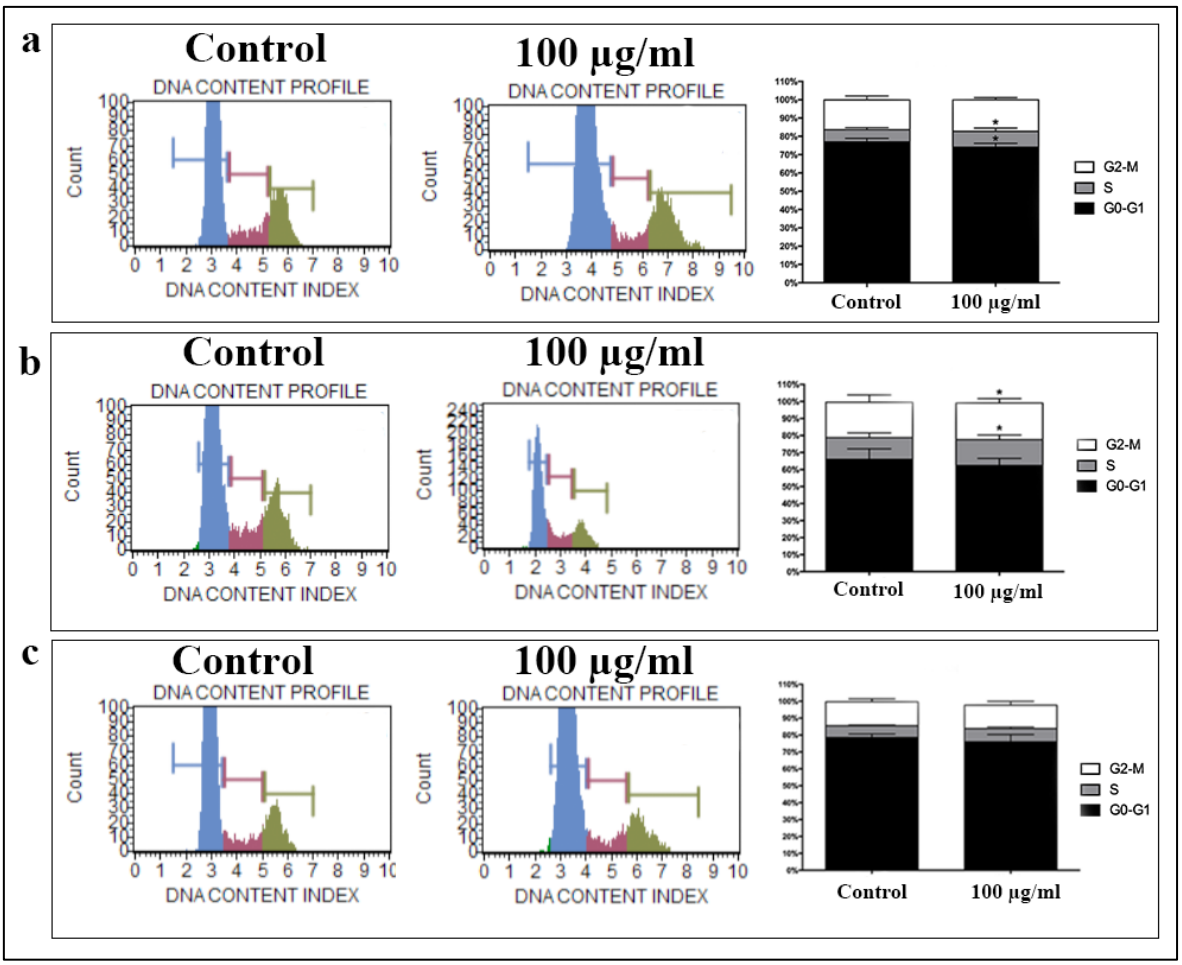

Figure 3.11. Cell cycle analysis of fibroblasts upon exosome treatment. (a) Cell cycle results of Fibroblasts at 12th hour. (b) Cell cycle results of Fibroblasts at 24th hour. (c) Cell cycle results of Fibroblasts at 48th hour. Data are shown with ± SEM, n=4, *P<0.05

3.6. SCRATCH ASSAY

Scratch assay was conducted with the object of detecting the effects of pineapple exosomes on cell migration and wound closure. For that purpose, both 50- and 100 µg/ml of exosomes which were shown by MTS analysis results to have proliferative effects on dermal cells were used.

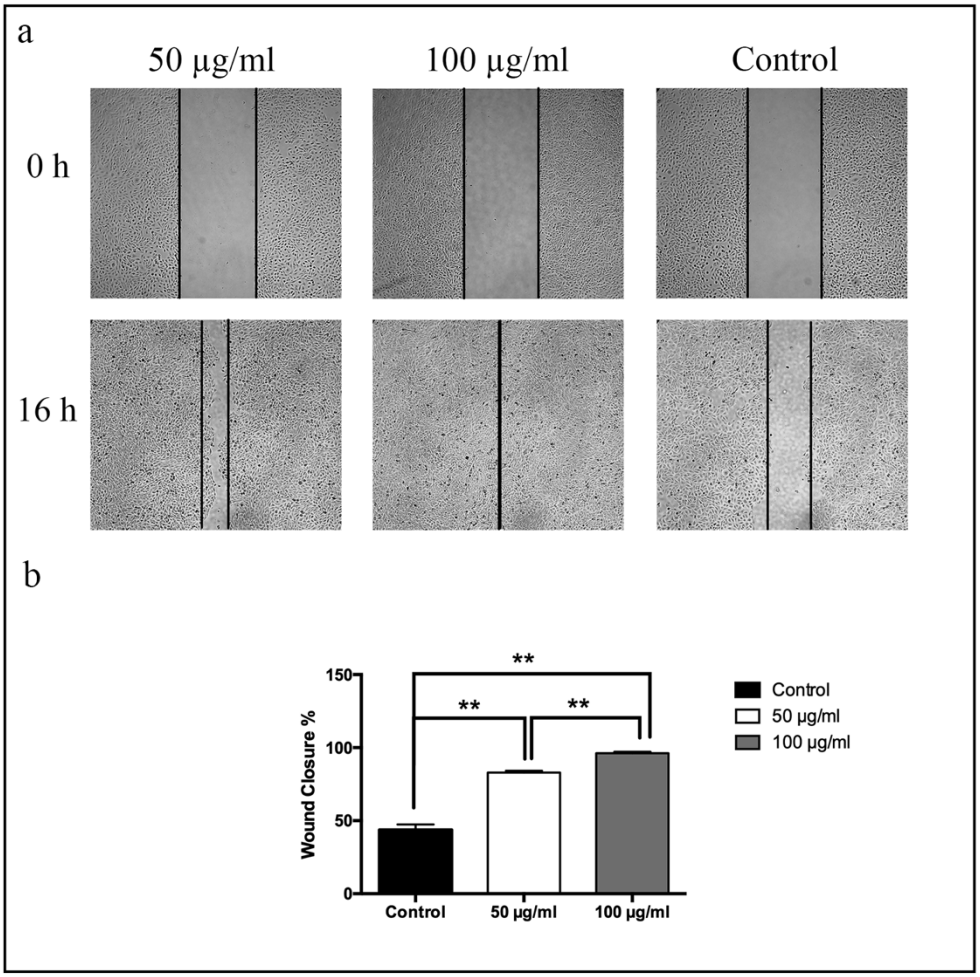

Figure 3.12. Scratch assay analysis of HaCaT cells. (a) Representative images of *A. comosus* treated HaCaT cells at 0- and 16-hour. (b) Wound closure rates of HaCaT cells treated with exosomes. Data are shown with ± SD, n=10, **P<0.01.

Results displayed that 50 and 100 µg/ml of exosome treatment on HaCaT cells resulted in 82.78±1.315 percent and 96.18 ± 1.045 percent closure rates of the wound while growth medium treated control cells only showed 43.67±3.747 percent wound closure rate within 16 hour. Migration rate of the 100 µg/ml exosome treatment was significantly higher than that of 50 µg/ml treatment in addition to significant difference between control and both treatments (Figure 3.12).

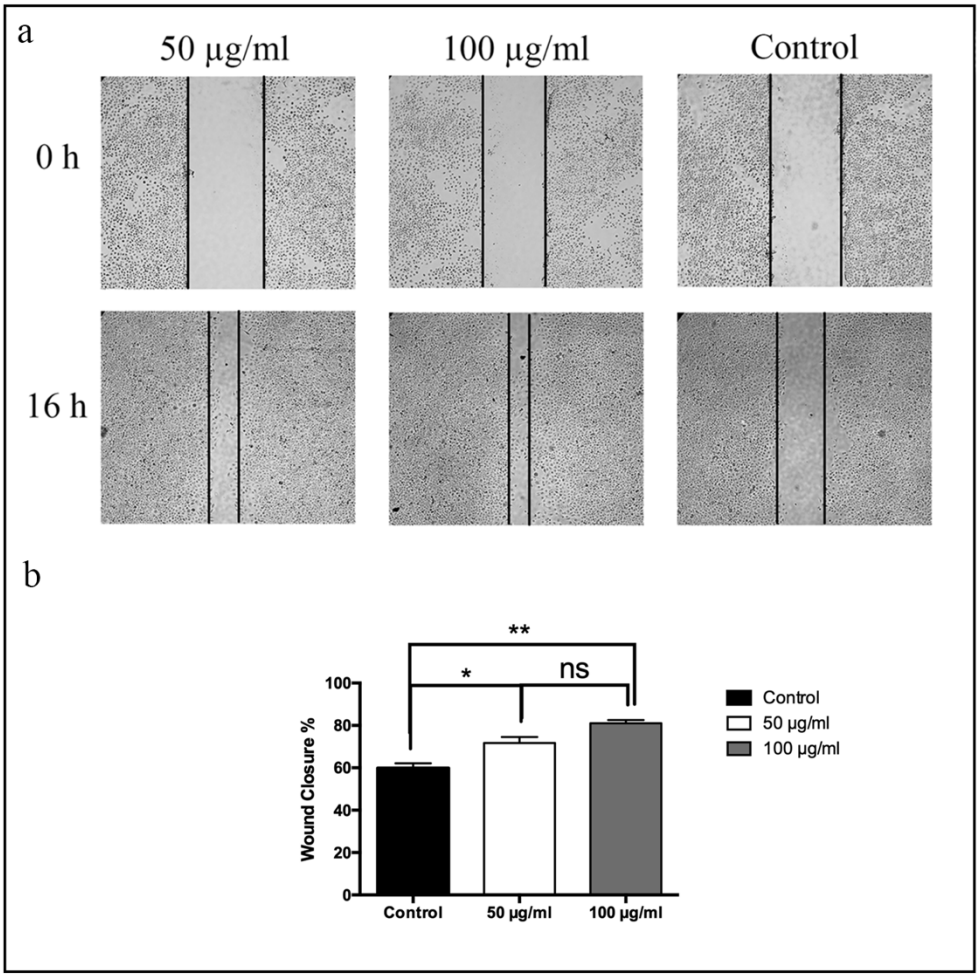

Figure 3.13. Scratch assay analysis of HUVEC cells. (a) Representative images of *A. comosus* treated HUVEC cells at 0- and 16-hour. (b) Wound closure rates of HUVEC cells treated with exosomes. Data are shown with ± SD, n=10, *P<0.05, **P<0.01, ns: non-significant.

Results revealed that 50 and 100 µg/ml of exosome treated HUVEC cells showed 71.74±2.799 percent and 81.06 ± 1.458 percent closure rate of the wound while growth medium treated control cells only showed 59.87 ± 2.240 percent wound closure rate within 16 hour. Although closure rates of 50 µg/ml and 100 µg/ml treatments did not significantly differ, both treatments caused a significantly higher closure rates than that of growth medium treated control (Figure 3.13).

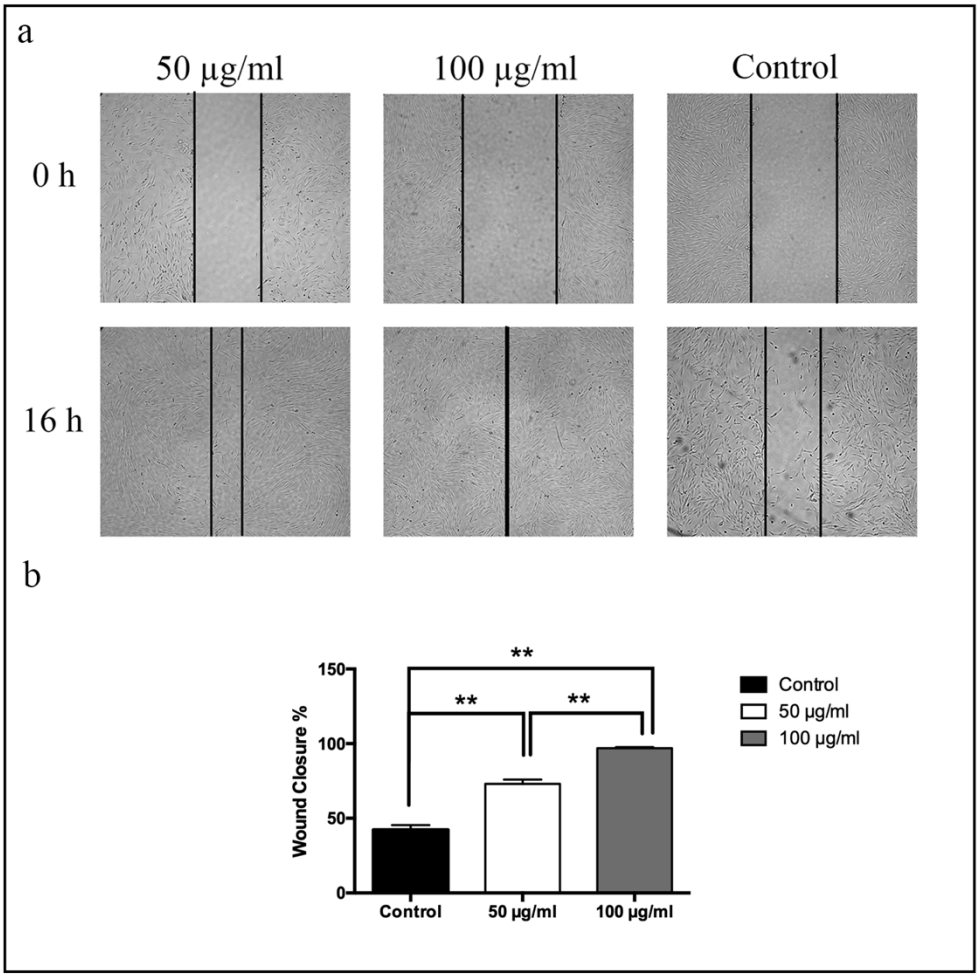

Figure 3.14. Scratch assay analysis of fibroblast cells. (a) Representative images of *A. comosus* treated fibroblasts at 0- and 16-hour. (b) Wound closure rates of Fibroblasts treated with exosomes. Data are shown with ± SD, n=10, **P<0.01.

Results revealed that 50 and 100 µg/ml of exosome treated fibroblast cells showed 73.12±2.828 percent and 96.92 ± 0.7735 percent closure rate of the wound while growth medium treated control cells only showed 42.35 ± 3.054 percent wound closure rate within 16 hour. Migration rate of the 100 µg/ml exosome treatment was significantly higher than that of 50 µg/ml treatment in addition to significant difference between control and both treatments (Figure 3.14).

3.7. TRANSMEMBRANE CELL INVASION ASSAY

Trans membrane cell invasion assay was done to detect the chemoattractant properties of the *A. comosus* exosomes to evaluate whether they induce cell motility among dermal cells. Results showed that, upon 100 µg/ml exosome treatment, invaded Hacat cell number rose from approximately 13 cell/view to 436 cells/view (Figure 3.15).

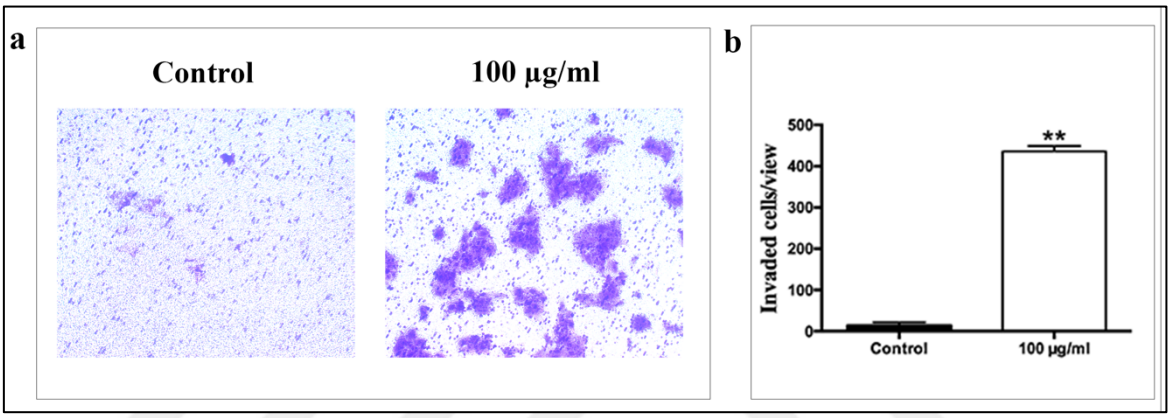

Figure 3.15. Transmembrane cell invasion assay of HaCaT cells. (a) Representative transmembrane invasion images of HaCat cells. (b) Invaded cell per view of HaCaT cells. Data are shown with ± SD, n=5, **P<0.0001

Number of HUVEC cells invaded to the exosome containing medium from control treated medium rose from approximately 147 cells/view to 578 cell/view (Figure 3.16).

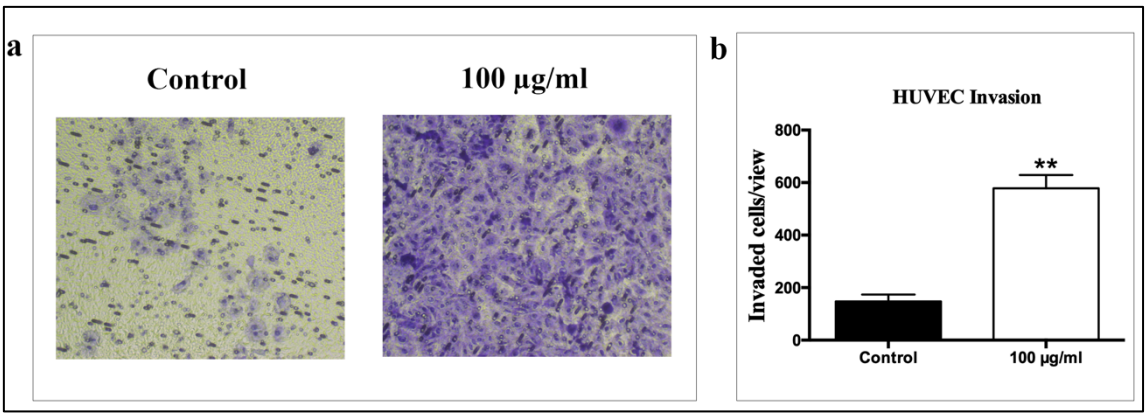

Figure 3.16. Transmembrane cell invasion assay of HUVEC cells. (a) Representative transmembrane invasion images of HUVEC cells. (b) Invaded cell per view of HUVEC cells. Data are shown with ± SD, n=5, **P<0.0001

3.8. TRANSMEMBRANE CELL MIGRATION ASSAY

The effects of *A. comosus* exosomes on cell migration was detected by transmembrane migration assay was also performed. Results revealed that while nearly 1080 HaCaT cells migrate to the to the control medium present well, nearly 4600 cells migrate to exosome present medium within 24 hours (Figure 3.17).

In line with migration results of HaCaT cells, HUVEC cells are also affected with the exosome treatment and nearly doubles its migration rates from 486 cell/view to 881 cells/view (Figure 3.18).

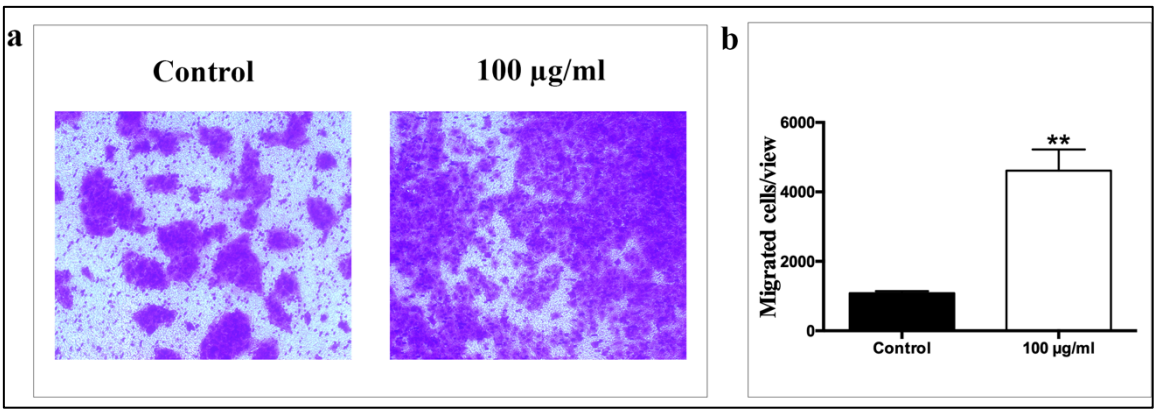

Figure 3.17. Transmembrane cell migration assay of HaCaT cells. (a) Representative transmembrane migration images of HaCaT cells. (b) Migrated cell per view of HaCaT cells. Data are shown with ± SD, n=3, **P<0.005

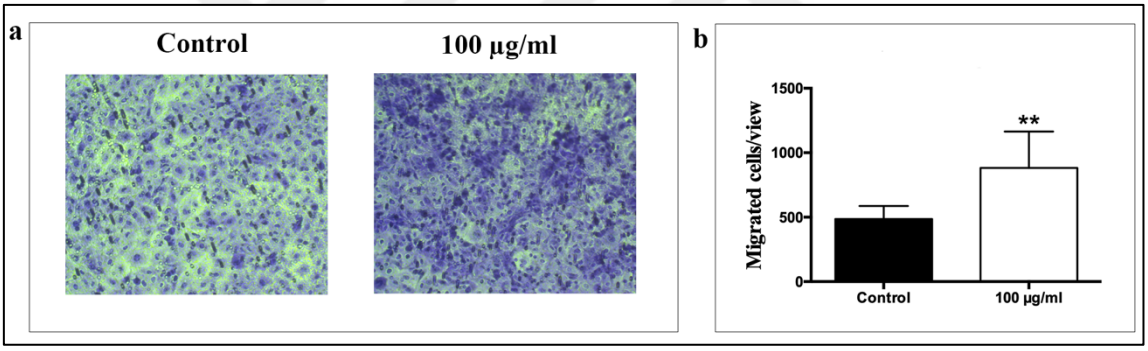

Figure 3.18. Transmembrane cell migration assay of HUVEC cells. (a) Representative transmembrane migration images of HUVEC cells. (b) Migrated cell per view of HUVEC cells. Data are shown with ± SD, n=6, **P<0.005

3.9. CELLULAR REACTIVE OXYGEN SPECIES (ROS) DETECTION

ROS detection was performed upon exosome treatment and detected by conversion of 2',7' –dichlorofluorescin diacetate (DCFDA) to a fluorescence dye 2', 7' –dichlorofluorescein (DCF) with two different concentrations of DCFDA (1- and 10 µM). When HaCaT cells treated with 1 µM of DCFDA without no exosome treatment, florescence intensity of positive control cells was at 34.30 percent while ROS production of 50 µg/ml and 100 µg/ml

exosome treatment reduced the fluorescence intensity to 28.07 percent and 5.88 percent respectively. On the other hand, when HaCaT cells were processed with 10 µM of DCFDA, positive control cells were 94.54 percent positive. Upon exosome treatment positive cells were 95.07 percent and 68.85 percent respectively (Figure 3.19).

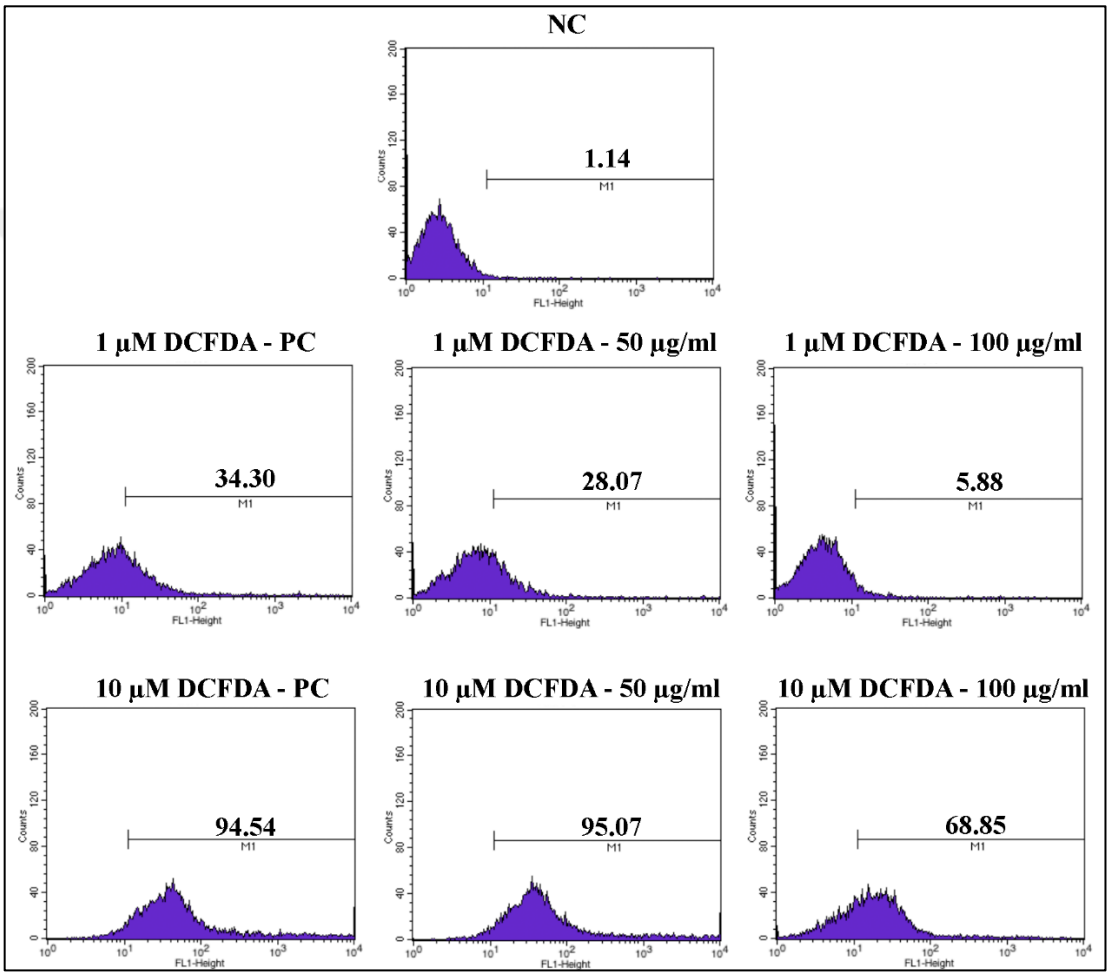

Figure 3.19. Detected ROS measured within HaCaT cells. Abbreviations: PC: Positive Control, NC: Negative Control, DCFDA: 2',7' –dichlorofluorescin diacetate.

HUVEC cells, on the other hand, were 46.82 percent positive when treated with 1 µM DCFDA. Cell percentage was evaluated at 46.65 percent and 96.44 percent upon 50 µg/ml and 100 µg/ml exosome treatment respectively when 1 µM DCFDA applied. When 10 µM DCFDA was applied to HUVEC cells, 98.98 percent of cells were positive as a control.

Upon 50- and 100 µg/ml exosome treatment, percentage of the cells were detected at 98.90 percent and 30.11 percent respectively (Figure 3.20).

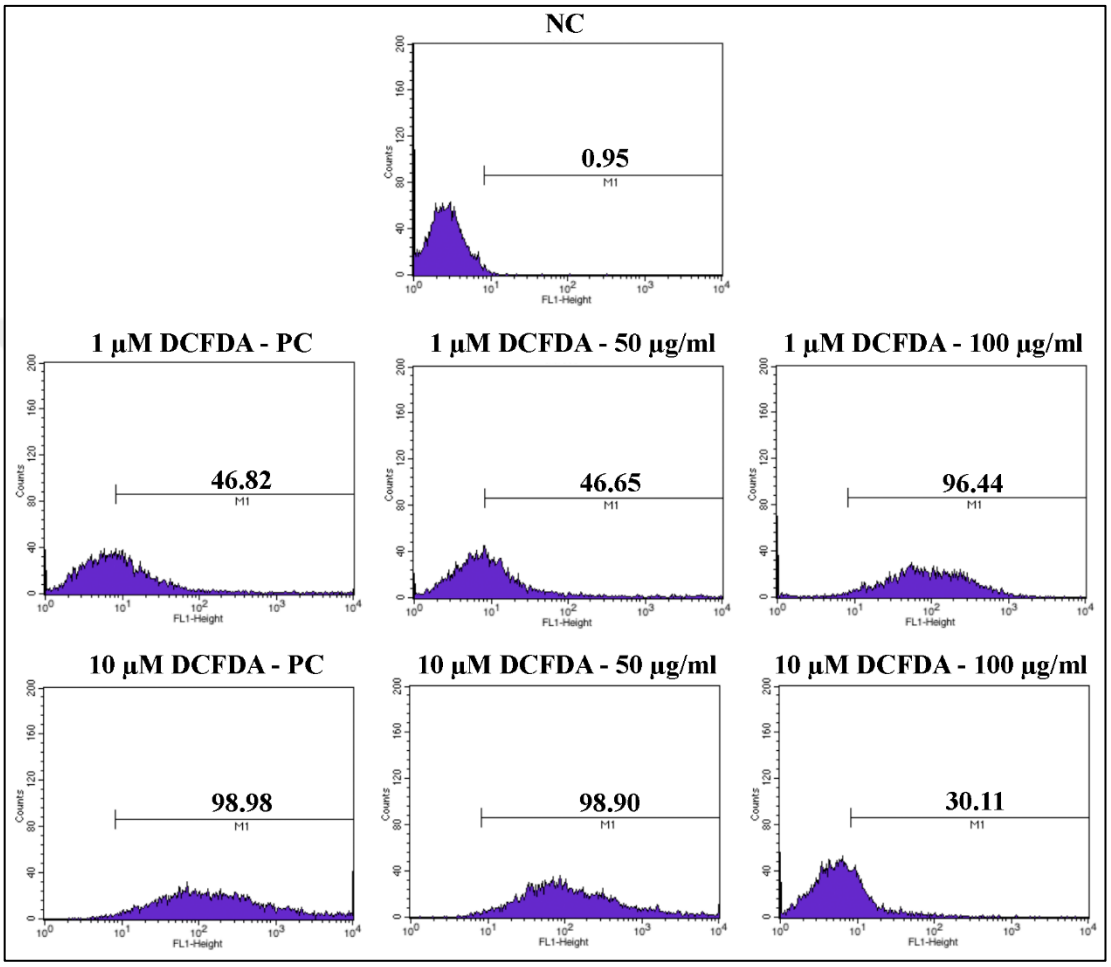

Figure 3.20. Detected ROS measured within HUVEC cells. Abbreviations: PC: Positive Control, NC: Negative Control, DCFDA: 2',7'–dichlorofluorescin diacetate.

3.10. ANGIOGENESIS ASSAY

Seeded on Matrigel, HUVEC cells were either given growth medium as a control or 100 µg/ml of *A. comosus* exosome and their tube formation ability as well as length of the tubes were determined at 7th and 20th hours. Although length of the tubes significantly increases from 39589 ± 112,5 to 41826,5 ± 154,5 during 7th hour, no significant difference was

observed at 20th hour. Moreover, tube number was significantly higher upon exosome treatment at 7th hour where control group has 225,5 ± 10,6066 while treated group has 270,5 ± 21,92031 tube number. On the other hand, at 20th hour there was no statistical changes in tube numbers (Figure 3.21).

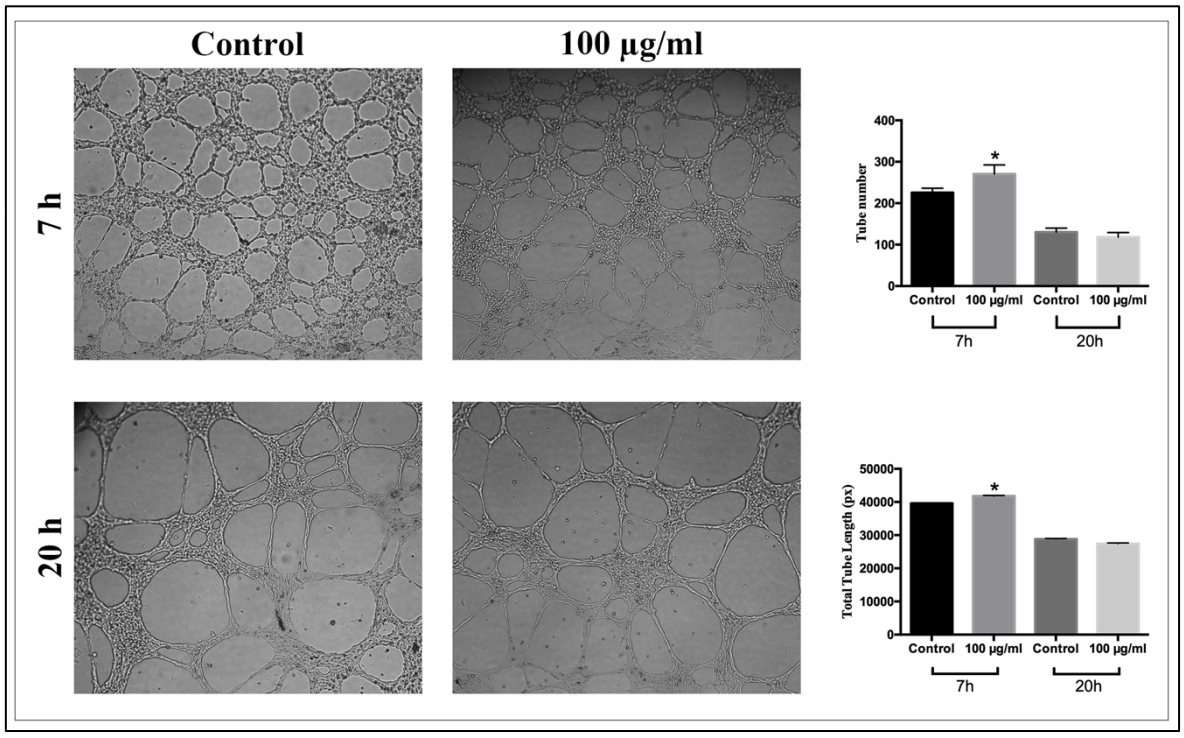

Figure 3.21. Effect of 100 µg/ml *A. comosus* exosome on tube formation ability of HUVEC cells at 7th and 20th hours. Results were analysed by two-tailed multiple t tests. Data are shown with ± SD, n=5, *P<0.05.

3.11. RT-PCR ANALYSIS

To comprehend the molecular mechanisms that *A. comosus* exosomes affect, dermal cells (HaCaT and Fibroblast) were subjected to 100 µg/ml of exosomes for 16 hours and then wound healing associated genes along with those related in scar formation was assessed with RT-PCR. Results indicate that upon treatment with 100 µg/ml of exosomes, col1A1, MMP2 and TGF-β1 levels did not significantly changed however, COL3A1, MMP9 and TGF-β3

levels rose by 3-,4- and 2 folds respectively. With that, ratio of COL3A1 to col1a1 rose 3.33 fold and that of TGF-β3 to TGF-β1 rose by 5 folds. Nevertheless, as another important regulator in scar formation fibromodulin remains unaffected upon treatment. On the other hand, wound healing related genes such as AKT, vimentin and laminin gene expression levels increased by 6-, 4- and 3 folds respectively while α-SMA mRNA expression levels significantly decrease by 4 folds upon exosome treatment (Figure 3.22).

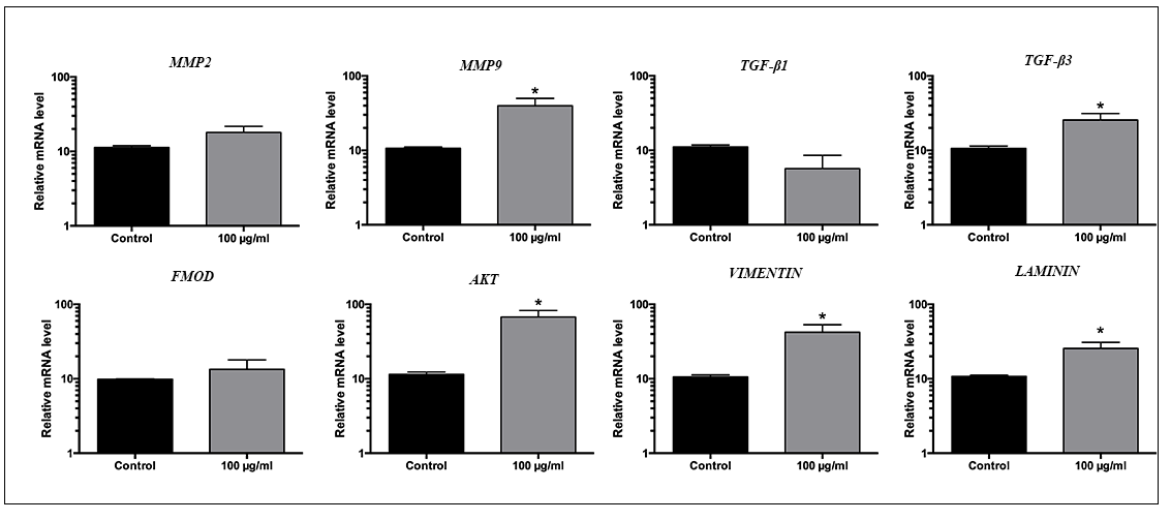

Figure 3.22. mRNA expression levels of HaCaT cells upon 100 µg/ml exosome treatment. Abbreviations: MMP2: Matrix metalloproteinase-2, MMP9: Matrixmetalloproteinase-9, TGF-β1: Transforming Growth Factor beta 1, TGF-β3: Transforming Growth Factor beta 3, FMOD: fibromodulin, AKT: Protein kinase B. Results were analysed by two-tailed multiple t tests. Data are shown with ± SEM, n=6, *P<0.05.

HUVEC cells when treated with 100 µg/ml of exosomes, MMP2 levels did not significantly change while MMP9 expression levels upregulated by 5 folds upon 24 hours of exosome treatment in addition to 5 folds of increase in fibromodulin expression levels. mRNA expression of AKT did not significantly change besides to apparent 4 fold increase (Figure 3.23).

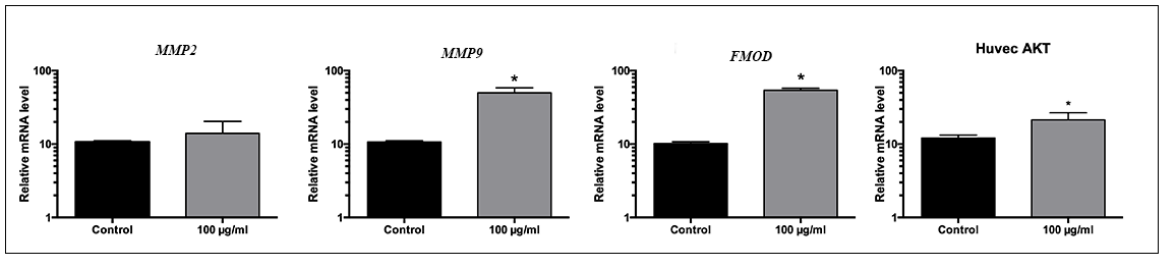

Figure 3.23. mRNA expression levels of HUVEC cells upon 100 µg/ml exosome treatment. Abbreviations: MMP2: Matrix metalloproteinase-2, MMP9: Matrixmetalloproteinase-9, FMOD: fibromodulin, AKT: Protein kinase B. Results were analysed by two-tailed multiple t tests. Data are shown with ± SEM, n=6, *P<0.05.

Fibroblasts when treated with 100 µg/ml of exosomes showed a significant downregulation in scar formation related genes of COL1A1 and TGF-β1 mRNA expressions by 6- and 8 folds. On the other hand, COL3A1 and TGF-β3 mRNA expressions upregulated by 4 folds each. Moreover, MMP2 mRNA expression downregulated by 4 fold while MMP9 and AKT mRNA expression levels are upregulated by 5 folds upon exosome treatment. Fibromodulin and Vimentin mRNA expression levels also increased by 4- and 2 folds. Interestingly, mRNA expression levels of Laminin decreases 6 fold in addition to 4 fold downregulation of α-SMA mRNA expression level (Figure 3.24).

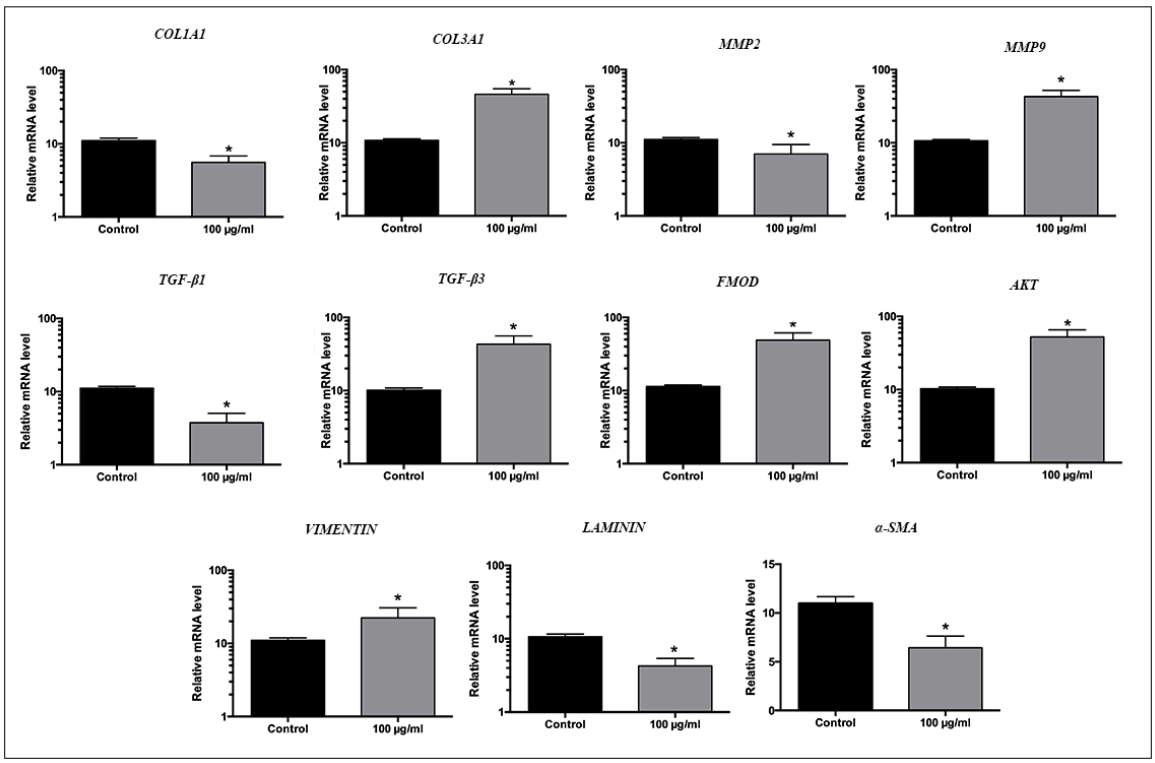

Figure 3.24. mRNA expression levels of fibroblast cells upon 100 µg/ml exosome treatment. Abbreviations: COL1A1: Collagen type I alpha 1, COL3A1: Collagen type III alpha 1, MMP2: Matrix metalloproteinase-2, MMP9: Matrixmetalloproteinase-9, TGF-β1: Transforming Growth Factor beta 1, TGF-β3: Transforming Growth Factor beta 3, FMOD: fibromodulin, AKT: Protein kinase B, α-SMA: alpha smooth muscle actin. Results were analysed by two-tailed multiple t tests. Data are shown with ± SEM, n=6, *P<0.05.

3.12. ENZYME-LINKED IMMUNOSORBENT ASSAYS

3.12.1. Human MMP1 Elisa

Human MMP1 ELISA was performed to evaluate MMP1 levels on dermal cells upon exosome application. According to the results derived from the assay, MMP1 expression level significantly upregulated to 4411.133 ± 455.341 pg/ml from 750.333 ± 32.416 pg/ml when treated with 100 µg/ml of *A. comosus* exosomes. Moreover, MMP1 expression level

of fibroblasts also upregulated to 3394.667 ± 150.512 pg/ml from 2853.033 ± 180.525 pg/ml. (Figure 3.25).

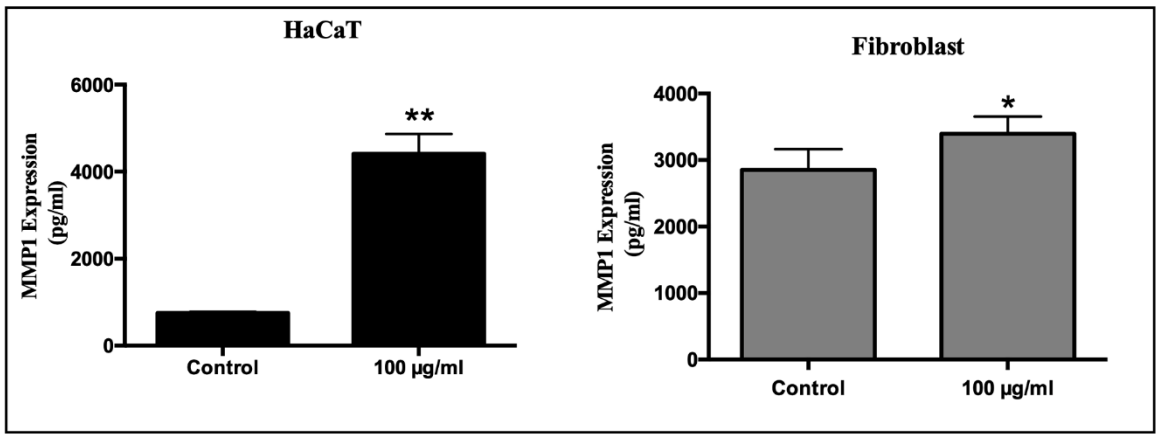

Figure 3.25. MMP1 expression levels of HaCaT and fibroblast cells. Control was treated with growth medium. Results were analysed by two-tailed multiple t tests. Data are shown with ± SEM, n=3, *P<0.05, **P<0.01

3.12.2. Human MMP3 Elisa

Human MMP3 ELISA was performed to evaluate MMP3 levels on dermal cells upon exosome application. According to the results derived from the assay, MMP3 expression levels significantly upregulated in both HaCaT and fibroblast cells. In HaCaT cells, MMP3 expression upregulated from 268.492 ± 11.665 pg/ml to 341.953 ± 13.161 pg/ml and in fibroblasts, the expression rose from 139.017 ± 6.342 pg/ml to 193.837 ± 11.826 pg/ml when treated with 100 µg/ml of *A. comosus* exosomes (Figure 3.26).

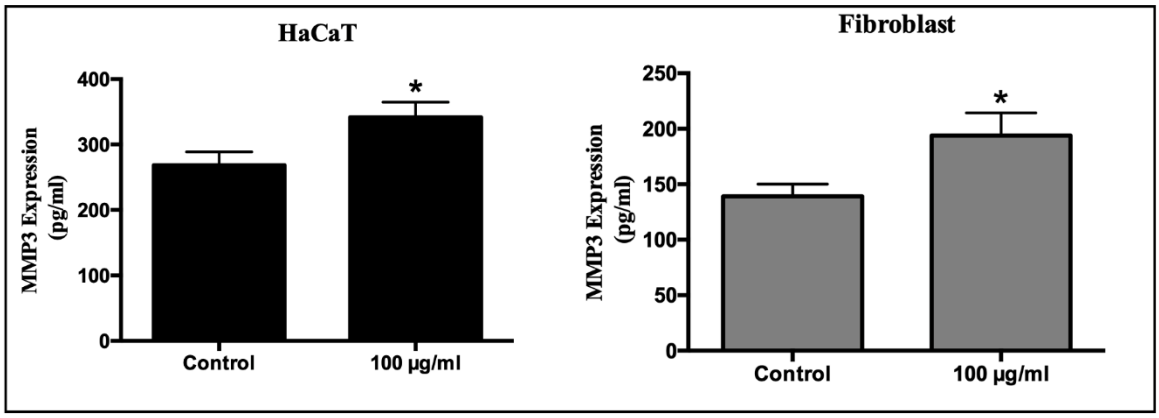

Figure 3.26. MMP3 expression levels of HaCaT and fibroblast cells. Control was treated with growth medium. Results were analysed by two-tailed multiple t tests. Data are shown with ± SEM, n=3, *P<0.05.

3.12.3. Human VEGF Elisa

Human VEGF ELISA was performed to evaluate VEGF levels on dermal cells upon exosome application. According to the results derived from the assay, VEGF expression of HaCaT cells was not significantly affected with the exosome treatment. However, that of HUVEC and fibroblasts were significantly upregulated. In HUVEC cells, VEGF expression was observed at 617.137 ± 59.082 pg/ml for growth medium treated control and it rose to 822.497 ± 32.113 pg/ml upon exosome treatment. In fibroblasts, VEGF expression was rather less than that of HUVEC cells, as expected. VEGF expression in fibroblasts was observed at 35.0 ± 2.309 pg/ml in growth medium treated controls and it rose to 48.667 ± 2.603 pg/ml upon exosome treatment (Figure 3.27).

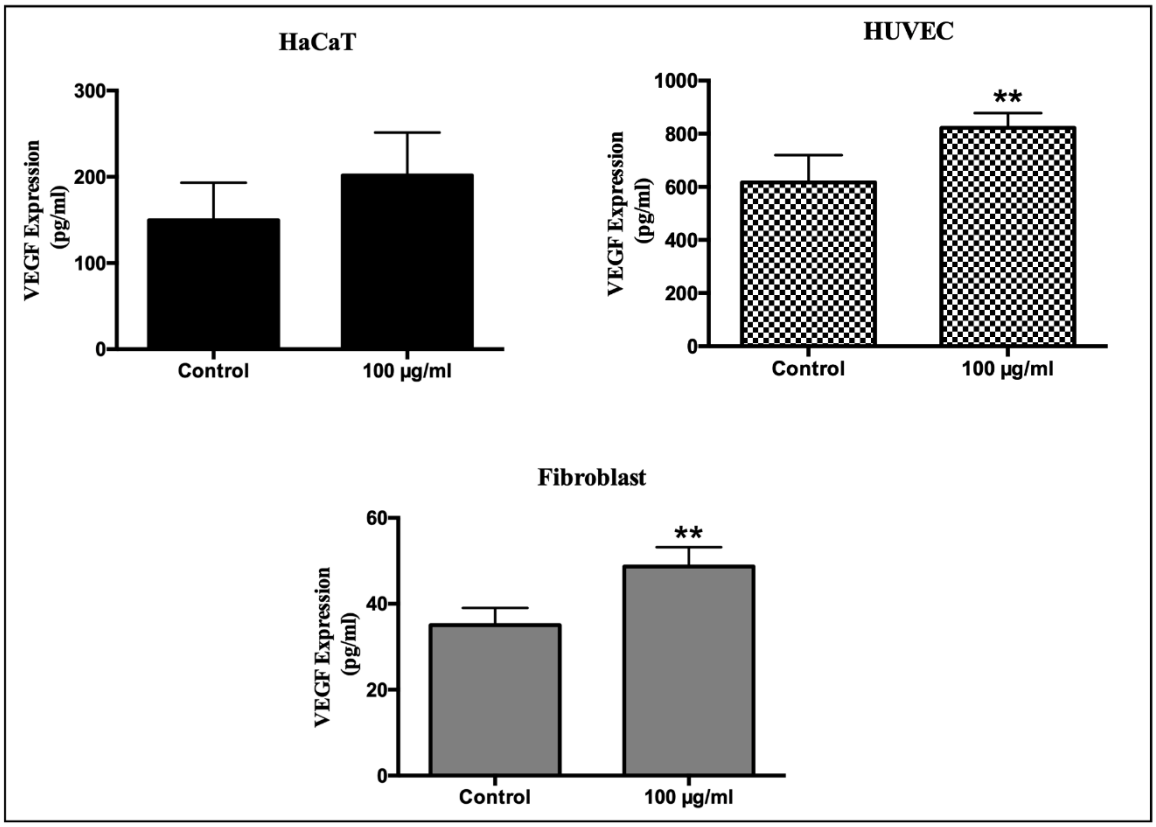

Figure 3.27. VEGF expression levels of HaCaT, HUVEC and fibroblast cells. Control was treated with growth medium. Results were analysed by two-tailed multiple t tests. Data are shown with ± SEM, n=3, *P<0.05.

3.12.4. Human TGF-Beta 1 Elisa

Human TGF-β1 ELISA was performed to evaluate TGF-β1 levels on dermal cells upon exosome application. According to the results derived from the assay, TGF-β1 expression levels significantly downregulated in each cell line. In HaCaT cells, TGF-β1 expression downregulated from 53.857 ± 7.789 pg/ml to 38.768 ± 7.082 pg/ml. In fibroblasts, TGF-β1 expression was evaluated at 436.028 ± 66.307 pg/ml for growth medium treated control cells and it decreased to 104.361 ± 3.639 pg/ml upon exosome treatment (Figure 3.28).

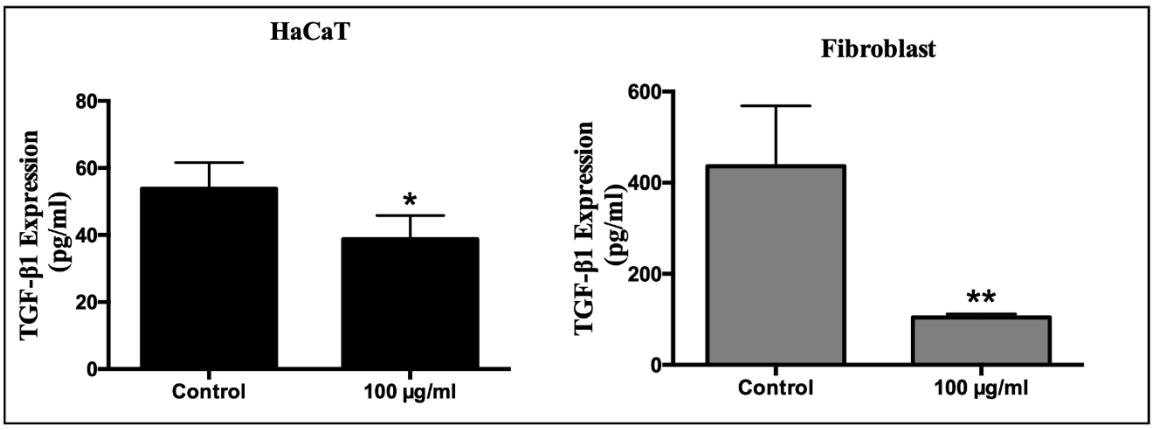

Figure 3.28. TGF-β1 expression levels of HaCaT and fibroblast cells. Control was treated with growth medium. Results were analysed by two-tailed multiple t tests. Data are shown with ± SEM, n=3, *P<0.05, **P<0.01

3.12.5. Human Pro-Collagen I Alpha 1 Elisa

Human COL1A1 ELISA was performed to evaluate collagen 1 levels on fibroblast cells upon exosome application. However protein expression levels did not significantly change (Figure 3.29).

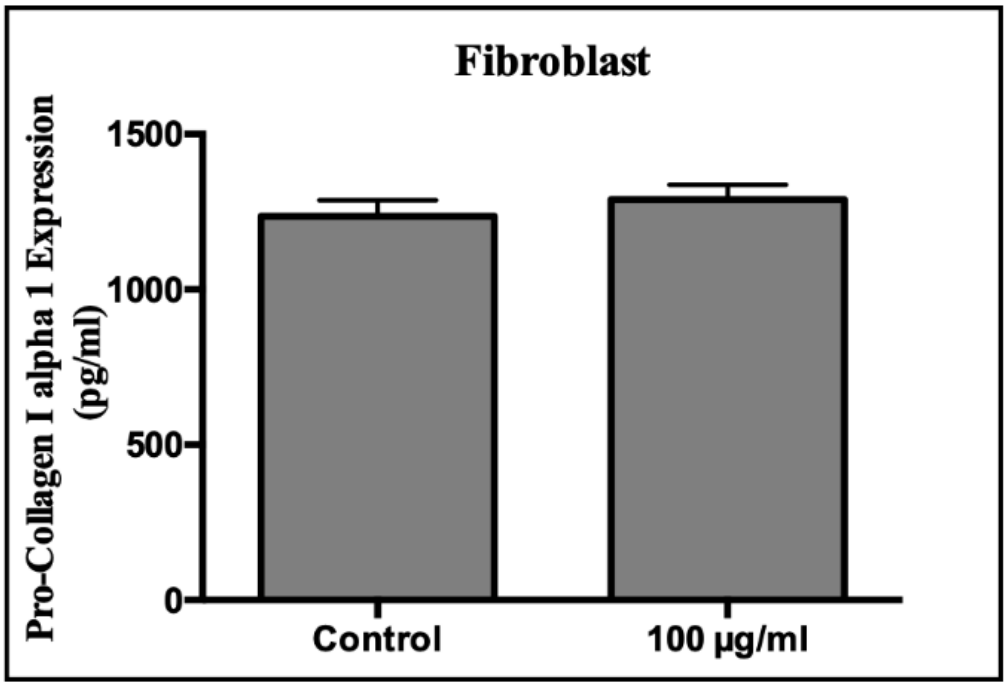

Figure 3.29. COL1A1 expression levels of fibroblast cells. Control was treated with growth medium. Results were analysed by two-tailed multiple t tests. Data are shown with ± SEM, n=3.

3.13. WESTERN BLOT

AKT, p-p44/42 MAPK and p-p38 MAPK protein expression levels were evaluated by immunoblotting technique. According to the results, protein expression levels of AKT, p-p44/42 MAPK and p-p38 MAPK increased 1.52-, 1.27- and 1.76 fold among HaCaT cells upon 100 µg/ml exosome treatment (Figure 3.30).

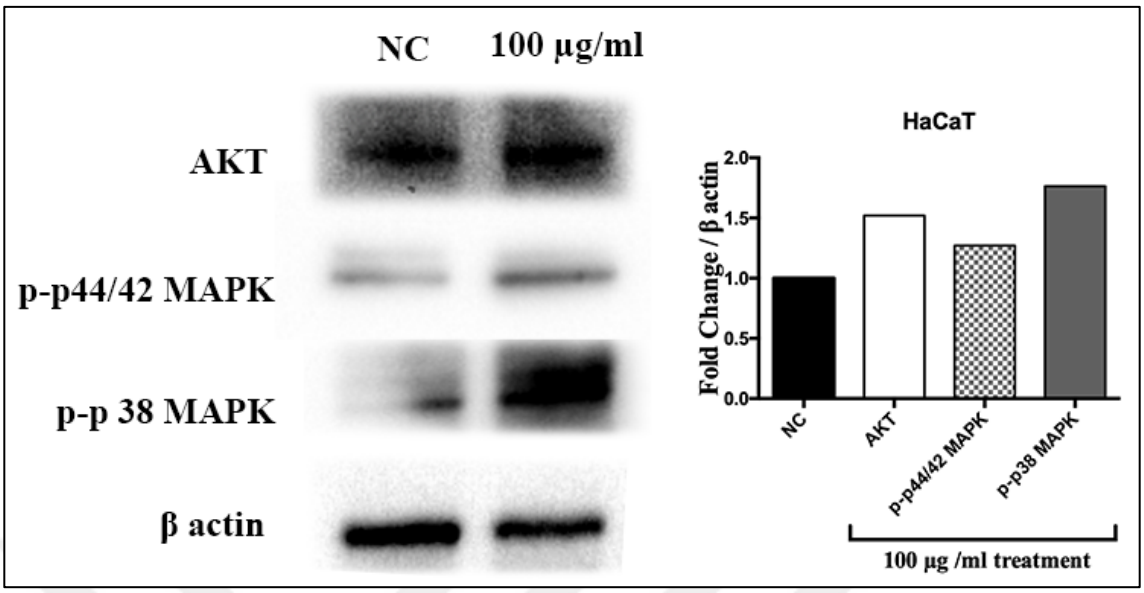

Figure 3.30. Western blot analysis of total AKT, p-p44/42 MAPK and p-p38 MAPK protein levels of HaCaT cells.

On the other hand, while AKT protein expression levels of HUVEC cells remain still, that of p-p44/42 MAPK and p-p38 MAPK were upregulated by3.36- and 2.06 fold among exosome treated group in contrast to growth medium treated group (Figure 3.31).

Among fibroblasts AKT and p-p44/42 MAPK protein expression levels did not dramatically change among all, p-p38 MAPK expression level increased by 1.18 fold upon exosome treatment (Figure 3.32).

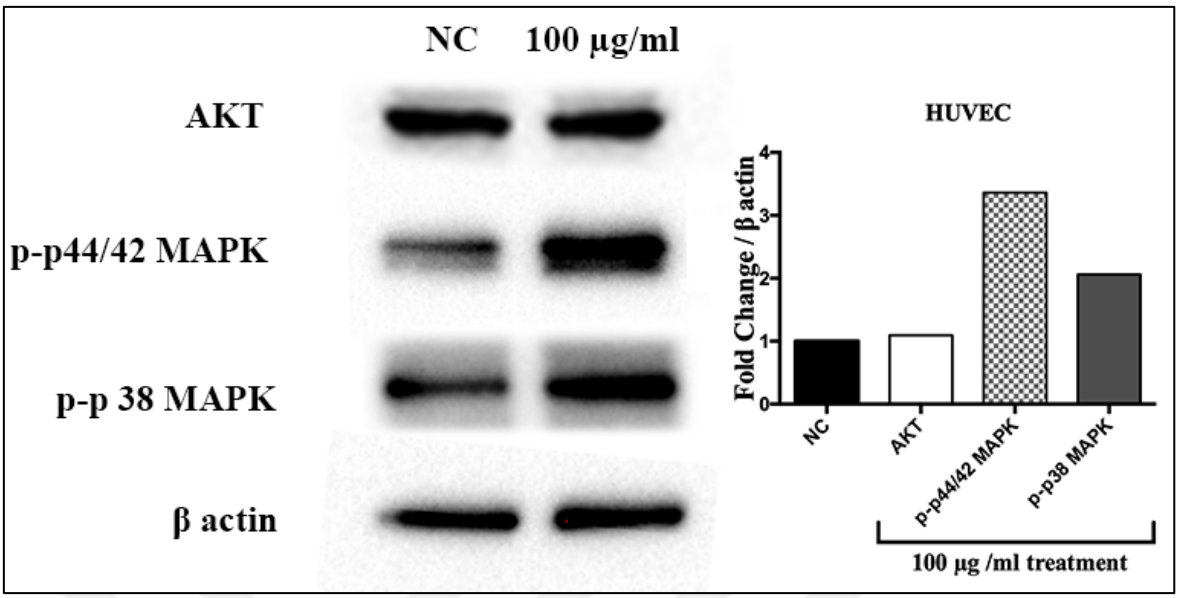

Figure 3.31. Western blot analysis of total AKT, p-p44/42 MAPK and p-p38 MAPK protein levels of HUVEC cells.

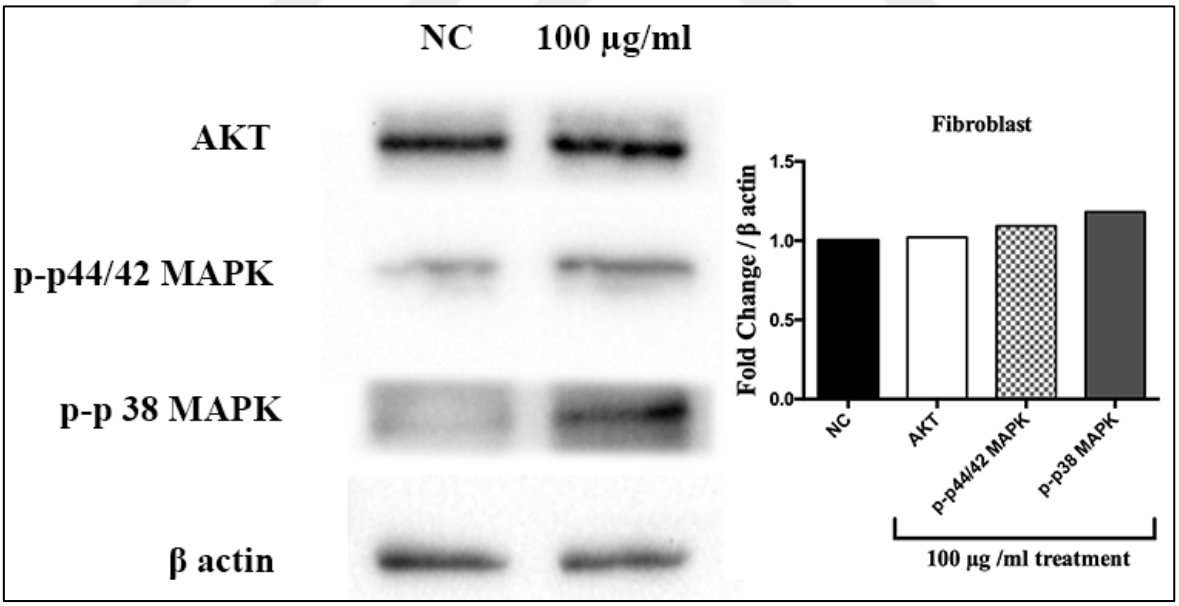

Figure 3.32. Western blot analysis of total AKT, p-p44/42 MAPK and p-p38 MAPK protein levels of fibroblast cells.

3.14. IMMUNOCYTOCHEMISTRY ANALYSIS

Immunocytochemistry analysis was performed to project and quantify protein expression levels on cells. According to the ICC images, ERK1/2 and fibronectin protein expression levels cells significantly increased while SMAD3 expression was significantly downregulated among HaCaT cells after treatment (Figure 3.33, Figure 3.34 and Figure 3.35). On the other hand, ERK1/2 expression levels of HUVEC cells were also significantly upregulated after treatment (Figure 3.36).

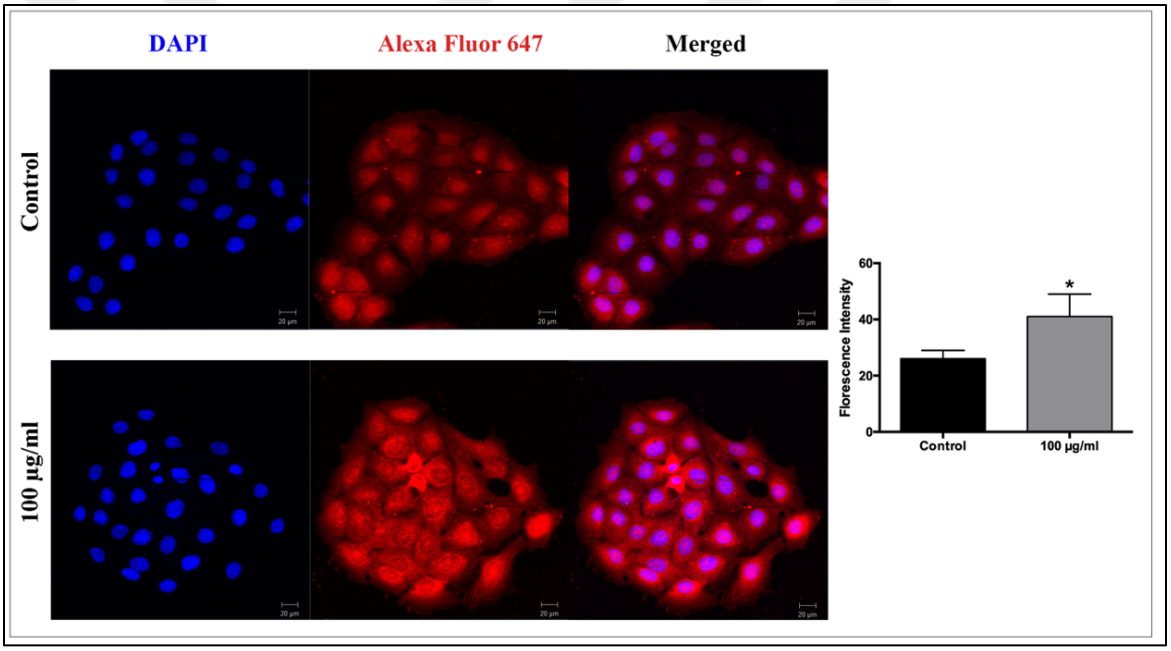

Figure 3.33. Immunocytochemistry location and quantification of ERK1/2 protein expression of HaCaT cells by confocal microscopy. Results were analysed by two-tailed multiple t tests. Data are shown with ± SD, n=3.

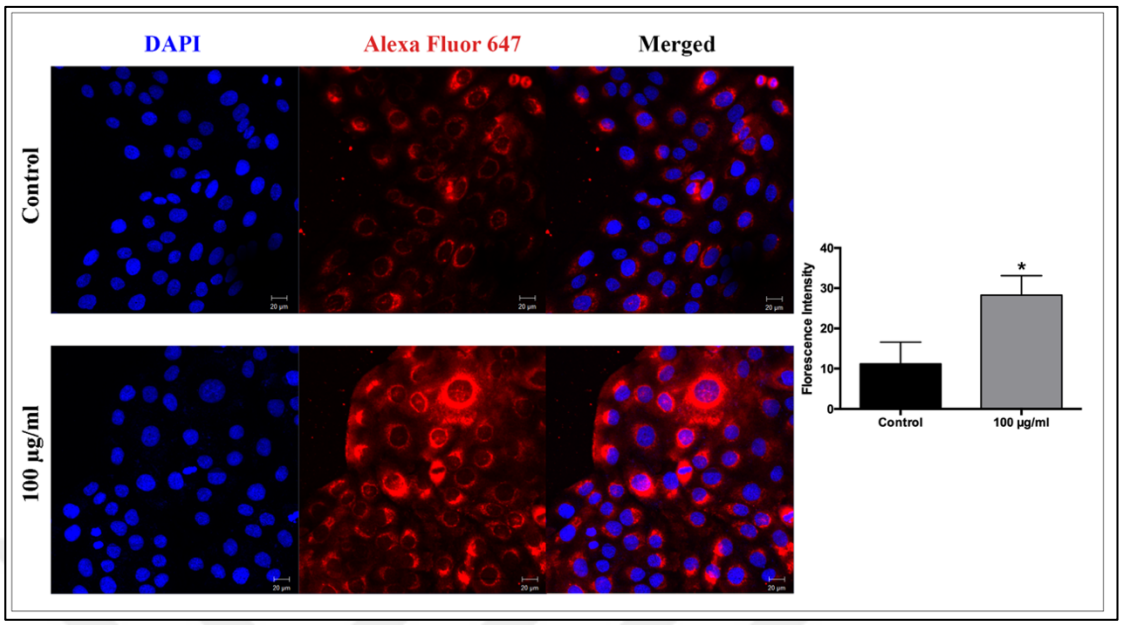

Figure 3.34. Immunocytochemistry location and quantification of fibronectin protein expression of HaCaT cells by confocal microscopy. Results were analysed by two-tailed multiple t tests. Data are shown with ± SD, n=3.

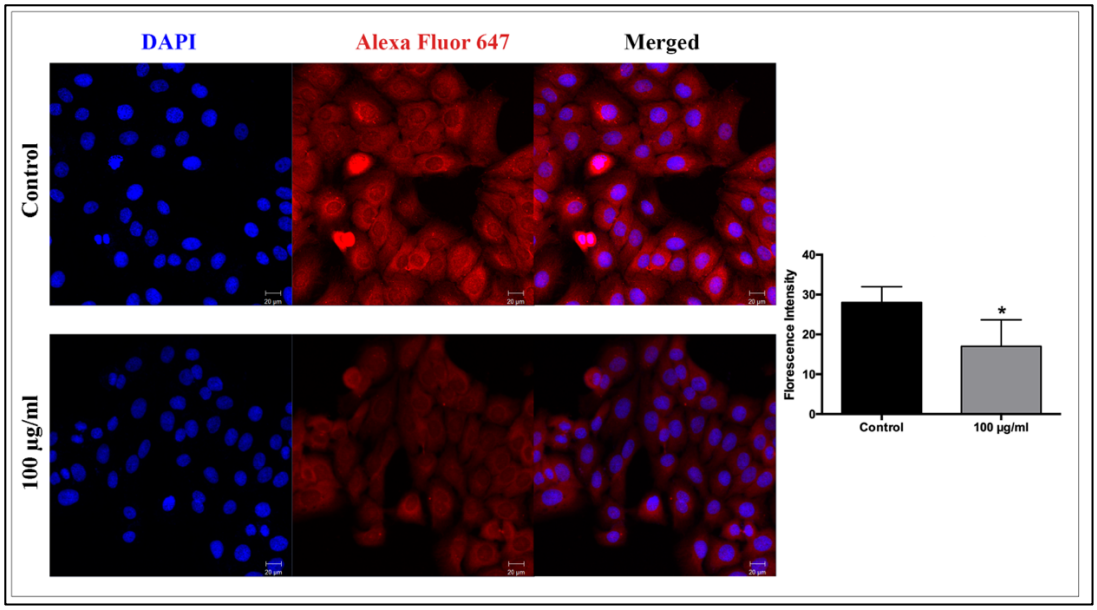

Figure 3.35. Immunocytochemistry location and quantification of SMAD3 protein expression of HaCaT cells by confocal microscopy. Results were analysed by two-tailed multiple t tests. Data are shown with ± SD, n=3.

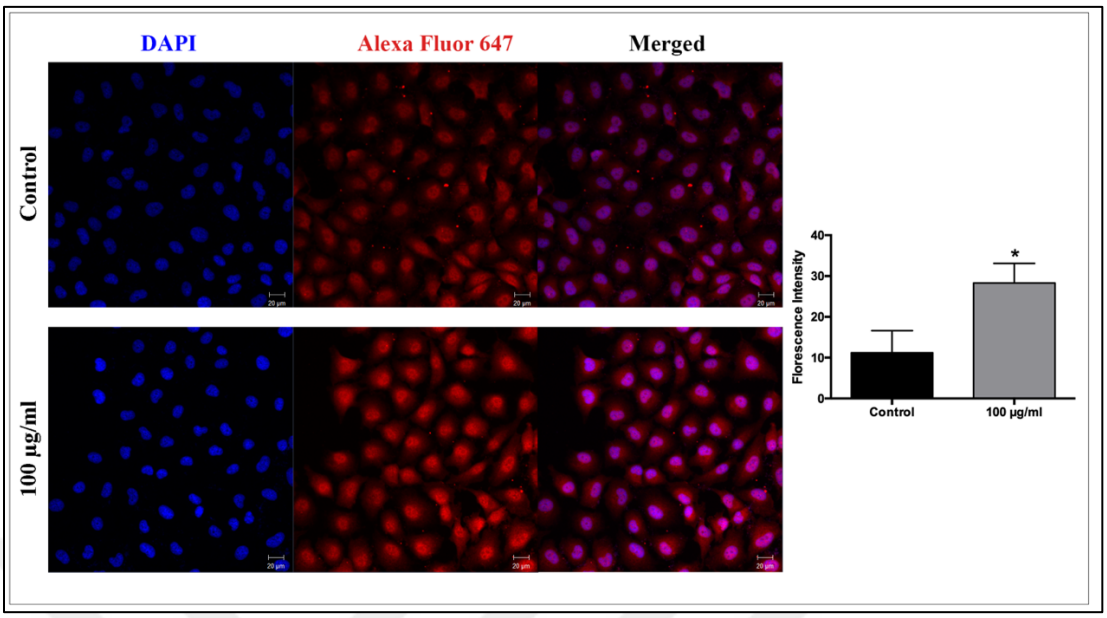

Figure 3.36. Immunocytochemistry location and quantification of ERK1/2 protein expression of HUVEC cells by confocal microscopy. Results were analysed by two-tailed multiple t tests. Data are shown with ± SD, n=3.

4. DISCUSSION

The interaction of different cells types and their interplay makes wound healing a very composite process. In depth studies about the wound healing mechanism is continuously being undertaken by scientists for a better comprehension of the process. Wound healing field and used technologies are constantly changing with the development of more accessible, effective and cheaper healing agents. Ever since the revelation of scarless healing of foetuses, the research in this area has broadened and shifted to overcome scar formation while developing an effective wound healing agent at the same time.

Exosomes, on the other hand, are nanosized secreted vesicles that play a fundamental role in cellular interaction even though when first discovered they were thought to be the garbage bins of the cells [292]. Increased numbers of publications about extracellular vesicles (EV) proved that they are also vital for aging, cancer development, infectious diseases, and many more [320]. However, rapidly increasing number of publications with poor or insufficient information about extracellular content has raised the question of developing a guide (Minimal Information for Studies of Extracellular Vesicles – MISEV) for all EV studies to underline differences exosomes, microvesicles and apoptotic bodies [293]. These extracellular vesicles vary according to their size and biogenesis pathways [321]. According to guideline of MISEV, exosomes should be quantified, at least 3 positive exosome protein markers should be present and they should be visualized by either electron microscopy or NTA [293, 322]. Moreover, the guideline strongly suggests the observation of cellular uptake of the exosomes inside the target cells. In this thesis, exosomes were derived from *A. comosus* and were characterized according to these guidelines. Presence of tetraspanin proteins of CD9, CD63 and HSP70 which are widely known biomarkers to be present on exosomal membrane were determined via flow cytometry [323]. Nanoparticle tracking analysis was performed to quantify and to acquire size distribution of the exosomes. According to the literature, size distribution may vary between 40-160 nm and the mean exosome size determined by NTA is within the limits for exosome size. However, the size differences are predicted for the exosome content since the source of the exosomes is a plant rather than a biological fluid. Brownian motion of the exosomes were also observed during

the analysis, a property unique to exosomes. Although particle number was determined by NTA, rest of the experiments were carried out according to protein content of the exosomes due to variances in size distribution. Therefore exosome quantification was performed by Lowry protein assay and this method was carried out throughout the whole study [319]. Studying towards perfecting the purity of exosomes is one of the future prospects of this study. In addition, uptake analysis proved the cross-kingdom communication between exosomes and the dermal cells as they become more and more visible inside the cells at and after 2 hour upon application. Even after 12th hour their application, their presence inside the cells are apparent.

Skin integrity is crucial for keeping the internal organs intact and undamaged. However, whenever the skin integrity is insulted, tissues as well as organs become susceptible to outside pathogens [324]. Regardless, bacterial contamination is seen in all types of wounds however the extent of keeping the contamination from turning into infection solely depends on the immune system of the patient [325]. As mentioned earlier, after the homeostasis phase, inflammatory phase takes control in the wound area to eliminate pathogens from the surrounding area. The time required for inflammatory phase varies for each wound however it is especially delayed in chronic wounds therefore it is especially important to test antimicrobial properties of healing agents for chronic wounds. Infection control also partially depends on the production of reactive oxygen species (ROS) and maintaining their levels inside the cells [326]. Radical derivatives of oxygen act as secondary messenger by signalling to many non-lymphoid cells and immunocytes, recruiting lymphoid cells around the wound and regulating angiogenesis [327]. It has been proven that various concentrations of ROS have various consequences. While cell cycle arrest is induced by extremely low levels of ROS, its presence maintain normal homeostasis and cell functions. On the other hand, extreme levels of ROS promote cell death and necrosis [328]. Main purpose during the wound healing is to reduce amount of oxidative stress caused by ROS production so that normal wound healing may take place. It has been proved that *A. comosus* exosomes help reduce ROS production among keratinocytes and endothelial cells with a few exceptions. However, low levels of ROS is also not a good option since these chemical species help in obliterating the microbial invaders, therefore it is important to have a balance between the two.

In acute wounds, proliferative phase takes place following the inflammatory phase. This phase includes both the migration and proliferation of cells to close the gap. This phase is crucial for proper healing and are considered as rate limiting factor for healing. It has been established with MTS assays that *A. comosus* exosome application to each of these cell lines causes a significant increase in the rates of cell proliferation as the exosome concentration increases. 3 different time points were investigated for cell proliferation rates, however, for investigating the changes in cell cycle distributions different time points were studied since it has been established that exosomes are taken up by cells rapidly. Hourly exosome uptake analysis showed that exosomes become visible inside the cells around after 2 hour. Therefore, we assume a change in cell cycle distributions in earlier time points. As expected, exosome application caused significant changes in cell cycle distributions of each cell line with an increasing proliferation rate. Cell cycle distribution of HaCaT cells significantly change after 24 hours of exosome treatment as more cells are in the G2-M phase than the control cells as a consequence of increased proliferation. On the other hand, HUVEC cells change their cell cycle distribution right after 12^{th} hour of exosome application. As a result, more cells leave G0-G1 phase in which cells are not dividing in this phase. These cells enter either S phase in which they prepare to synthesize DNA or G2-M phase where they are dividing during the first 12^{th} hour and this phenomenon lasts through the 24^{th} hour. Unlike keratinocytes and endothelial cells, fibroblasts generally reside in G0-G1 phase if there is no stimulus for them to divide. However, just like HUVEC cells, fibroblasts are also directly affected from exosome application right after 12^{th} hour of the treatment and fibroblast cells prepare to divide by entering S phase. After 24 hours of exosome application, number of cells preparing to divide in S phase or that of dividing in G2-M phase are significantly higher than control cells. Nonetheless, among all cell lines, none of them show a significant change in their cell cycle distributions.

As an another rate limiting factor in healing, migration is crucial to the living cells for normal development, prevention of inflammation, disease, and immune response [329]. Scratch assay and migration & invasion assays are two common practices to evaluate wound closure. Therefore as a first method, scratch assay was conducted with 2 separate concentrations of *A. comosus* exosomes to evaluate their effects on migration of dermal cells. Within 16 hours

of exosome application, both keratinocytes and fibroblasts showed magnificent migration rates and completely closed the gap in scratch assays. Additionally endothelial cells also showed significant increase in their migration rate and closed nearly 80 percent of the gap within 16 hour of exosome application. Aside from scratch assay, transmembrane cell migration and invasion assays were conducted. Even though cell migration assay determines almost the same properties of cell motility as a scratch assay, an invasion assay gauges the potential of cells to move through an ECM by breaching through it. These assays are also used to detect the cell response to a certain chemo-attractants, in our case *A. comosus* exosomes. It has been made clear with the studies that exosome application causes a great difference in migration and invasion rates of the dermal cells which suggest that these exosomes may strongly attract dermal cells to the wound site upon application.

The main factor inducing the dermal cell migration is the interaction between cell surface proteins with ECM proteins like laminin, vimentin, collagen, and fibronectin [165, 330]. In addition, actin and microtubules specifically cooperate with vimentin for elongation of cells for invasion [331]. These ECM proteins directly or indirectly regulate the cellular behaviour and are the key factors for normal wound healing. For example, laminin and collagen turnover is specifically related to the keratinocyte and fibroblast proliferation and migration. Upregulation of vimentin and laminin among HaCaT cells may be the primary reason of their increased cell proliferation. On the other hand, while vimentin levels increased in fibroblasts, that of laminin significantly decreased which is an important protein separating epidermis from dermis [332]. Fibronectin is also another vital ECM protein involved in cellular behaviour such as attachment, migration, and proliferation [333]. In that regard, upregulation of fibronectin protein expression upon exosome treatment also contribute to the increase in cellular proliferation and migration. Another reason for increased cell proliferation and migration rates may be due to increased AKT mRNA expression levels as well as protein expression levels. AKT is one of the core mediators of PI3K pathway that regulates cellular proliferation, migration, invasion, and angiogenesis via MMPs and VEGF [334]. In line with increased mRNA expression AKT protein levels in HaCaT cells also increased but that of fibroblasts and HUVEC cells was not completely different from their controls. However, in order to further investigate if *A. comosus* derived exosomes induce a change in PI3K pathway, downstream signalling proteins of the pathway such as expression

levels of pAKT should be studied. In addition, since PI3K pathway play a role in angiogenesis, pro-angiogenic properties of the exosomes were also studied. Increasing the angiogenesis level is a standard way to successfully heal a wound, however it is also crucial during the healing of chronic wounds where venous insufficiency commonly occurs [335]. In order to address angiogenic properties, HUVEC cells were seeded on Matrigel with or without *A. comosus* exosomes. It has been shown that exosome treatment significantly increased tube formation rate as well as tube length at 7th hour, however, no significant change was observed at neither of these properties at 20th hour. Regardless, just like any other endothelial cells, angiogenetic potential of HUVECs are also regulated by several cytokines and growth factors. Increased mRNA expression of MMP-2 and MMP-9 gelatinases may have caused HUVECs to increase their angiogenic potentials, as well [336, 337]. Moreover, HUVEC cells secreted more VEGF upon exosome treatment. Regardless, it is important to maintain capillary tube-like structures of micro- and macro-vascular endothelial cells, therefore anti apoptotic mechanism of these exosomes should also be studied. VEGF is crucial for endothelial cell chemotaxis and mitogenesis. Therefore VEGF is also produced by other cells like keratinocytes and fibroblasts [338]. Although VEGF levels in HaCaT cells did not significantly change, VEGF protein expression and its secretion by fibroblasts significantly increased upon exosome application. All in all, increased VEGF expression levels induce wound closure, re-epithelization and increased repair quality.

In addition to PI3K pathway, it has been shown with this study that *A. comosus* derived exosomes affect p38 MAPK and ERK1/2 pathways as well. Both pathways are extensively involved in cellular proliferation and migration [339]. Matrix metalloproteinases are also important regulators of ERK/MAPK pathway which are activated during proliferation, differentiation and development. One of the activators of ERK/MAPK pathway is skin injury. Previous studies showed that ERK/MAPK pathway is directly related to cellular migration [340]. In this study, western blot studies showed that *A. comosus* exosome application upregulated the levels of phosphorylated p44/42 (ERK1/2) in HaCaT and HUVEC cells while fibroblasts cells were not affected. In addition, ICC images also proved a significant upregulation of ERK1/2 protein concentration in both keratinocytes and endothelial cells. As an another signal in MAPK pathway, phosphorylation of p38 was also

increased in keratinocytes and endothelial cells even though that of fibroblast did not increase as much [341]. Altogether according to these findings, exosome treatment had an effect on various pathways such as MAPK, ERK, PI3K/AKT signals. Activation of these signals upon exosome treatment can be attributed to increased cellular proliferation, migration, and angiogenesis rates of the dermal cells.

Evidences have so far proved that *A. comosus* derived exosomes are beneficial for dermal wound healing. Further analysis was performed to see if these exosomes help mitigate scar formation. Although scar formation is a result of normal wound repair process, it is a compelling health issue that arise once the wounds have healed [161]. Excessive collagen accumulation contributes to hypertrophic scar formation. Besides, MMPs play a vital role in preventing collagen aggregation since they include gelatinases (MMP-2,-9), collagenases (MMP-1,-8-13), stromelysins (MMP-3,10) and many more [342]. Matrix metalloproteinases are especially important for the re-epithelization step and ECM degradation and deposition [343]. If found in excess amounts, MMPs lead to chronic wound formation, however their timely activation is crucial for neat and scarless healing [344]. Among all, MMP-2 and MMP-9 have a very broad substrate spectrum where MMP-2 utilizes gelatin, collagen-I,-IV,-VII,-X, fibronectin and laminin as substrate it accelerates cell migration by the wound margin. In addition, MMP-9 (also expressed by keratinocytes at the wound margin) also utilizes gelatin, collagen-I,-III,-V, and elastin and it serves as the same purpose as MMP-2 [345]. Although MMP-2 levels did not significantly change in HaCaT cells, it was significantly decreased in fibroblasts. Nonetheless, increased migratory responses may stem from increased levels of MMP-9 in both HaCaT cells and fibroblasts. Levels of MMP-1 together with MMP-3 and MMP-9 are important in the chemokine (family of small cytokines) regulation [346]. MMP-1 is also highly expressed by fibroblasts to remodel the ECM [347]. In addition, while MMP-1 promotes keratinocytes to migrate on fibrillar collagen, MMP-3 affects wound contraction and they are both synthesized by keratinocytes at the wound edge. Therefore, increased levels of MMP-1 in both HaCaT and fibroblasts might also be triggered by the migratory activity of these cells. It is a good practice to keep in mind that although MMP-1 peaks at day 1 among keratinocytes, its sustained overexpression delays the re-epithelization phase. Aside from MMP-1, MMP-3 has wider range of substrates from the ECM such as fibronectin, gelatin, E-cadherin, collagen-IV, -V,

-IX, and –X. MMP-3 is also capable of activating other pro-metalloprotease and ERK/MAPK pathway which contributes to the high MMP3/TIMP1 ratio. Although TIMP-1 levels was not measured, high ratio of MMP-3 over TIMP-1 is beneficial for scarless regeneration in addition to remodelling of the ECM.

The ratio of collagen III over collagen I and that of TGF-β3 over TGF-β1 are highly important in scarless healing [348]. Scarless tissue formation especially requires less cross linkage between fine reticular collagens [349]. Collagen accumulation results from any imbalance that may occur in collagen synthesis and degradation, hence this situation further feeds scar formation. While sufficient collagen type III formation prevents scar formation, excess collagen I secretion results in a disorganized structure [350]. Therefore switching from collagen I to collagen III is necessary for a scarless healing since fetal ECM contains more collagen III over collagen I. As a strong effector of scar formation, dermal fibroblasts are the main regulators of ECM and collagen. RT-PCR results revealed a significant decrease in COL1A1 levels while COL3A1 levels significantly increased in fibroblasts. These results propose that increased ratio of COL3A1/COL1A1 upon the exosome treatment favors scarless healing. Contrarily, COL1A1 ELISA results showed a nonsignificant increase in COL1A1 expression levels in fibroblasts. Further *in vivo* studies are needed to visualize collagen arrangement of the tissues in order to better observe structural changes in collagen.

In addition, ratio of TGF-β family isoforms were also evaluated to understand the effect of *A. comosus* exosomes on scarless healing. Although TGF-β family is involved in a lot of steps of the wound repair process, there are lots of controversial reports about its function in wound heling. Regardless, it has been established that TGF-β exerts its effects through type-I and -II receptors and SMAD pathway [351]. Although some reports suggest that both TGF-β1 and TGF-β3 have pro-migratory and proliferative properties, latest studies showed that scarless healing seen among the fetuses is due to elevated levels of TGF-β3. On the other hand, elevated levels of TGF-β1 is associated with hypertrophic scar formation. For example, addition of TGF-β1 to fetal wounds result in scar formation where these wound normally heal without scars [173]. In this study, TGF-β3/TGF-β1 significantly increased upon addition of *A. comosus* exosomes in both HaCaT cells and fibroblasts even though TGF-β1 mRNA expression of HaCaT cells did not change significantly. Regardless, secretion of TGF-β1 protein in both keratinocytes and fibroblasts significantly decreased.

Moreover, since most of the profibrotic properties of TGF-β mediates through SMAD pathway, its expression in HaCaT cells were also studied. ICC images showed that, SMAD3 protein expression levels significantly decrease upon exosome treatment in keratinocytes.

As a potent regulator of TGF-β family, fibromodulin may bind to TGF-β receptors and inhibit their action especially during scarring with a specific affinity for the TGF-β1 receptor [197]. Although fibromodulin levels elevate after the injury occurs, adult wound healing does not generally include fibromodulin whereas fetal injuries contain high doses of fibromodulin contributing to scarless healing. Opposite to fetal wounds, adult wounds are deficient in fibromodulin expression, however its expression may start increasing later in the healing process. In this study, although fibromodulin expression levels of keratinocytes did not change significantly, that of fibroblasts significantly increased which ultimately promote scarless healing. Fibromodulin also regulate fibril formation of collagens and the tensile strength by binding fibrillar collagens and ultimately delaying the fibrillogenesis. Consequently, early upregulation of fibromodulin expression may promote scarless healing in the adult skin by contributing antifibrotic effect on collagens.

Another contribution to scar formation is the elevated levels of alpha smooth muscle actin (α-SMA) expression by fibroblasts. This protein usually found on the vessel walls and affects scar contraction and increases fibrosis just like collagen type I [352]. Differentiation of fibroblasts to myofibroblasts is associated with an increase in α-SMA which is generally found in nodular structures in hypertrophic scars. RT-PCR studies revealed that exosome application significantly reduced α-SMA mRNA expression in fibroblasts which correlates with decreased levels of TGF-β1 expression in line with the earlier finding that TGF-β1 promotes α-SMA expression [353].

On the whole, exploring the molecular mechanisms of scar formation in the field of tissue regeneration is continuing to expand beyond majority of the previous studies that had initially focused on wound phenotype and healing mechanisms. In order to reduce scar tissue which results from replacing damaged tissue by a pathological connective tissue [354], the

focus has shifted to fetal healing where the only example of impeccable tissue regeneration takes place in human lifespan. Although underlying mechanisms of the scarless wound healing are yet to be discovered, findings in this study has lightened that *A. comosus* derived exosomes promote wound healing, ECM remodeling, and have anti-scar properties.

5. CONCLUSIONS

In conclusion, *A. comosus* derived exosomes enhance wound repair via multiple mechanisms. In particular, these exosomes activate proliferative and migrative properties of dermal cells via ERK/MAPK and PI3K/AKT mechanisms, increase angiogenic properties of endothelial cells via transient upregulation of MMPs and VEGF. Elevated levels of migrative properties of keratinocytes and fibroblasts can also be attributed to increased levels of ECM proteins upon exosome treatment. Although antimicrobial activity of the exosomes were not studied in this work, certain exosome concentrations reduced ROS levels. Provided the data, *A. comosus* derived exosomes increase dermal cell proliferation, accelerate wound repair, enhance angiogenesis and have anti-scar properties. These results indicate that *A. comosus* exosomes are promising agents in cutaneous wound healing and reducing scars. Further studies are, however, needed in order to elucidate the effect of *A. comosus* exosomes on wound healing both *in vitro* and *in vivo.*

REFERENCES

1. Schilling JA. Wound healing. *Surg Clin North Am.* 1976;56(4):859–74.

2. Serhan CN, Chiang N. Novel endogenous small molecules as the checkpoint controllers in inflammation and resolution: Entrée for resoleomics. *Rheumatic Disease Clinics of North America*. 2004;30(1):69-95.

3. Singer AJ, Clark RAF. Cutaneous wound healing. *N Engl J Med.* 1999;341(10):738–46.

4. Robson MC. Wound healing: biologic features and approaches to maximum healing trajectories. *Curr Probl Surg.* 2001;38(2):72–141.

5. Robson MC. Growth factors as wound healing agents. *Curr Opin Biotechnol.* 1991; 2(6):863–7.

6. Clark RAF. Biology of dermal wound repair. *Dermatologic Clinics*. 1993;11(4):647-66.

7. McGrath MH, Simon RH. Wound geometry and the kinetics of wound contraction. *Plast Reconstr Surg*. 1983;72(1):66-73.

8. Kennedy DF, Cliff WJ. A systematic study of wound contraction in mammalian skin. *Pathology*. 1979;11(2):207-22.

9. Pecoraro RE, Ahroni JH, Boyko EJ, et al. Chronology and determinants of tissue repair in diabetic lower-extremity ulcers. *Diabetes*. 1991;40(10):1305-13.

10. Margolis DJ, Gross EA, Wood CR, et al. Planimetric rate of healing in venous ulcers of the leg treated with pressure bandage and hydrocolloid dressing. *J Am Acad Dermatol*. 1993;28(3):418-21.

11. Tallman P, Muscare E, Carson P, et al. Initial rate of healing predicts complete healing of venous ulcers. *Arch Dermatol*. 1997;133(10):1231-4.

12. Snowden JM. Wound closure: An analysis of the relative contributions of contraction and epithelialization. *J Surg Res*. 1984;37(6):453-63.

13. Stromberg K, Chapekar MS, Goldman BA, et al. Regulatory concerns in the development of topical recombinant ophthalmic and cutaneous wound healing biologics. *Wound Repair Regen*. 1994;2(3):155-64.

14. Robson MC, Maggi SP, Smith PD, et al. Ease of wound closure as an endpoint of treatment efficacy. *Wound Repair Regen*. 1999;7(2):90-6.

15. Robson MC, Hill DP, Woodske ME, et al. Wound healing trajectories as predictors of effectiveness of therapeutic agents. *Arch Surg.* 2000; 135(7): 773–7.

16. Nwomeh BC, Yager DR, Cohen IK. Physiology of the chronic wounds. *Clin Plast Surg*. 1999;25:341-6.

17. Witte MB, Barbul A. General principles of wound healing. *Surg Clin North Am.* 1997; 77(3): 509–28.

18. Kirsner, Robert S. M, H. Eaglstein, William M. The wound healing process. *Surgical Inflammation.* 1993;11(4):629-40.

19. Santoro SA. Identification of a 160,000 dalton platelet membrane protein that mediates the initial divalent cation-dependent adhesion of platelets to collagen. *Cell*. 1986;46(6):913-20.

20. Meyer FA, Frojmovic XX. Characteristics of the major platelet membrone-site used in binding to collagen. *Thromb Res.* 1979; 15(5-6): 755–67.

21. Plow EF, Loftus JC, Levin EG, et al. Immunologic relationship between platelet membrane glycoprotein GPIIb/IIIa and cell surface molecules expressed by a variety of cells. *Proc Natl Acad Sci U S A.* 1986; 83(16): 6002–6.

22. Plow EF, McEver RP, Coller BS, et al. Related binding mechanisms for fibrinogen, fibronectin, von Willebrand factor, and thrombospondin on thrombin-stimulated human platelets. *Blood*. 1985;66(3):724-7.

23. Fang J, Hodivala-Dilke K, Johnson BD, et al. Therapeutic expression of the platelet-specific integrin, αIIbβ3, in a murine model for glanzmann thrombasthenia. *Blood*. 2005;106(8):2671-9.

24. Moncada S, Gryglewski R, Bunting S, et al. An enzyme isolated from arteries

transforms prostaglandin endoperoxides to an unstable substance that inhibits platelet aggregation. *Nature*. 1976;263(5579):663-5.

25. Grinnell F, Billingham RE, Burgess L. Distribution of fibronectin during wound healing in vivo. *J Invest Dermatol*. 1981;76(3):181-9.

26. Brown LF, Lanir N, McDonagh J, et al. Fibroblast migration in fibrin gel matrices. *Am J Pathol*. 1993;142(1):273-83.

27. Katz MH, Alvarez AF, Kirsner RS, et al. Human wound fluid from acute wounds stimulates fibroblast and endothelial cell growth. *J Am Acad Dermatol*. 1991;25(6 Pt 1):1054-8.

28. Rothe MJ, Falanga V. Growth factors and wound healing. *Clin Dermatol.* 1991; 9(4): 553–9.

29. Assoian RK, Komoriya A, Meyers CA, et al. Transforming growth factor-β in human platelets. Identification of a major storage site, purification, and characterization. *J Biol Chem*. 1983;258(11):7155-60.

30. Kaplan DR, Chao FC, Stiles CD, et al. Platelet α granules contain a growth factor for fibroblasts. *Blood*. 1979;53(6):1043-52.

31. Oka Y, Orth DN. Human plasma epidermal growth factor/β-urogastrone is associated with blood platelets. *J Clin Invest*. 1983;72(1):249-59.

32. Pierce GF, Mustoe TA, Altrock BW, et al. Role of platelet-derived growth factor in wound healing. *J Cell Biochem*. 1991;45(4):319-26.

33. Pierce GF, Vande Berg J, Rudolph R, et al. Platelet-derived growth factor-BB and transforming growth factor beta1 selectively modulate glycosaminoglycans, collagen, and myofibroblasts in excisional wounds. *Am J Pathol*. 1991;138(3):629-46.

34. Mustoe TA, Pierce GF, Morishima C, et al. Growth factor-induced acceleration of tissue repair through direct and inductive activities in a rabbit dermal ulcer model. *J Clin Invest*. 1991;87(2):694-703.

35. Pohlman TH, Stanness KA, Beatty PG, et al. An endothelial cell surface factor(s) induced in vitro by lipopolysaccharide, interleukin 1, and tumor necrosis factor-α

increases neutrophil adherence by a CDw18-dependent mechanism. *J Immunol*. 1986;136(12):4548-53.

36. Bevilacqua MP, Pober JS, Wheeler ME, et al. Interleukin 1 acts on cultured human vascular endothelium to increase the adhesion of polymorphonuclear leukocytes, monocytes, and related leukocyte cell lines. *J Clin Invest*. 1985;76(5):2003-11.

37. Werner S, Grose R. Regulation of wound healing by growth factors and cytokines. *Physiol Rev*. 2003;83(3):835-70.

38. Andoniou CE, Bryan MA, Cooley S. Natural killer cells: Basic science and clinical application. Elsevier-Academic Press; 2010.

39. Broughton G, Janis JE, Attinger CE. Wound healing: An overview. *Plast Reconstr Surg.* 2006; 117 (7 Suppl): 1–32.

40. Sen CK. Wound healing essentials: Let there be oxygen. *Wound Repair and Regeneration*. 2009;17(1):1-18.

41. Diegelmann RF, Evans MC. Wound healing: An overview of acute, fibrotic and delayed healing. *Frontiers in Bioscience*. 2004;9:283-9.

42. Hart J. Inflammation. 1: Its role in the healing of acute wounds. *Journal of Wound Care*. 2002;11(6):205-9.

43. Hunt TK, Hopf H, Hussain Z. Physiology of wound healing. *Advances in skin & wound care*. 2000;13(2 Suppl):6-11.

44. Velnar T, Bailey T, Smrkolj V. The wound healing process: an overview of the cellular and molecular mechanisms. *J Int Med Res*. 2009;37(5):1528-42.

45. Ramasastry SS. Acute wounds. *Clinics in Plastic Surgery*. 2005;32(2):195-208

46. Witte MB, Barbul A. Role of nitric oxide in wound repair. *Am J Surg.* 2002;183(4):406-12.

47. Koh TJ, DiPietro LA. Inflammation and wound healing: the role of the macrophage. *Expert Reviews In Molecular Medicine*. 2011;13:e23

48. Martin P, Leibovich SJ. Inflammatory cells during wound repair: The good, the bad

and the ugly. *Trends in Cell Biology*. 2005;15(11):599-607.

49. Malawista SE, Montgomery RR, Van Blaricom G. Evidence for reactive nitrogen intermediates in killing of staphylococci by human neutrophil cytoplasts. A new microbicidal pathway for polymorphonuclear leukocytes. *J Clin Invest*. 1992;90(2):631-6.

50. Buchmüller-Rouiller Y, Mauel J. Macrophage activation for intracellular killing as induced by calcium ionophore: Correlation with biologic and biochemical events. *J Immunol*. 1991;146(1):217-23.

51. Schmidt HHHW, Zernikow B, Baeblich S, et al. Basal and stimulated formation and release of L-arginine-derived nitrogen oxides from cultured endothelial cells. *J Pharmacol Exp Ther*. 1990;254(2):591-7.

52. Werner-Felmayer G, Werner ER, Fuchs D, et al. Tetrahydrobiopterin-dependent formation of nitrite and nitrate in murine fibroblasts. *J Exp Med*. 1990;172(6):1599-1607.

53. Xiao L, Eneroth Phe, Qureshi Ga. Nitric Oxide Synthase Pathway May Mediate Human Natural Killer Cell Cytotoxicity. *Scand J Immunol*. 1995;42(5):505-11.

54. Mautino G, Paul-Eugene N, Chanez LP, et al. Heterogeneous spontaneous and interleukin-4-induced nitric oxide production by human monocytes. *J Leukoc Biol*. 1994;56(1):15-20.

55. Schäffer MR, Tantry U, Gross SS, et al. Nitric oxide regulates wound healing. *Journal of Surgical Research*. 1996;63(1):237-40.

56. Henry G, Garner WL. Inflammatory mediators in wound healing. *Surgical Clinics of North America*. 2003;83(3):483-507.

57. Barrientos S, Stojadinovic O, Golinko MS, et al. Growth factors and cytokines in wound healing. *Wound Repair and Regeneration*. 2008;16(5):585-601.

58. Lowry SF. Cytokine mediators of immunity and inflammation. *Arch Surg*. 1993;128(11):1235-41.

59. Nissen NN, Polverini PJ, Koch AE, et al. Vascular endothelial growth factor mediates

angiogenic activity during the proliferative phase of wound healing. *Am J Pathol*. 1998;152(6):1445-52.

60. Mosser DM, Edwards JP. Exploring the full spectrum of macrophage activation. *Nature Reviews Immunology*. 2008;8(12):958-69.

61. Gillitzer R, Goebeler M. Chemokines in cutaneous wound healing. *J Leukoc Biol*. 2001;69(4):513-21.

62. Ito M, Cotsarelis G. Is the hair follicle necessary for normal wound healing? *Bone.* 2008; 128(5): 1059–61.

63. Ohyama M. Hair follicle bulge: A fascinating reservoir of epithelial stem cells. *J Dermatol Sci.* 2007; 46(2): 81–9.

64. Martin P. Wound healing--aiming for perfect skin regeneration. *Science.* 1997;276(5309):75-81.

65. Garlick JA, Taichman LB. Fate of human keratinocytes during reepithelialization in an organotypic culture model. *Lab Investig*. 1994;70(6):916-24.

66. Dominique Kubler M, Watt FM. Changes in the distribution of actin-associated proteins during epidermal wound healing. *J Invest Dermatol*. 1993;100(6):785-9.

67. Cavani A, Zambruno G, Marconi A, et al. Distinctive integrin expression in the newly forming epidermis during wound healing in humans. *J Invest Dermatol*. 1993;101(4):600-4.

68. Breuss JM, Gallo J, DeLisser HM, et al. Expression of the β6 integrin subunit in development, neoplasia and tissue repair suggests a role in epithelial remodeling. *J Cell Sci*. 1995;108 (Pt 6):2241-51.

69. Clark RAF, An JQ, Greiling D, et al. Fibroblast migration on fibronectin requires three distinct functional domains. *J Invest Dermatol*. 2003;121(4):695-705.

70. Haapasalmi K, Zhang K, Tonnesen M, et al. Keratinocytes in human wounds express alpha v beta 6 integrin. *J Invest Dermatol*. 1996;106(1):42-8.

71. Mitchison TJ, Cramer LP. Actin-based cell motility and cell locomotion. *Cell*.

1996;84(3):371-9.

72. Nguyen BP, Ryan MC, Gil SG, et al. Deposition of laminin 5 in epidermal wounds regulates integrin signaling and adhesion. *Current Opinion in Cell Biology*. 2000;12(5):554-62.

73. Pilcher BK, Wang M, Qin XJ, et al. Role of matrix metalloproteinases and their inhibition in cutaneous wound healing and allergic contact hypersensitivity. *Annals of the New York Academy of Sciences*. 1999;878:12-24.

74. Grøndahl-Hansen J, Lund LR, Ralfkiær E, et al. Urokinase- and tissue-type plasminogen activators in keratinocytes during wound reepithelialization in vivo. *J Invest Dermatol*. 1988;90(6):790-5.

75. Salo T, Makela M, Kylmaniemi M, et al. Expression of matrix metalloproteinase-2 and -9 during early human wound healing. *Lab Investig*. 1994;70(2):176-82.

76. Saarialho-Kere UK, Chang ES, Welgus HG, et al. Distinct localization of collagenase and tissue inhibitor of metalloproteinases expression in wound healing associated with ulcerative pyogenic granuloma. *J Clin Invest*. 1992;90(5):1952-7.

77. Muller M, Trocme C, Lardy B, et al. Matrix metalloproteinases and diabetic foot ulcers: The ratio of MMP-1 to TIMP-1 is a predictor of wound healing. *Diabet Med*. 2008;25(4):419-26.

78. Gipson IK, Spurr-Michaud SJ, Tisdale AS. Hemidesmosomes and anchoring fibril collagen appear synchronously during development and wound healing. *Dev Biol*. 1988;126(2):253-62.

79. Cribbs RK, Harding PA, Luquette MH, et al. Endogenous production of heparin-binding EGF-like growth factor during murine partial-thickness burn wound healing. *J Burn Care Rehabil*. 2002;23(2):116-25.

80. Brown GL, Curtsinger L, Brightwell JR, et al. Enhancement of epidermal regeneration by biosynthetic epidermal growth factor. *J Exp Med*. 1986;163(5):1319-24.

81. Schultz GS, White M, Mitchell R, et al. Epithelial wound healing enhanced by

transforming growth factor-α and vaccinia growth factor. *Science.* 1987;235(4786):350-2.

82. Ridley AJ, Hall A. The small GTP-binding protein rho regulates the assembly of focal adhesions and actin stress fibers in response to growth factors. *Cell*. 1992;70(3):389-99.

83. Ridley AJ, Comoglio PM, Hall A. Regulation of scatter factor/hepatocyte growth factor responses by Ras, Rac, and Rho in MDCK cells. *Mol Cell Biol*. 1995;15(2):1110-22.

84. Nobes CD, Hall A. Rho, Rac, and Cdc42 GTPases regulate the assembly of multimolecular focal complexes associated with actin stress fibers, lamellipodia, and filopodia. *Cell*. 1995;81(1):53-62.

85. Werner S, Smola H, Liao X, et al. The function of KGF in morphogenesis of epithelium and reepithelialization of wounds. *Science.* 1994;266(5186):819-22.

86. Pierce GF, Yanagihara D, Klopchin K, et al. Stimulation of all epithelial elements during skin regeneration by keratinocyte growth factor. *J Exp Med*. 1994;179(3):831-40.

87. Ornitz DM, Xu J, Colvin JS, et al. Receptor specificity of the fibroblast growth factor family. *J Biol Chem*. 1996;271(25):15292-7.

88. Sivamani RK, Garcia MS, Rivkah Isseroff R. Wound re-epithelialization: Modulating keratinocyte migration in wound healing. *Frontiers in Bioscience*. 2007;12:2849-68.

89. Santoro MM, Gaudino G. Cellular and molecular facets of keratinocyte reepithelization during wound healing. *Exp Cell Res.* 2005; 304(1): 274–86.

90. Maas-Szabowski N, Shimotoyodome A, Fusenig NE. Keratinocyte growth regulation in fibroblast cocultures via a double paracrine mechanism. *J Cell Sci*. 1999;112 (Pt 12):1843-53.

91. Gallucci RM, Sloan DK, Heck JM, et al. Interleukin 6 indirectly induces keratinocyte migration. *J Invest Dermatol*. 2004;122(3):764-72.

92. Kane CJM, Hebda PA, Mansbridge JN, et al. Direct evidence for spatial and temporal

regulation of transforming growth factor β1 expression during cutaneous wound healing. *J Cell Physiol*. 1991;148(1):157-73.

93. O'Kane S, Ferguson MWJ. Transforming growth factor βs and wound healing. *International Journal of Biochemistry and Cell Biology*. 2006;18(1):55-62.

94. Le Poole IC, Boyce ST. Keratinocytes suppress transforming growth factor-β1 expression by fibroblasts in cultured skin substitutes. *Br J Dermatol*. 1999;140(3):409-16.

95. Gailit J, Welch MP, Clark RAF. TGF-β1 stimulates expression of keratinocyte integrins during re-epithelialization of cutaneous wounds. *J Invest Dermatol*. 1994;103(2):221-27.

96. Sellheyer K, Bickenbach JR, Rothnagel JA, et al. Inhibition of skin development by overexpression of transforming growth factor β1 in the epidermis of transgenic mice. *Proceedings of the National Academy of Sciences of the United States of America*. 1993, 90 (11) 5237-41.

97. Tredget EB, Demare J, Chandran G, et al. Transforming growth factor-β and its effect on reepithelialization of partial-thickness ear wounds in transgenic mice. *Wound Repair Regen*. 2005;13(1):61-7.

98. Grotendorst GR, Soma Y, Takehara K, et al. EGF and TGF-alpha are potent chemoattractants for endothelial cells and EGF-like peptides are present at sites of tissue regeneration. *J Cell Physiol*. 1989;139(3):617-23.

99. Liarte, Bernabé-García, Nicolás. Role of TGF-β in skin chronic wounds: A keratinocyte perspective. *Cells.* 2020;9(2):306.

100. Pastar I, Stojadinovic O, Yin NC, et al. Epithelialization in wound healing: A comprehensive review. *Adv Wound Care.* 2014;3(7):445–64.

101. Williamson D, Harding K. Wound healing. *Medicine*. 2004; 32(12):4-7.

102. Ehrlich HP, Krummel TM. Regulation of wound healing from a connective tissue perspective. *Wound Repair and Regeneration*. 1996;4(2):203-10

103. Regan MC, Kirk SJ, Wasserkrug HL, et al. The wound environment as a regulator of

fibroblast phenotype. *J Surg Res*. 1991;50(5):442-48.

104. McClain SA, Simon M, Jones E, et al. Mesenchymal cell activation is the rate-limiting step of granulation tissue induction. *Am J Pathol*. 1996;149(4):1257-70.

105. Meckmongkol TT, Harmon R, McKeown-Longo P, et al. The fibronectin synergy site modulates TGF-β-dependent fibroblast contraction. *Biochem Biophys Res Commun*. 2007;360(4):709-14.

106. Desmouliere A, Geinoz A, Gabbiani F, et al. Transforming growth factor-β1 induces α-smooth muscle actin expression in granulation tissue myofibroblasts and in quiescent and growing cultured fibroblasts. *J Cell Biol*. 1996;4(2):278-87.

107. Jiang CK, Tomic-Canic M, Lucas DJ, et al. TGFβ promotes the basal phenotype of epidermal keratinocytes: Transcriptional induction of k#5 and k#14 keratin genes. *Growth Factors*. 1995;12(2):87-97.

108. Brown RL, Breeden MP, Greenhalgh DG. PDGF and TGF-α act synergistically to improve wound healing in the genetically diabetic mouse. *J Surg Res*. 1994;56(6):562-70.

109. Heldin CH, Westermark B. Mechanism of action and in vivo role of platelet-derived growth factor. *Physiological Reviews*. 1999;79(4):1283-1316.

110. Greiling D, Clark RAF. Fibronectin provides a conduit for fibroblast transmigration from collagenous stroma into fibrin clot provisional matrix. *J Cell Sci*. 1997;110 (Pt 7):861-70.

111. Toole BP. Proteoglycans and hyaluronan in morphogenesis and differentiation. *Cell Biology of Extracellular Matrix*. 1991.

112. Hinz B. The role of myofibroblasts in wound healing. *Curr Res Transl Med*. 2016;64(4):171-7.

113. Frank S, Hubner G, Breier G, et al. Regulation of vascular endothelial growth factor expression in cultured keratinocytes. Implications for normal and impaired wound healing. *J Biol Chem*. 1995;270(21):12607-13.

114. Abraham JA, Klagsbrun M. Modulation of wound repair by members of the fibroblast

growth factor family. *The Molecular and Cellular Biology of Wound Repair*. 1988.

115. Broadley KN, Aquino AM, Woodward SC, et al. Monospecific antibodies implicate basic fibroblast growth factor in normal wound repair. *Lab Investig*. 1989;61(5):571-5.

116. Detmar M, Brown LF, Berse B, et al. Hypoxia regulates the expression of vascular permeability factor/vascular endothelial growth factor (VPF/VEGF) and its receptors in human skin. *J Invest Dermatol*. 1997;108(3):263-8.

117. Brown LF, Yeo KT, Berse B, et al. Expression of vascular permeability factor (vascular endothelial growth factor) by epidermal keratinocytes during wound healing. *J Exp Med.* 1992; 176(5): 1375–9.

118. Berse B, Brown LF, Van de Water L, et al. Vascular permeability factor (vascular endothelial growth factor) gene is expressed differentially in normal tissues, macrophages, and tumors. *Mol Biol Cell*. 1992;3(2):211-20.

119. Brooks PC, Clark RA, Cheresh DA. Requirement of vascular integrin alpha v beta 3 for angiogenesis. *Science*. 1994;264(5158):569-71.

120. Clark RAF, Tonnesen MG, Gailit J, et al. Transient functional expression of αvβ3 on vascular cells during wound repair. *Am J Pathol*. 1996;148(5):1407-21.

121. Ho QT, Kuo CJ. Vascular endothelial growth factor: Biology and therapeutic applications. *International Journal of Biochemistry and Cell Biology*. 2007;39(7-8):1349-57.

122. Reinke JM, Sorg H. Wound repair and regeneration. *European Surgical Research*. 2012;49(1):35-43.

123. Fisher G, Gilbertson-Beadling S, Powers EA, et al. Interstitial collagenase is required for angiogenesis in vitro. *Dev Biol*. 1994;162(2):499-510.

124. Li J, Zhang Y-P, Kirsner RS. Angiogenesis in wound repair: Angiogenic growth factors and the extracellular matrix. *Microsc Res Tech*. 2003;60(1):107-14.

125. Tejero-Trujeque R. How do fibroblasts interact with the extracellular matrix in wound contraction? *Journal of Wound Care*. 2001;10(6):237-42.

126. Baranoski, Sharon, Elizabeth A. Ayello, and Sharon Baranoski. *Wound Care Essentials: Practice Principles*. Philadelphia: Wolters Kluwer Health/Lippincott Williams & Wilkins, 2012.

127. Li J, Chen J, Kirsner R. Pathophysiology of acute wound healing. *Clin Dermatol*. 2007;25(1):9-18

128. Gabbiani G, Ryan GB, Majno G. Presence of modified fibroblasts in granulation tissue and their possible role in wound contraction. *Experientia*. 1971;27(5):549-50.

129. Gabbiani G, Hirschel BJ, Ryan GB, et al. Granulation tissue as a contractile organ: Study of structure and function. *J Exp Med*. 1972;135(4):719-34.

130. Ryan GB, Cliff WJ, Gabbiani G, et al. Myofibroblasts in human granulation tissue. *Hum Pathol*. 1974;5(1):55-67.

131. Gabbiani G, Le Lous M, Bailey AJ, et al. Collagen and myofibroblasts of granulation tissue - A Chemical, ultrastructural and immunologic study. *Virchows Arch B Cell Pathol*. 1976;21(2):133-145.

132. Porter S. The role of the fibroblast in wound contraction and healing. *Wounds UK.* 2007; 3: 33–40.

133. Welch MP, Odland GF, Clark RAF. Temporal relationships of F-actin bundle formation, collagen and fibronectin matrix assembly, and fibronectin receptor expression to wound contraction. *J Cell Biol*. 1990;110(1):133-45.

134. Werner S, Grose R. Regulation of wound healing by growth factors and cytokines. *Physiol Rev*. 2003;83(3):835-70.

135. Singh S, Young A, McNaught CE. The physiology of wound healing. *Surg (United Kingdom).* 2017; 35: 473–77.

136. Bailey AJ, Sims TJ, Le Lous M, et al. Collagen polymorphism in experimental granulation tissue. *Biochem Biophys Res Commun*. 1975;66(4):1160-65.

137. Miller EJ. Biochemical characteristics and biological significance of the genetically-distinct collagens. *Mol Cell Biochem*. 1976;13(3):165-92.

138. Antoniades HN, Galanopoulos T, Neville-Golden J, et al. Injury induces in vivo expression of platelet-derived growth factor (PDGF) and PDGF receptor mRNAs in skin epithelial cells and PDGF mRNA in connective tissue fibroblasts. *Proc Natl Acad Sci U S A*. 1991;88(2):565-9.

139. Buckley-Sturrock A, Woodward SC, Senior RM, et al. Differential stimulation of collagenase and chemotactic activity in fibroblasts derived from rat wound repair tissue and human skin by growth factors. *J Cell Physiol*. 1989;138(1):70-8.

140. Herron GS, Banda MJ, Clark EJ, et al. Secretion of metalloproteinases by stimulated capillary endothelial cells. II. Expression of collagenase and stromelysin activities is regulated by endogenous inhibitors. *J Biol Chem*. 1986;261(6):2814-18.

141. Inoue M, Kratz G, Haegerstrand A, et al. Collagenase expression wound-edge keratinocytes after acute injury in human skin, persists during healing, and stops at re-epithelialization. *J Invest Dermatol*. 1995;104(4):479-83.

142. Armstrong DG, Jude EB. The role of matrix metalloproteinases in wound healing. *Journal of the American Podiatric Medical Association*. 2002;92(1):12-18.

143. Birkedal-Hansen H. Proteolytic remodeling of extracellular matrix. *Curr Opin Cell Biol*. 1995;7(5):728-35.

144. Borregaard N, Kjeldsen L, Lollike K, et al. Granules and vesicles of human neutrophils. The role of endomembranes as source of plasma membrane proteins. *Eur J Haematol*. 1993;51(5):318-22.

145. Tremble P, Chiquet-Ehrismann R, Werb Z. The extracellular matrix ligands fibronectin and tenascin collaborate in regulating collagenase gene expression in fibroblasts. *Mol Biol Cell*. 1994;5(4):439-53.

146. Unemori EN, Werb Z. Reorganization of polymerized actin: A possible trigger for induction of procollagenase in fibroblasts cultured in and on collagen gels. *J Cell Biol*. 1986;103(3):1021-31.

147. Leask A, Abraham DJ. TGF-beta signaling and the fibrotic response. *FASEB J*. 2004;18(7):816-27.

148. Gurtner GC, Werner S, Barrandon Y, et al. Wound repair and regeneration. *Nature*. 2008;453(7193):314-21.

149. DiPietro LA, Nissen NN, Gamelli RL, et al. Thrombospondin 1 synthesis and function in wound repair. *Am J Pathol*. 1996;148(6):1851-60.

150. Zhang JL, Chen GW, Liu YC, et al. Secreted protein acidic and rich in cysteine (sparc) suppresses angiogenesis by down-regulating the expression of VEGF and MMP-7 in gastric cancer. *PLoS One*. 2012;7(9):e44618.

151. Watt FM, Hogan BLM. Out of eden: Stem cells and their niches. *Science*. 2000;287(5457):1427-30.

152. Spradling A, Drummond-Barbosa D, Kai T. Stem cells find their niche. *Nature*. 2001;414(6859):98-104.

153. Bailey AJ, Bazin S, Sims TJ, et al. Characterization of the collagen of human hypertrophic and normal scars. *BBA - Protein Struct*. 1975;405(2):412-21

154. Levenson Sm, Geever Ef, Crowley L V., et al. The healing of rat skin wounds. *Ann Surg*. 1965;161(2):293-308.

155. Cecelia C. Yates*, Hebda P, Wells A. Skin wound healing and scarring: Fetal wounds and regenerative restitution. *Birth Defects Res C Embryo Today.* 2012; 96(4): 325–33.

156. Potter DA, Veitch D, Johnston GA. Scarring and wound healing. *Br J Hosp Med.* 2019; 80(11):166–71.

157. Larson BJ, Nauta A, Kawai K, et al. Scarring and scarless wound healing. *Adv Wound Repair Ther.* 2011; 77–111.

158. Niessen FB, Spauwen PHM, Schalkwijk J, et al. On the nature of hypertrophic scars and keloids: A review. *Plastic and Reconstructive Surgery*. 1999;104(5):1435-58.

159. Hynes RO. The extracellular matrix: Not just pretty fibrils. *Science*. 2009;326(5957):1216-9.

160. Shaffer JJ, Taylor SC, Cook-Bolden F. Keloidal scars: A review with a critical look

at therapeutic options. *J Am Acad Dermatol*. 2002;46(2 Suppl Understanding):63-97.

161. Karppinen S, Heljasvaara R, Gullberg D, et al. Toward understanding scarless skin wound healing and pathological scarring. 2019; 8:1–11.

162. Rowlatt U. Intrauterine wound healing in a 20 week human fetus. *Virchows Arch A Pathol Anat Histol*. 1979;381(3):353-61.

163. Armstrong JR, Ferguson MWJ. Ontogeny of the skin and the transition from scar-free to scarring phenotype during wound healing in the pouch young of a marsupial, Monodelphis domestica. *Dev Biol*. 1995;169(1):242-60.

164. Lian N, Li T. Growth factor pathways in hypertrophic scars: Molecular pathogenesis and therapeutic implications. *Biomedicine and Pharmacotherapy*. 2016;84:42-50.

165. Xue M, Jackson CJ. Extracellular matrix reorganization during wound healing and its impact on abnormal scarring. *Adv Wound Care*. 2015;4(3):119-36.

166. Reed CC, Iozzo R V. The role of decorin in collagen fibrillogenesis and skin homeostasis. *Glycoconjugate Journal*. 2002;19(4-5):249-55.

167. Miura T, Kishioka Y, Wakamatsu JI, et al. Decorin binds myostatin and modulates its activity to muscle cells. *Biochem Biophys Res Commun*. 2006;340(2):675-80.

168. Wang P, Liu X, Xu P, et al. Decorin reduces hypertrophic scarring through inhibition of the TGF-β1/Smad signaling pathway in a rat osteomyelitis model. *Exp Ther Med*. 2016;12(4):2102-8.

169. Zhang Z, Li XJ, Liu Y, et al. Recombinant human decorin inhibits cell proliferation and downregulates TGF-β1 production in hypertrophic scar fibroblasts. *Burns*. 2007;33(5):634-41.

170. Smith P, Mosiello G, Deluca L, et al. TGF-β2 activates proliferative scar fibroblasts. *J Surg Res*. 1999;82(2):319-23.

171. Polo M, Smith PD, Kim YJ, et al. Effect of TGF-β2 on proliferative scar fibroblast cell kinetics. *Ann Plast Surg*. 1999;43(2):185-90.

172 Krummel TM, Michna BA, Thomas BL, et al. Transforming growth factor beta (TGF-

β) induces fibrosis in a fetal wound model. *J Pediatr Surg*. 1988;23(7):647-52.

173. Shah M, Foreman DM, Ferguson MWJ. Neutralisation of TGF-β1 and TGF-β2 or exogenous addition of TGF-β3 to cutaneous rat wounds reduces scarring. *J Cell Sci*. 1995;108 (Pt 3):985-1002.

174. Hsu M, Peled ZM, Chin GS, et al. Ontogeny of expression of transforming growth factor-β1 (TGF-β1), TGF-β3, and TGF-β receptors I and II in fetal rat fibroblasts and skin. *Plast Reconstr Surg*. 2001;107(7):1787-96.

175. Wierzbicka-Patynowski I, Schwarzbauer JE. The ins and outs of fibronectin matrix assembly. *Journal of Cell Science*. 2003;116(Pt 16):3269-76.

176. Schwarzbauer JE. Alternative splicing of fibronectin: Three variants, three functions. *BioEssays*. 1991;13(10):527-33.

177. Maseruka H, Bonshek RE, Tullo AB. Tenascin-C expression in normal, inflamed, and scarred human corneas. *Br J Ophthalmol*. 1997;81(8):677-82.

178. Rodrigues M, Kosaric N, Bonham CA, et al. Wound healing: A cellular perspective. *Physiol Rev*. 2019;99(1):665-706.

179. Mackie EJ, Halfter W, Liverani D. Induction of tenascin in healing wounds. *J Cell Biol*. 1988;107(6 Pt 2):2757-67.

180. Midwood KS, Orend G. The role of tenascin-C in tissue injury and tumorigenesis. *Journal of Cell Communication and Signaling*. 2009;3(3-4):287-310.

181. Yates CC, Krishna P, Whaley D, et al. Lack of CXC chemokine receptor 3 signaling leads to hypertrophic and hypercellular scarring. *Am J Pathol*. 2010;176(4):1743-55.

182. Tensen CP, Flier J, Van Der Raaij-Helmer EMH, et al. Human IP-9: A keratinocyte-derived high affinity CXC-chemokine ligand for the IP-10/Mig receptor (CXCR3). *J Invest Dermatol*. 1999;112(5):716-22.

183. Yates CC, Whaley D, Kulasekeran P, et al. Delayed and deficient dermal maturation in mice lacking the CXCR3 ELR-negative CXC chemokine receptor. *Am J Pathol*. 2007;171(2):484-95.

184. Bullard KM, Longaker MT, Lorenz HP. Fetal wound healing: Current biology. *World Journal of Surgery*. 2003;27(1):54-61.

185. Hopkinson-Woolley J, Hughes D, Gordon S, et al. Macrophage recruitment during limb development and wound healing in the embryonic and foetal mouse. *J Cell Sci*. 1994;107 (Pt 5):1159-67.

186. Gilbert RWD, Vickaryous MK, Viloria-Petit AM. Signalling by transforming growth factor beta isoforms in wound healing and tissue regeneration. *J Dev Biol*. 2016;4(2):21.

187. Liechty KW, Adzick NS, Crombleholme TM. Diminished interleukin 6 (IL-6) production during scarless human fetal wound repair. *Cytokine*. 2000;12(6):671-76.

188. Liechty KW, Crombleholme TM, Cass DL, et al. Diminished interleukin-8 (IL-8) production in the fetal wound healing response. *J Surg Res*. 1998;77(1):80-4.

189. Nodder S, Martin P. Wound healing in embryos: A review. *Anatomy and Embryology*. 1997;195(3):215-28.

190. Estes JM, Berg JSV, Adzick NS, et al. Phenotypic and functional features of myofibroblasts in sheep fetal wounds. *Differentiation*. 1994;56(3):173-81.

191. Merkel JR, Dipaolo BR, Hallock GG, et al. Type I and type III collagen content of healing wounds in fetal and adult rats. *Proc Soc Exp Biol Med*. 1988;187(4):493-7.

192. Larson BJ, Longaker MT, Lorenz HP. Scarless fetal wound healing: A basic science review. *Plastic and Reconstructive Surgery*. 2010;126(4):1172-80.

193. Leavitt T, Hu MS, Marshall CD, et al. Scarless wound healing: Finding the right cells and signals. *Cell and Tissue Research*. 2016;365(3):483-93.

194. Sawai T, Usui N, Sando K, et al. Hyaluronic acid of wound fluid in adult and fetal rabbits. *J Pediatr Surg*. 1997;32(1):41-3.

195. Mast BA, Diegelmann RF, Krummel TM, et al. Hyaluronic acid modulates proliferation, collagen and protein synthesis of cultured fetal fibroblasts. *Matrix*. 1993;13(6):441-46.

196. Alaish SM, Yager D, Diegelmann RF, et al. Biology of fetal wound healing: Hyaluronate receptor expression in fetal fibroblasts. *J Pediatr Surg*. 1994;29(8):1040-3.

197. Soo C, Hu FY, Zhang X, et al. Differential expression of fibromodulin, a transforming growth factor-β modulator, in fetal skin development and scarless repair. *Am J Pathol*. 2000;157(2):423-33.

198. Longaker MT, Whitby DJ, Jennings RW, et al. Fetal diaphragmatic wounds heal with scar formation. *J Surg Res*. 1991;50(4):375-85.

199. Wilgus TA, Bergdall VK, Tober KL, et al. The impact of cyclooxygenase-2 mediated inflammation on scarless fetal wound healing. *Am J Pathol*. 2004;165(3):753-61.

200. Lobmann R, Schultz G, Lehnert H. Proteases and the diabetic foot syndrome: Mechanisms and therapeutic implications. *Diabetes Care*. 2005;28(2):461-71.

201. Richmond NA, Maderal AD, Vivas AC. Evidence-based management of common chronic lower extremity ulcers. *Dermatol Ther*. 2013;26(3):187-96.

202. Nolan CM, Beaty HN, Bagdade JD. Further characterization of the impaired bactericidal function of granulocytes in patients with poorly controlled diabetes. *Diabetes*. 1978;27(9):889-94.

203. Tsioufis C, Bafakis I, Kasiakogias A, et al. The Role of Matrix Metalloproteinases in Diabetes Mellitus. *Curr Top Med Chem*. 2012;12(10):1159-65.

204. Bullen EC, Longaker MT, Updike DL, et al. Tissue inhibitor of metalloproteinase-1 is decreased and activated gelatinases are increased in chronic wounds. *J Invest Dermatol*. 1995;104(2):236-40.

205. Frykberg RG, Banks J. Challenges in the treatment of chronic wounds. *Adv Wound Care*. 2015;4(9):560-82.

206. James TJ, Hughes MA, Cherry GW, et al. Evidence of oxidative stress in chronic venous ulcers. *Wound Repair Regen*. 2003;11(3):172-6

207. Shankaran V, Brooks M, Mostow E. Advanced therapies for chronic wounds: NPWT, engineered skin, growth factors, extracellular matrices. *Dermatol Ther*.

2013;26(3):215-21.

208. Guo S, DiPietro LA. Critical review in oral biology & medicine: Factors affecting wound healing. *J Dent Res* 2010; 89: 219–29.

209. Bishop A. Role of oxygen in wound healing. *Journal of wound care*. 2008;17(9):399-402.

210. Rodriguez PG, Felix FN, Woodley DT, et al. The role of oxygen in wound healing: A review of the literature. *Dermatologic Surgery*. 2008;34(9):1159-69.

211. Tandara AA, Mustoe TA. Oxygen in wound healing: More than a nutrient. *World Journal of Surgery*. 2001;9(3):175-7.

212. Gordillo GM, Sen CK. Revisiting the essential role of oxygen in wound healing. *American Journal of Surgery*. 2003;186(3):259-63.

213. Bryan N, Ahswin H, Smart N, et al. Reactive oxygen species (ROS) - A family of fate deciding molecules pivotal in constructive inflammation and wound healing. *Eur Cells Mater*. 2012;24:249-65.

214. Edwards R, Harding KG. Bacteria and wound healing. *Current Opinion in Infectious Diseases*. 2004;17(2):91-6.

215. Gardner SE, Frantz RA, Doebbeling BN. The validity of the clinical signs and symptoms used to identify localized chronic wound infection. *Wound Repair Regen*. 2001;9(3):178-86.

216. Menke NB, Ward KR, Witten TM, et al. Impaired wound healing. *Clin Dermatol*. 2007;25(1):19-25.

217. Sibbald RG, Orsted H, Schultz GS, et al. Preparing the wound bed 2003: Focus on infection and inflammation. *Ostomy Wound Manage*. 2003;49(11):24-51.

218. Bjarnsholt T, Kirketerp-Møller K, Jensen PØ, et al. Why chronic wounds will not heal: A novel hypothesis. *Wound Repair and Regeneration*. 2008;16(1):2-10.

219. Bowler PG. Wound pathophysiology, infection and therapeutic options. *Annals of Medicine*. 2002;34(6):419-27.

220. Rowland Payne CME, Bladin C, Colchester ACF, et al. Argyria from excessive use of topical silver sulphadiazine. *The Lancet*. 1992;340(8811):126.

221. Murray CK, Loo FL, Hospenthal DR, et al. Incidence of systemic fungal infection and related mortality following severe burns. *Burns*. 2008;34(8):1108-12.

222. Gosain A, DiPietro LA. Aging and wound healing. *World Journal of Surgery*. 2004;28(3):321-6.

223. Swift ME, Burns AL, Gray KL, et al. Age-related alterations in the inflammatory response to dermal injury. *J Invest Dermatol*. 2001;117(5):1027-35.

224. Swift ME, Kleinman HK, DiPietro LA. Impaired wound repair and delayed angiogenesis in aged mice. *Lab Investig*. 1999;79(12):1479-87.

225. Mascarucci P, Taub D, Saccani S, et al. Age-related changes in cytokine production by leukocytes in rhesus monkeys. *Aging Clin Exp Res*. 2001;13(2):85-94.

226. Plackett TP, Schilling EM, Faunce DE, et al. Aging enhances lymphocyte cytokine defects after injury. *FASEB J*. 2003;17(6):688-9.

227. Plisko A, Gilchrest BA. Growth factor responsiveness of cultured human fibroblasts declines with age. *Journals Gerontol*. 1983;38(5):513-18.

228. Huijberts MSP, Schaper NC, Schalkwijk CG. Advanced glycation end products and diabetic foot disease. *Diabetes/Metabolism Research and Reviews*. 2008;24 Suppl 1:19-24.

229. Woo K, Ayello EA, Sibbald RG. The edge effect: current therapeutic options to advance the wound edge. *Advances in skin & wound care*. 2007;20(2):99-119.

230. King GL, Loeken MR. Hyperglycemia-induced oxidative stress in diabetic complications. *Histochemistry and Cell Biology*. 2004;122(4):333-8.

231. Calhoun JH, Overgaard KA, Stevens CM, et al. Diabetic foot ulcers and infections: Current concepts. *Advances in skin & wound care*. 2002;15(1):31-45.

232. Sibbald RG, Woo KY. The biology of chronic foot ulcers in persons with diabetes. *Diabetes/Metabolism Research and Reviews*. 2008;24 Suppl 1:25-30.

233. Loots MAM, Lamme EN, Mekkes JR, et al. Cultured fibroblasts from chronic diabetic wounds on the lower extremity (non-insulin-dependent diabetes mellitus) show disturbed proliferation. *Arch Dermatol Res*. 1999;291(2-3):93-9.

234. Galkowska H, Wojewodzka U, Olszewski WL. Chemokines, cytokines, and growth factors in keratinocytes and dermal endothelial cells in the margin of chronic diabetic foot ulcers. *Wound Repair Regen*. 2006;14(5):558-65.

235. Quattrini C, Jeziorska M, Boulton AJM, et al. Reduced vascular endothelial growth factor expression and intra-epidermal nerve fiber loss in human diabetic neuropathy. *Diabetes Care*. 2008;31(1):140-5.

236. Charles CA, Romanelli P, Martinez ZB, et al. Tumor necrosis factor-alfa in nonhealing venous leg ulcers. *J Am Acad Dermatol*. 2009;60(6):951-5.

237. Bell HE, Openshaw P. The cause of venous ulceration. *The Lancet*. 1982;2(8295):437-8.

238. Juge-Aubry CE, Henrichot E, Meier CA. Adipose tissue: A regulator of inflammation. *Best Practice and Research: Clinical Endocrinology and Metabolism*. 2005;19(4):547-66.

239. Trent JT, Kirsner RS. Wounds and malignancy. *Advances in skin & wound care*. 2003;16(1):31-4.

240. Wilson JA, Clark JJ. Obesity: impediment to postsurgical wound healing. *Advances in skin & wound care*. 2004;17(8):426-35.

241. Sen CK, Gordillo GM, Roy S, et al. Human skin wounds: A major snoballing threat to public health and economy. *Wound Repair Regen.* 2009;17(6):763-71.

242. Phillips TJ, Kehinde O, Green H, et al. Treatment of skin ulcers with cultured epidermal allografts. *J Am Acad Dermatol*. 1989;21(2 Pt 1):191-9.

243. Wainwright DJ. Use of an acellular allograft dermal matrix (AlloDerm) in the management of full-thickness burns. *Burns*. 1995;21(4):243-8.

244. Sheridan RL, Tompkins RG. Skin substitutes in burns. *Burns*. 1999;25(2):97-103.

245. Leigh IM, Navsaria HA. Pre-confluent keratinocyte grafting: The future for cultured skin replacements? *Burns*. 1998;24(7):591-3.

246. Stanulis-Praeger BM, Gilchrest BA. Growth factor responsiveness declines during adulthood for human skin-derived cells. *Mech Ageing Dev*. 1986;35(2):185-98.

247. Rinnerthaler M, Duschl J, Steinbacher P, et al. Age-related changes in the composition of the cornified envelope in human skin. *Exp Dermatol*. 2013;22(5):329-35.

248. Gilchrest BA, Karassik RL, Wilkins LM, et al. Autocrine and paracrine growth stimulation of cells derived from human skin. *J Cell Physiol*. 1983;117(2):235-40.

249. Ferguson MWJ, O'Kane S. Scar-free healing: From embryonic mechanism to adult therapeutic intervention. *Philosophical Transactions of the Royal Society B: Biological Sciences*. 2004;359(1445):839-50.

250. Green H, Kehinde O, Thomas J. Growth of cultured human epidermal cells into multiple epithelia suitable for grafting. *Proc Natl Acad Sci U S A*. 1979;76(11):5665-68.

251. Barrandon Y, Green H. Cell migration is essential for sustained growth of keratinocyte colonies: The roles of transforming growth factor-α and epidermal growth factor. *Cell*. 1987;50(7):1131-7.

252. Lam PK, Chan ESY, To EWH, et al. Development and evaluation of a new composite laserskin graft. *Journal of Trauma - Injury, Infection and Critical Care*. 1999;47(5):918-22.

253. Wood F, Martin L, Lewis D, et al. A prospective randomised clinical pilot study to compare the effectiveness of Biobrane ® synthetic wound dressing, with or without autologous cell suspension, to the local standard treatment regimen in paediatric scald injuries. *Burns*. 2012;38(6):830-9.

254. Böttcher-Haberzeth S, Biedermann T, Reichmann E. Tissue engineering of skin. *Burns*. 2010;36(4):450-60.

255. Leigh Im, Purkis Pe, Navsaria Ha, et al. Treatment of chronic venous ulcers with

sheets of cultured allogenic keratinocytes. *Br J Dermatol*. 1987;117(5):591-7.

256. Dreifke MB, Jayasuriya AA, Jayasuriya AC. Current wound healing procedures and potential care. *Mater Sci Eng. C* 2015; 48: 651–62.

257. Boateng JS, Matthews KH, Stevens HNE, et al. Wound healing dressings and drug delivery systems: A review. *J Pharm Sci*. 2008;97(8):2892-923.

258. Dumville JC, Deshpande S, O'Meara S, et al. Hydrocolloid dressings for healing diabetic foot ulcers. *Cochrane Database of Systematic Reviews*. 2013;(8):CD009099.

259. Mogoşanu GD, Grumezescu AM. Natural and synthetic polymers for wounds and burns dressing. *Int J Pharm*. 2014;463(2):127-36.

260. Dreifke MB, Ebraheim NA, Jayasuriya AC. Investigation of potential injectable polymeric biomaterials for bone regeneration. *Journal of Biomedical Materials Research - Part A*. 2013;101(8):2436-47.

261. Chen WYJ, Abatangelo G. Functions of hyaluronan in wound repair. *Wound Repair and Regeneration*. 1999;7(2):79-89

262. Turley EA, Torrance J. Localization of hyaluronate and hyaluronate-binding protein on motile and non-motile fibroblasts. *Exp Cell Res*. 1985;161(1):17-28.

263. Moczar M, Robert L. Stimulation of cell proliferation by hyaluronidase during in vitro aging of human skin fibroblasts. *Exp Gerontol*. 1993;28(1):59-68

264. Campo GM, Avenoso A, Campo S, et al. Molecular size hyaluronan differently modulates toll-like receptor-4 in LPS-induced inflammation in mouse chondrocytes. *Biochimie*. 2010;92(2):204-15.

265. Ghazi K, Deng-Pichon U, Warnet JM, et al. Hyaluronan fragments improve wound healing on in vitro cutaneous model through P2X7 Purinoreceptor basal activation: Role of molecular weight. *PLoS One*. 2012;7(11):e48351.

266. Gowan J, Roller L. Diabetes complications. *Aust J Pharm*. 2013.

267. Bradley T, Brown RE, Kucan JO, et al. Toxic epidermal necrolysis: A review and report of the successful use of biobrane for early wound coverage. *Ann Plast Surg*.

1995;35(2):124-32.

268. Kirwan L. Management of difficult wounds with Biobrane®. *Conn Med*. 1995;59(9):523-9.

269. Gerding RL, Imbembo AL, Fratianne RB. Biosynthetic skin substitute vs. 1% silver sulfadiazine for treatment of inpatient partial-thickness thermal burns. *J Trauma - Inj Infect Crit Care*. 1988;28(8):1265-9.

270. Morgan D. Wounds: What should a dressings formulary include? *Hospital Pharmacist*. 2002;9(9):261-6.

271. Steed DL, Study Group the DU. Clinical evaluation of recombinant human platelet - derived growth factor for the treatment of lower extremity diabetic ulcers. *J Vasc Surg*. 1995;21(1):71-81.

272. Yao C, Yao P, Wu H, et al. Acceleration of wound healing in traumatic ulcers by absorbable collagen sponge containing recombinant basic fibroblast growth factor. *Biomed Mater*. 2006;1(1):33-7.

273. Geer DJ, Swartz DD, Andreadis ST. Biomimetic delivery of keratinocyte growth factor upon cellular demand for accelerated wound healing in vitro and in vivo. *Am J Pathol*. 2005;167(6):1575-86.

274. Pandit A, Ashar R, Feldman D. The effect of TGF-β delivered through a collagen scaffold on wound healing. *J Investig Surg*. 1999;12(2):89-100.

275. Khavari PA, Rollman O, Vahlquist A. Cutaneous gene transfer for skin and systemic diseases. *Journal of Internal Medicine*. 2002;252(1):1-10.

276. Escámez MJ, Carretero M, García M, et al. Assessment of optimal virus-mediated growth factor gene delivery for human cutaneous wound healing enhancement. *J Invest Dermatol*. 2008;128(6):1565-75.

277. Krebs MD, Jeon O, Alsberg E. Localized and sustained delivery of silencing RNA from macroscopic biopolymer hydrogels. *J Am Chem Soc*. 2009;131(26):9204-6.

278. Viñas-Castells R, Holladay C, Di Luca A, et al. Snail1 down-regulation using small interfering RNA complexes delivered through collagen scaffolds. *Bioconjug Chem*.

2009;20(12):2262-9.

279. Nguyen PD, Tutela JP, Thanik VD, et al. Improved diabetic wound healing through topical silencing of p53 is associated with augmented vasculogenic mediators. *Wound Repair Regen*. 2010;18(6):553-9.

280. Van Solingen C, Seghers L, Bijkerk R, et al. Antagomir-mediated silencing of endothelial cell specific microRNA-126 impairs ischemia-induced angiogenesis. *J Cell Mol Med*. 2009;13(8A):1577-85.

281. Pastar I, Khan AA, Stojadinovic O, et al. Induction of specific microRNAs inhibits cutaneous wound healing. *J Biol Chem*. 2012;287(35):29324-35.

282. Wu Y, Huang S, Enhe J, et al. Bone marrow-derived mesenchymal stem cell attenuates skin fibrosis development in mice. *Int Wound J*. 2014;11(6):701-10.

283. Laverdet B, Micallef L, Lebreton C, et al. Use of mesenchymal stem cells for cutaneous repair and skin substitute elaboration. *Pathol Biol*. 2014;62(2):108-117.

284. Beddington RSP, Robertson EJ. An assessment of the developmental potential of embryonic stem cells in the midgestation mouse embryo. *Development*. 1989;105(4):733-7.

285. Coraux C, Hilmi C, Rouleau M, et al. Reconstituted skin from murine embryonic stem cells. *Curr Biol*. 2003;13(10):849-53.

286. Gutierrez-Aranda I, Ramos-Mejia V, Bueno C, et al. Human induced pluripotent stem cells develop teratoma more efficiently and faster than human embryonic stem cells regardless the site of injection. *Stem Cells*. 2010;28(9):1568-70.

287. Gimble JM, Katz AJ, Bunnell BA. Adipose-derived stem cells for regenerative medicine. *Circulation Research*. 2007;100(9):1249-60.

288. Gathier W, Türktaş Z, Duckers HJ. Adipose-derived stem cells. *Stem Cell and Gene Therapy for Cardiovascular Disease*. 2015.

289. Huang SP, Hsu CC, Chang SC, et al. Adipose-derived stem cells seeded on acellular dermal matrix grafts enhance wound healing in a murine model of a full-thickness defect. *Ann Plast Surg*. 2012;69(6):656-62.

290. Luo G, Cheng W, He W, et al. Promotion of cutaneous wound healing by local application of mesenchymal stem cells derived from human umbilical cord blood. *Wound Repair Regen*. 2010;18(5):506-13.

291. Park SJ, Moon SH, Lee HJ, et al. A comparison of human cord blood- and embryonic stem cell-derived endothelial progenitor cells in the treatment of chronic wounds. *Biomaterials*. 2013;34(4):995-1003.

292. Théry C, Zitvogel L, Amigorena S. Exosomes: composition, biogenesis and function. *Nat Rev Immunol*. 2002;2(8):569-79.

293. Théry C, Witwer KW, Aikawa E, et al. Minimal information for studies of extracellular vesicles 2018 (MISEV2018): a position statement of the International Society for Extracellular Vesicles and update of the MISEV2014 guidelines. *J Extracell Vesicles*. 2018;7(1):1535750.

294. Rashed MH, Bayraktar E, Helal GK, et al. Exosomes: From garbage bins to promising therapeutic targets. *International Journal of Molecular Sciences*. 2017;18(3):538.

295. Masyuk AI, Masyuk T V., Larusso NF. Exosomes in the pathogenesis, diagnostics and therapeutics of liver diseases. *Journal of Hepatology*. 2013;59(3):621-5.

296. Vella LJ, Sharples RA, Nisbet RM, et al. The role of exosomes in the processing of proteins associated with neurodegenerative diseases. *European Biophysics Journal*. 2008. 2008;37(3):323-32.

297. Hanson PI, Cashikar A. Multivesicular body morphogenesis. *Annu Rev Cell Dev Biol*. 2012;28:337-62.

298. Mathivanan S, Simpson RJ. ExoCarta: A compendium of exosomal proteins and RNA. *Proteomics*. 2009;9(21):4997-5000.

299. Théry C, Ostrowski M, Segura E. Membrane vesicles as conveyors of immune responses. *Nature Reviews Immunology*. 2009;9(8):581-93.

300. Record M, Carayon K, Poirot M, et al. Exosomes as new vesicular lipid transporters involved in cell-cell communication and various pathophysiologies. *Biochimica et Biophysica Acta - Molecular and Cell Biology of Lipids*. 2014;1841(1):108-20.

301. Xiang X, Poliakov A, Liu C, et al. Induction of myeloid-derived suppressor cells by tumor exosomes. *Int J Cancer*. 2009;124(11):2621-33.

302. Valadi H, Ekström K, Bossios A, et al. Exosome-mediated transfer of mRNAs and microRNAs is a novel mechanism of genetic exchange between cells. *Nat Cell Biol*. 2007;9(6):654-9.

303. Ostenfeld MS, Jeppesen DK, Laurberg JR, et al. Cellular disposal of miR23b by RAB27-dependent exosome release is linked to acquisition of metastatic properties. *Cancer Res*. 2014;74(20):5758-71.

304. McKelvey KJ, Powell KL, Ashton AW, et al. Exosomes: Mechanisms of uptake. *Journal of Circulating Biomarkers*. 2015;4:7.

305. Marchant R, Robards AW. Membrane systems associated with the plasmalemma of plant cells. *Ann Bot*. 1968;32(3):457-72.

306. Rutter BD, Innes RW. Extracellular vesicles isolated from the leaf apoplast carry stress-response proteins. *Plant Physiol*. 2017;173(1):728-41.

307. Rutter B, Rutter K, Innes R. Isolation and quantification of plant extracellular vesicles. *BIO-PROTOCOL*. 2017;89(23):12968-75.

308. An Q, Ehlers K, Kogel KH, et al. Multivesicular compartments proliferate in susceptible and resistant MLA12-barley leaves in response to infection by the biotrophic powdery mildew fungus. *New Phytol* 2006; 172(3): 563–76.

309. Hansen LL, Nielsen ME. Plant exosomes: Using an unconventional exit to prevent pathogen entry? *Journal of Experimental Botany*. 2017;69(1):59-68.

310. Zeyen RJ, Bushnel WR. Papilla response of barley epidermal cells caused by Erysiphe graminis : rate and method of deposition determined by microcinematography and transmission electron microscopy. *Can J Bot*. 1979; 57(8):898-913.

311. Samuel M, Bleackley M, Anderson M, et al. Extracellular vesicles including exosomes in cross kingdom regulation: A viewpoint from plant-fungal interactions. *Front Plant Sci*. 2015;6:766.

312. Golezar S. Ananas comosus effect on perineal pain and wound healing after episiotomy: A randomized double-blind placebo-controlled clinical trial. *Iran Red Crescent Med J*. 2016;18(3):e21019.

313. Suhrabi Z, Taghinejad H. A comparative study on the efficacy of ibuprofen and celecoxib on the intensity of perineal pain following episiotomy: A randomized clinical trial. *Iran Red Crescent Med J*. 2013;15(12):e9980.

314. Maurer HR. Bromelain: Biochemistry, pharmacology and medical use. *Cellular and Molecular Life Sciences*. 2001;58(9):1234-45.

315. Dušková M, Wald M. Orally administered proteases in aesthetic surgery. *Aesthetic Plast Surg*. 1999;23(1):41-4.

316. Vellini M, Desideri D, Milanese A, et al. Possible involvement of eicosanoids in the pharmacological action of bromelain. *Arzneimittel-Forschung/Drug Res*. 1986;36(1):110-2.

317. Zatuchni GI, Colombi DJ. Bromelains therapy for the prevention of episiotomy pain. *Obstet Gynecol*. 1967;29(2):275-8.

318. Halbert CL, Alexander IE, Wolgamot GM, et al. Adeno-associated virus vectors transduce primary cells much less efficiently than immortalized cells. *J Virol*. 1995;69(3):1473-9.

319. Kırbaş OK, Bozkurt BT, Asutay AB, et al. Optimized isolation of extracellular vesicles from various organic sources using aqueous two-phase system. *Sci Rep*. 2019;9(1):19159.

320. van der Pol E, Böing AN, Harrison P, et al. Classification, functions, and clinical relevance of extracellular vesicles. *Pharmacol Rev*. 2012;64(3):676-705.

321. György B, Szabó TG, Pásztói M, et al. Membrane vesicles, current state-of-the-art: Emerging role of extracellular vesicles. *Cellular and Molecular Life Sciences*. 2011;68(16):2667-88.

322. Gardiner C, Vizio D Di, Sahoo S, et al. Techniques used for the isolation and characterization of extracellular vesicles: Results of a worldwide survey. *J Extracell*

Vesicles. 2016;5:32945.

323. Andreu Z, Yáñez-Mó M. Tetraspanins in extracellular vesicle formation and function. *Front Immunol*. 2014;5:442.

324. Ellis S, Lin EJ, Tartar D. Immunology of wound healing. *Current Dermatology Reports*. 2018;7(4):350-8.

325. MacLeod AS, Mansbridge JN. The innate immune system in acute and chronic wounds. *Adv Wound Care*. 2016;5(2):65-78.

326. Paiva CN, Bozza MT. Are reactive oxygen species always detrimental to pathogens? *Antioxidants and Redox Signaling*. 2014;20(6):1000-37.

327. Dunnill C, Patton T, Brennan J, et al. Reactive oxygen species (ROS) and wound healing: the functional role of ROS and emerging ROS-modulating technologies for augmentation of the healing process. *Int Wound J*. 2017;14(1):89-96.

328. Auf Dem Keller U, Kümin A, Braun S, et al. Reactive oxygen species and their detoxification in healing skin wounds. *Journal of Investigative Dermatology Symposium Proceedings*. 2006;11(1):106-11.

329. Kramer N, Walzl A, Unger C, et al. In vitro cell migration and invasion assays. *Mutation Research - Reviews in Mutation Research*. 2013;752(1):10-24.

330. Schultz GS, Ladwig G, Wysocki A. Extracellular matrix: Review of its roles in acute and chronic wounds. *World Wide Wounds*. 2005.

331. Schoumacher M, Goldman RD, Louvard D, et al. Actin, microtubules, and vimentin intermediate filaments cooperate for elongation of invadopodia. *J Cell Biol*. 2010;189(3):541-56.

332. Woodley DT, Stanley JR, Reese MJ, et al. Human dermal fibroblasts synthesize laminin. *J Invest Dermatol*. 1988.

333. Johnson MB, Pang B, Gardner DJ, et al. Topical fibronectin improves wound healing of irradiated skin. *Sci Rep*. 2017;7:3876.

334. Adya R, Tan BK, Punn A, et al. Visfatin induces human endothelial VEGF and MMP-

2/9 production via MAPK and PI3K/Akt signalling pathways: Novel insights into visfatin-induced angiogenesis. *Cardiovasc Res*. 2008;78(2):356-65.

335. Tonnesen MG, Feng X, Clark RAF. Angiogenesis in wound healing. *J Investig Dermatology Symp Proc*. 2000;5(1):40-6.

336. Webb AH, Gao BT, Goldsmith ZK, et al. Inhibition of MMP-2 and MMP-9 decreases cellular migration, and angiogenesis in in vitro models of retinoblastoma. *BMC Cancer*. 2017;17(1):434.

337. Manuel JA, Gawronska-Kozak B. Matrix metalloproteinase 9 (MMP-9) is upregulated during scarless wound healing in athymic nude mice. *Matrix Biol*. 2006;25(8):505-14.

338. Shibuya M. Vascular Endothelial Growth Factor (VEGF) and Its Receptor (VEGFR) Signaling in Angiogenesis: A Crucial Target for Anti- and Pro-Angiogenic Therapies. *Genes and Cancer*. 2011;2(12):1097-1105.

339. Lee S, Kim MS, Jung SJ, et al. ERK activating peptide, AES16-2M promotes wound healing through accelerating migration of keratinocytes. *Sci Rep*. 2018;8(1):14398.

340. Sun Y, Liu WZ, Liu T, et al. Signaling pathway of MAPK/ERK in cell proliferation, differentiation, migration, senescence and apoptosis. *Journal of Receptors and Signal Transduction*. 2015;35(6):600-4.

341. Cuenda A, Rousseau S. p38 MAP-Kinases pathway regulation, function and role in human diseases. *Biochimica et Biophysica Acta - Molecular Cell Research*. 2007;1773(8):1358-75.

342. Nguyen TT, Mobashery S, Chang M. Roles of matrix metalloproteinases in cutaneous wound healing. *Wound Healing - New insights into Ancient Challenges*. 2016.

343. Keane TJ, Horejs CM, Stevens MM. Scarring vs. functional healing: Matrix-based strategies to regulate tissue repair. *Advanced Drug Delivery Reviews*. 2018;129:407-19.

344. Muller M, Trocme C, Lardy B, et al. Matrix metalloproteinases and diabetic foot ulcers: The ratio of MMP-1 to TIMP-1 is a predictor of wound healing. *Diabet Med*

2008; 25(4): 419–26.

345. Caley MP, Martins VLC, O'Toole EA. Metalloproteinases and wound healing. *Adv Wound Care*. 2015;4(4):225-34.

346. Gill SE, Parks WC. Metalloproteinases and their inhibitors: Regulators of wound healing. *International Journal of Biochemistry and Cell Biology*. 2008;40(6-7):1334-47.

347. Parks WC. Matrix metalloproteinases in repair. *Wound Repair and Regeneration*. 1999;7(6):423-32.

348. Rolfe KJ, Richardson J, Vigor C, et al. A role for TGF-β1-induced cellular responses during wound healing of the non-scarring early human fetus? *J Invest Dermatol*. 2007;127(11):2656-67.

349. Wang L, Hu L, Zhou X, et al. Exosomes secreted by human adipose mesenchymal stem cells promote scarless cutaneous repair by regulating extracellular matrix remodelling. *Sci Rep*. 2017;7(1):13321.

350. Cuttle L, Nataatmadja M, Fraser JF, et al. Collagen in the scarless fetal skin wound: Detection with picrosirius-polarization. *Wound Repair Regen*. 2005;13(2):198-204.

351. Colwell AS, Faudoa R, Krummel TM, et al. Transforming growth factor-β, Smad, and collagen expression patterns in fetal and adult keratinocytes. *Plast Reconstr Surg*. 2007;119(3):852-7.

352. Kwan P, Desmoulière A, Tredget EE. Molecular and cellular basis of hypertrophic scarring. *Elsevier Inc.* 2018:455–65.

353. Ornitz D, Sannes P. Fibroblast growth factors. *Encyclopedia of Respiratory Medicine*. Four-Volume Set. Elsevier Inc. 2006;210-3.

354. Eming SA, Martin P, Tomic-Canic M. Wound repair and regeneration: Mechanisms, signaling, and translation. *Science Translational Medicine*. 2014;6:265.